Designing a passive dynamic SLS-3D printable ankle-foot orthosis

Master thesis Integrated Product Design

by Falko Baatsen

"Designing a passive dynamic SLS-3D printable ankle-foot orthosis with specific stiffness characteristics"

Master thesis
Integrated Product Design
Faculty of Industrial Design Engineering
University of Technology Delft

Author

Falko Baatsen
4594274

Supervisory team

Mentor
Joris van Dam
Dept./section: SDE/EM

Chair
Erik Thomassen
Dept./section: SDE/TS

Client supervisors

Parts on Demand B.V.
Anne van den Dool

Livit Ottobock Care.
Tim de Roo

Special thanks to:
Rein Miedema from the UMC for his help with conducting the BRUCE tests and Chantal Engel from Livit Ottobock Care for her orthopedic expertise and help in conducting the user test

30-06-2023

Summary

An ankle-foot orthosis (AFO) is a medical aid that helps individuals with deficient walking patterns achieve a more natural gait. There are various types of AFOs prescribed for different reasons. This thesis specifically focuses on passive dynamic ankle-foot orthoses (PD-AFOs) and even within that branch a very specific type: the carbon dorsal leaf spring orthosis. This type of AFO leverages the body's biomechanics and gravitational forces to store and release energy at precise phases of the gait pattern, helping to restore some of the ankle function. Furthermore, they address the issue of excessive plantar flexion during the swing phase of gait, which can result in foot drop or an undesirable foot-slamming motion.

To ensure optimal fit and functionality, these orthoses are custom-made to provide the best fit for the lower leg and foot of each individual. Currently, the manufacturing process for these orthoses involves labour-intensive carbon composite layering techniques, which require significant effort and expertise.

An alternative AFO concept was designed, which aims to replicate the behaviour of existing carbon dorsal leaf spring orthoses using SLS-3D printing. This direction was explored as additive manufacturing excels in one-off production and eliminates the need for manual labour, offering cost-effective and efficient production of personalized items. This case is therefore carried out for the companies Parts on Demand, a selective laser sintering (SLS) 3D-printing company, and Livit Ottobock Care, an orthopedics company, to further investigate the feasibility of such an orthosis.

This study involved multiple design iterations, primarily focused on the stiffness behaviour of the AFO to create a novel SLS printable design that exhibits similar stiffness characteristics and gait influence compared to the existing carbon dorsal leaf spring AFOs produced by Livit Ottobock Care, whilst maintaining comparable weight and cost.

A model was created to parametrically refine SLS printable AFOs based on scanned lower leg and foot data for repeatable results using different feet. Subsequently, prototypes were fabricated using this model to validate the quantitative stiffness behaviour and qualitative correction of user gait resulting in an orthosis with a comparable function to the baseline carbon dorsal leaf spring orthosis.

Initial results seem promising for the feasibility of SLS printing PD-AFOs, but requires further validation, as many aspects related to their longevity were excluded from this study. These factors include its fracture resistance over longer periods of time, whether stiffness fatigue will occur, or how the AFO will behave mediolaterally. Nonetheless, producing an SLS-printed orthosis can provide benefits in the long run which for example include not only customized and well-fitting orthoses but also tailored stiffness characteristics for each individual, enhancing the function of the ankle and foot during walking. However, it is important to note that research in this area is currently insufficient.

Terminology

Anisotropic - (of a material) Has physical properties that differ depending on the direction of the material
Bilateral - Both sides (usually of the body)
Cadence - Walking steps per minute
Extension - Opening of a joint (increasing the angle between two bones)
Flexion - Closing of a joint (decreasing the angle between two bones)
Gait - A person's manner of walking
Gait analysis - An assessment of the way a body moves
Isotropic - (of a material) Has physical properties of the same value from different directions
Mediolateral stability - The ability to balance yourself whilst walking
Muscular dystrophy - Muscle disease caused by mutations of the genes
Step - Half a gait cycle
Stride - A full gait cycle
Unilateral - One-sided (usually of the body)

Abbreviations

AFO - Ankle-foot orthosis
AM - Additive manufacturing
BRUCE - The Bi-articular Reciprocating Universal Compliance Estimator
CAD - Computer-aided design
CAM - Computer-aided manufacturing
CarbonLW - Carbon reinforced Polyamide 12
CNC - Computerized numerical control
FBD - Fused deposition modelling
FDM - Free body diagram
FEA - Finite element analysis
MTP - Metatarsophalangeal joint
PA11 - Nylon 11 or Polyamide 11
PA11GF - Glass filled Polyamide 11
PA12 - Nylon 12 or Polyamide 12
PD-AFO - Passive dynamic ankle-foot orthosis
PVP - Premium vapour polishing
ROM - Range of motion
SLS - Selective laser sintering
SVA - Shank vertical angle

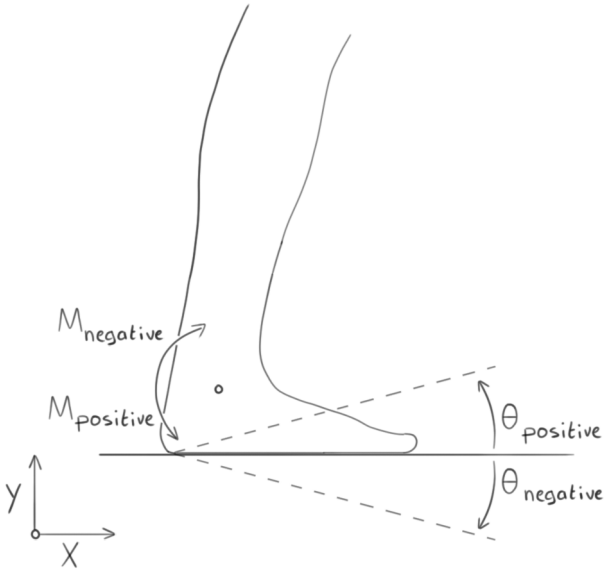
M negative
M positive
θ positive
θ negative
y
X

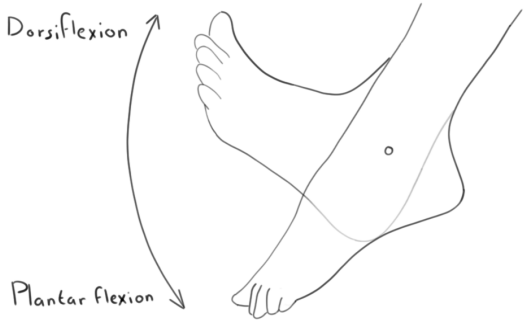
Dorsiflexion
Plantar flexion

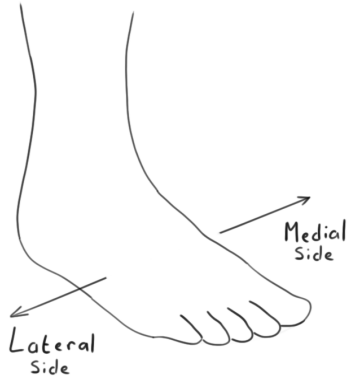
Medial Side
Lateral Side


Eversion
Inversion

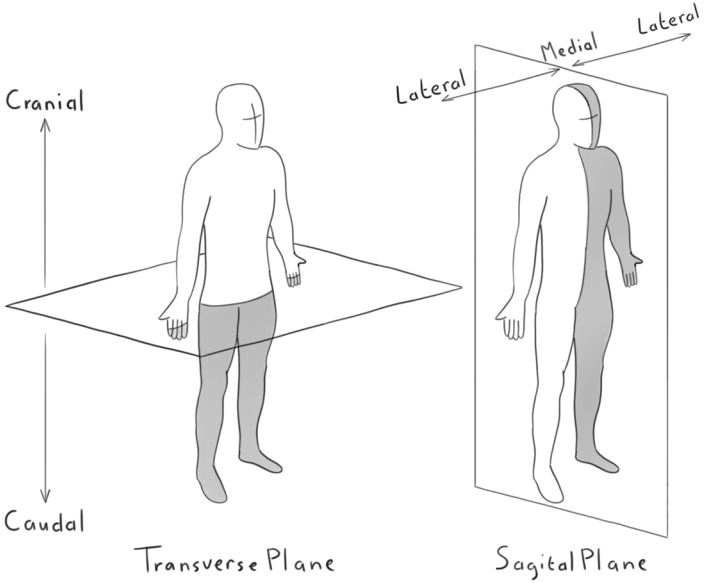
Cranial
Caudal
Transverse Plane

Medial
Lateral
Lateral
Sagital Plane

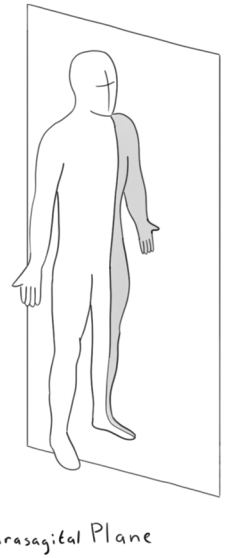
Parasagital Plane

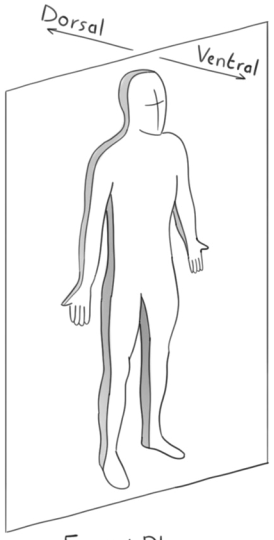
Dorsal
Ventral
Frontal Plane

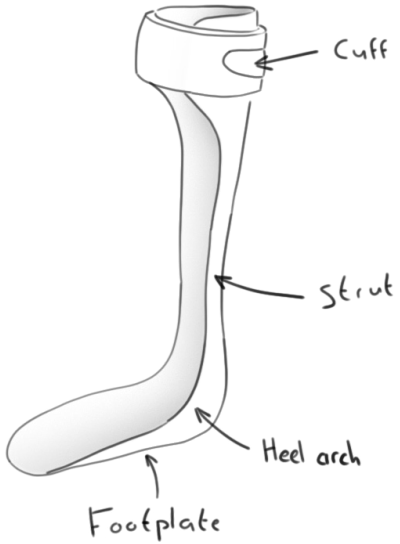
Cuff
Strut
Heel arch
Footplate

Assignment

An ankle-foot orthosis (commonly referred to as an AFO) is a wearable aid that improves walking patterns by reducing, preventing or helping the movement of the lower limbs to stabilise joints, support weak muscles and in general control the range of motion in the foot and ankle (*figure 1*)[1]. It is a supportive device that is strapped on the lower leg and extends into the shoe underneath the plantar surface of the foot. The need to wear an AFO usually results from an underlying condition such as nerve damage, brain/spinal cord problems, muscular dystrophy or an inherited condition[1], [2].

Off-the-shelf prefabricated orthoses are commonly used in the short term for an improvable condition. However, more commonly a long-term patient-specific AFO is needed as many ergonomic complaints arise when the device needs to be worn for longer periods. This project will focus on this second type of AFO. The current production methods of these AFOs consist of many manual labour-intensive steps. This is especially true for the dynamic AFOs with higher stiffness values as these require cutting and applying multiple layers of carbon fibre.

An alternative may be to introduce a more automated production process using 3D-printing[3]. This case is therefore carried out for the company Parts on Demand, a selective laser sintering (SLS) 3D-printing company for industrial parts. They, in collaboration with Livit Ottobock Care, an orthopedics company, have set up this case to explore the possibilities of manufacturing a SLS printable AFO providing a comfortable walking experience.

Livit Ottobock Care already has CAD files of all their clients and currently uses these to mill a positive cast of the lower leg and foot. This is consequently used for the manual application of either vacuum-formed plastic sheets or carbon layering. An alternative to this process may be to directly go from CAD to AFO through SLS printing.

Designing an orthosis using SLS printing as a starting point provides new design opportunities in terms of its form freedom. SLS-printed AFOs are deemed promising rigid orthoses with potential benefits like a better fit or customizable stiffness[3]. Compared to traditional orthopedic aids, 3D-printed AFOs can provide a more consistent product and a better distribution of pressure on the skin which results in a more comfortable device. However, 3D-printed orthoses are in the early stages of development and further research is needed in terms of their required strength and desired stiffness as they are still prone to fracturing due to the forces exerted at certain points when worn[4].

3D-printed othoses are also not yet widely employed as the hardware is considered to be too expensive and many parties are waiting for further validation of methods and materials before investing[5]. Parts on Demand in collaboration with Livit Ottobock Care is in a viable position to further explore this field, as they have the orthopaedic knowledge and hardware. Therefore it is researched in this project if a strong, patient-specific SLS-3D printed dynamic ankle-foot orthosis can be a viable alternative to the existing carbon dynamic AFOs currently being produced.

The full project brief can be found in Appendix A.

figure 1: An ankle-foot orthosis designed by Livit Ottobock Care

Parts on Demand

"There's 3D-printing, and 3D-printing. We know the difference."

Parts on Demand is an industrial selective laser sintering (SLS) production service company located in Utrecht. They specialize in fast series, one-off or repeatable production providing near isotropic high-strength 3D-printed parts. Parts on Demand actively assists clients in optimizing their products for SLS printing, enhancing their suitability and performance [6].

Parts on Demand can produce parts in various materials with multiple post-processing steps available to provide smooth, rough or coloured parts. They have experience with printing medical products such as custom-made braces or dental products and have ISO 13485 certification for the production of medical aids which makes it an ideal company to collaborate with an orthotics company[7].

They continue to introduce new printable materials and are continuously improving their printable repertoire. This case was partially set up because of recent innovations over at Parts on Demand through introducing new carbon-infused lightweight materials and the introduction of a more sustainably sourced material with increased material properties compared to the current standard.

Livit Ottobock Care

"Voor je lijf. Voor je leven."

Livit Ottobock Care is a Dutch orthopedics company, a part of Ottobock located in Dordrecht. With over 90 years of experience, Livit is dedicated to enabling mobility and promoting independent and unrestricted movement for all individuals.[8]

Livit is an orthopedic instrument maker producing a broad assortment of orthotic and prosthetic aids. They have a network of over 400 facilities in the Netherlands and produce their devices locally to ensure quality and fast delivery times.

They are collaborating on this project because of their aim to introduce more automation in the orthotics sector. They aim to move towards a more digitized future and slowly make the transition from more physically oriented labour and skill towards automation. They also already have a work flow that can, with minimal adaptation, suit the production of SLS-printed Ankle-foot orthoses and have a history of working together with Parts on Demand in the production of various other orthotic devices.

ANALYSIS

Ankle-foot orthoses

There is a broad range of ankle-foot orthoses. A distinction that has to be made is that an orthosis is not a prosthetic. A prosthetic is an artificial replacement for a limb or body part that is missing. An orthosis is an externally wearable aid that replaces or aids the function of a limb or body part, not replace it. An ankle-foot orthosis is a type of brace that is worn below the knee on the lower leg onto the foot[1]. This thesis will solely focus on this kind of orthosis and will commonly be abbreviated to AFO.

The need to wear an AFO is a result of a diagnosed deviating walking pattern where discomfort is experienced. A common condition for the prescription of an AFO is foot drop. This is a general conditional term where it is difficult for to lift the front part of the feet and thus drag their feet on the ground when they walk. It is seen commonly with people suffering from Charcot-Marie-Tooth disease, Cerebral Palsy, Spina Bifida, spasticity or stroke[1], [9]. Foot drop is in these cases caused by weak muscles, paralysis of muscles or nerve injuries/problems. It is consequently corrected by the ability of the AFO to correct the ankle angle.

Aside from foot drop, AFOs serve other purposes. They can provide mediolateral stability by limiting the inversion and eversion of the foot, to prevent toe walking or to correct the position of the knee to name a few. Usually, a combination of conditions is diagnosed and the best-fitting orthosis type is prescribed.

Different types

Ankle-foot orthoses can be divided into two classifications: prefabricated(or off-the-shelf AFOs) and custom-made AFOs. Prefabricated AFOs are mass-produced products based on average foot size groups. These orthoses are commonly used in the short term for an improvable condition. While they are less expensive, custom-made AFOs are generally recommended for better results and fit, especially when the device needs to be worn for longer periods[10].

These custom-made AFOs provide more comfort as they are tailor-made for the patient using a cast of the foot. They are more common because a better-fit results in a better functioning device and more customer satisfaction.

Within the categories of prefabricated and custom-made orthoses, there are various types available, each designed to treat specific irregular gaits[11]:

Posterior dynamic element ankle-foot orthosis (PDE AFO)
This type of AFO is designed for high-impact activities, such as sports. The strut stores and releases energy during gait and is interchangeable to increase or decrease the desired stiffness to suit different activities.

Articulated ankle-foot orthosis
Usually, a thermoplastic device that allows for ankle range of motion while limiting inversion and eversion of the foot, thus providing mediolateral stability.

Leaf spring ankle-foot orthosis
Usually a thermoplastic device which prevents foot drop through providing toe clearance and controlling plantar flexion. This type of orthosis does not aid in stabilizing inversion and eversion of the foot.

Passive dynamic ankle-foot orthosis (PD-AFO)
Commonly made through carbon fibre layering. This type has a flexible strut that stores energy during dorsiflexion and releases it right before the swing phase. This propels the user in a forward motion.

Solid / rigid ankle-foot orthosis
A custom orthosis used to lock the foot and ankle in place. This orthosis immobilizes the foot so almost no movement is possible.

There are more types of AFOs, and certain combinations of these types also exist to ensure more specific functionality. Each device has its advantages and drawbacks which might help or impair the user. It is therefore crucial to have a precise evaluation of the patient and their requirements.

Livit Ottobock Care has expressed the most interest in developing an SLS printable alternative for their passive dynamic carbon orthosis collection. These orthoses require many labor-intensive hours to produce and are estimated to be at a price-competitive point with an SLS-printed variant.

Carbon-layered ankle-foot orthoses are known for their lightweight and high stiffness values. The biggest challenge would be to replicate the same behavior of carbon AFOs while making them just as stiff, with minimal compromise to their sleek and lightweight design.

Livit Ottobock Care currently produces 7 different types of carbon ankle-foot orthoses:

- Carbon dorsal bilateral AFO
- Carbon dorsal unilateral AFO
- Carbon dorsal AFO with hinge
- Carbon dorsal leaf spring AFO
- Carbon ventral bilateral AFO
- Carbon ventral unilateral AFO
- Carbon ventral AFO with hinge

These AFOs can be split into two groups: dorsal AFOs and ventral AFOs. These terms regard the mounting of the AFO cuff and whether it attaches to the calf or the shin (*figure 2*).

Whether a dorsal or ventral AFO is desired depends greatly on the patient's condition. Typically, dorsal AFOs are more prescribed for stability and support and controlling ankle flexion whilst ventrally mounted AFOs are more prescribed to aid in dorsiflexion. Dorsal AFOs fit a more extended knee position better for stability whilst ventral AFOs are more suited for a flexed knee position. Further elaboration can be found on page 17.

The difference between a unilateral and bilateral AFO regards whether the cuff and footplate are connected only on the lateral side of the foot or on the lateral and medial side of the foot.

The hinged AFOs use a prefabricated hinge that is mounted between a carbon-layered rigid cuff and footplate. The stiffness required to aid in walking is derived from springs placed in this hinge component (*figure 3*).

The last type of carbon AFO produced by Livit Ottobock Care is the carbon dorsal leaf spring AFO. This AFO consists of one piece and provides passive dynamic walking aid through the flexibility and stiffness of the carbon strut.

The decision was made to focus on the carbon dorsal leaf spring AFO as it relies the most on the flexible and stiff properties of layered carbon. The stress is more evenly distributed in this type of orthosis as no bolts or other fasteners are used in this design which creates stress points. The material properties of SLS printable materials are lower than that of carbon composites which makes stress distribution more relevant. Concentrated stress points can be detrimental for an SLS printed design as the material properties of the available materials are lower than that of carbon[4].

Moreover, around 45% of the carbon orthoses produced by Livit Ottobock Care are this specific type of orthosis[12] making it a significant candidate for further investigation.

figure 2: (from left to right) An AFO mounted on the dorsal side of the leg and a AFO mounted on the ventral side of the leg

figure 3: An Ottobock Nextgear Tango AFO hinge

Gait

Ankle-foot orthoses help clients with a deviating walking pattern that experience discomfort to achieve a healthier range of motion. It is important to have an understanding of the way humans walk, how someone in need of an AFO deviates from this pattern and which AFO influence is desired. The manner or style of walking is commonly referred to as the gait pattern. Fully technical: walking occurs when moments are present where both feet are in contact with the ground which is not followed by periods where neither foot is touching the ground[1],[13]. IThis would be classified as running. The focus of this project remains on walking, as designing an AFO for running would require a different AFO type to handle more extreme loads and moments. Once an SLS passive dynamic posterior leaf spring AFO is validated for walking, other more stress-demanding types could be considered.

A full gait cycle involves multiple steps that can be described as a stride. The steps that make up a stride can be divided into a stance phase and a swing phase[13] as seen in figure 5. The gait pattern is typically divided into 7 or 8 'phases', representing moments in time from the sagittal plane for better understanding. The stance phase is when a foot is in contact with the ground, and the swing phase is when a foot is in the air.

The second row in figure 5 represents the ankle angle, defined as the angle between the tibia and the somewhat ambiguous sole axis. This axis is a perpendicular line with the ground, drawn at the ankle joint when the foot is standing on a flat surface. Although this angle is usually 90 degrees, it will further on be defined as 0.

A full gait cycle can, apart from the 7 or 8 phases, also be divided into 3 stages: weight acceptance, single limb support, and swing limb advancement. Taking a closer look at these stages tells us more about the function of the ankle during gait.

Ankle functions

During weight acceptance

The ankle prevents the front of the foot from slamming onto the ground during this stage. The ground reaction force, as a reaction to the weight of body, creates a moment around the ankle when the heel first touches the ground (*figure 4*). The muscles in the ankle typically counteract this moment to enable controlled plantar flexion. However, weak muscles are unable to control the moment, leading to toes slamming onto the ground or even making contact before the heel. An ideal AFO would prevent this by recreating a positive ankle moment to lift the toes before initial contact and to transfer into the loading response phase in a controlled manner.

During single limb support

All the body weight rests on a single foot during this phase. The ankle plays an important role in keeping the person stable during this phase. The foot will need to have full contact with the ground for a healthy gait between loading response and heel off. At the end of this phase, the ankle should aid in pushing off the ground by plantar flexing.

During swing limb advancement

The ankle should prevent toe dragging during this phase. It should help keep the foot in a neutral ankle position to ensure clearance from the ground. Failing to do so will result in plantar flexion of the foot, reducing clearance and causing a larger area of the foot to slam onto the ground at initial contact.

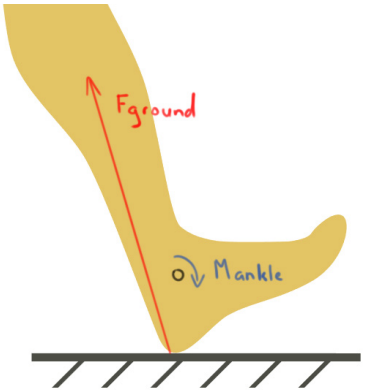

figure 4: ground reaction force (red) and resulting ankle moment (blue) during initial contact

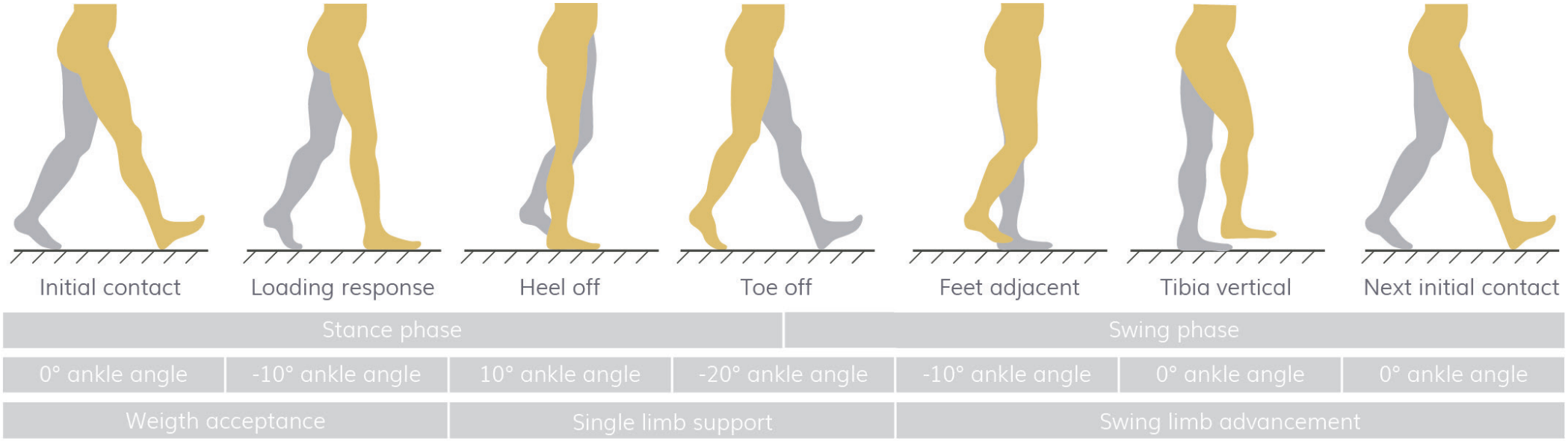

figure 5: Phases of a normal gait cycle

Initial contact	This stance is initiated once the heel of the foot touches the ground
Loading response	When the heel touches the ground, the weight shifts to this foot. The result is that the toes slam onto the ground as well and position the foot flat on the ground
Heel off	The foot dorsiflexes and the weight passes over the ball of the foot. This moment is identified when the heel starts to lift from the ground The
Toe off	Foot plantar flexes and pushes the foot off the ground. The toes lose contact with the ground and the right foot enters its swing phase
Feet adjacent	Both feet are next to each other as seen from the sagittal plane
Tibia vertical	The lower leg is in a vertical position and the foot makes the shape of an 'L'
Next initial contact	The leg touches the ground once again and a new gait cycle begins

PD-AFO working principle

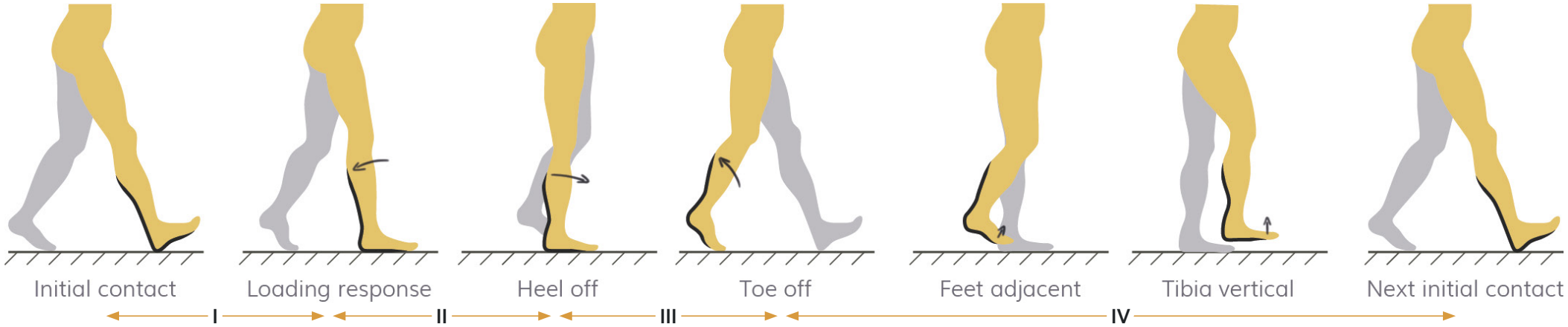

figure 6: Phases of a normal gait cycle whilst wearing an passive dynamic dorsal AFO

An AFO applies forces to the lower leg to maintain the correct position of the foot and ankle during the gait cycle. This is needed when muscles or nerves fail to keep the foot at the correct angle. An AFO is used to stabilise a joint and control its rotation. Typical applications are to limit either dorsiflexion or plantar flexion of the foot depending on the functional needs of the client[13].

Examining the different phases of gait in figure 5, we can draw in a passive dynamic ankle-foot orthosis to better visualize what the AFO is supposed to do when ankle function is impaired (*figure 6*)[14], [15].

Essentially an AFO works by providing the adjustments necessary to come as close as possible to the moment produced by a healthy ankle. It does this through exerting forces on the lower leg and foot that vary in magnitude during gait when the AFO deforms. Passive dynamic AFOs work through storing energy in the orthosis during deformation. This energy storage, combined with changes in ankle angle and body weight distribution, creates either a plantar flex or dorsiflex moment as close as possible to the ankle.

I As seen in figure 4, a negative moment is present in the ankle as a result from the ground reaction force. The AFO will need to create a positive moment to counteract this moment and ensure a controlled transition into the loading response phase.

II The left foot is released from the ground and the full bodyweight is supported on the right leg. As the body moves forward over the foot, dorsiflexion occurs, causing elastic deformation of the AFO, which stores energy and creates a negative moment around the ankle. However, the AFO should not be excessively rigid, as this would restrict dorsiflexion of the ankle and lead to an earlier heel off.

III The foot plantarflexes and the front part of the foot flexes around the metatarsophalangeal joint line. The energy stored in the AFO during dorsiflexion is released creating acceleration and lift. The AFO should not have a big positive moment at this phase, hampering the plantar flex muscles if these are still functional. It should provide a big positive moment if the plantarflex muscles are not functional ensuring a push from the ground

IV People suffering from drop foot will have the front part of the foot pointing downwards during the swing phase. The AFO should provide a positive moment in the ankle to prevent this from happening

The carbon dorsal leaf spring AFO produced by Livit Ottobock Care has another function regarding the knee position of the wearer.

When the client is anlysed it is determined which orthosis will be most suitable for them. Several methods can be used to classify the deviating gait and one such method is the Amsterdam Gait Classification[14], [17]. This classifies five types of gait as seen in figure 7.

Looking at the position of the knees gives us a direction of which AFO might be most suitable. A dorsal design might be more suitable for hyper extended knees as they force the lower leg more forward through the 3 point pressure woring of an dorsal ankle foot orthosis (*figure 8*). A more flexed knee might benefit more from a ventral design as this creates more backwards force that pushes the knee back.

The dorsal leaf spring orthosis will thus only focus on the first three classification types. Within these types, next to the knee position, there is also a difference present in the ankle angle of the foot. The foot contact with the ground is incomplete in gait type three for example. The client in this case tends to walk on their toes. A carbon dorsal leaf spring orthoses can counteract this by making the footplate more stiff. This limits the range of motion around the metatarsophalangeal joints (more on that later) and thus forces the wearer to make more complete foot contact with the ground. This limits the range of motion around the metatarsophalangeal joint line and thus forces the wearer to make more complete foot contact with the ground.

The Amsterdam Gait Classification is a tool that helps identify the needs of the client but is not completely leading in determining the type of AFO, as individual needs and goals can warrant the complete opposite.

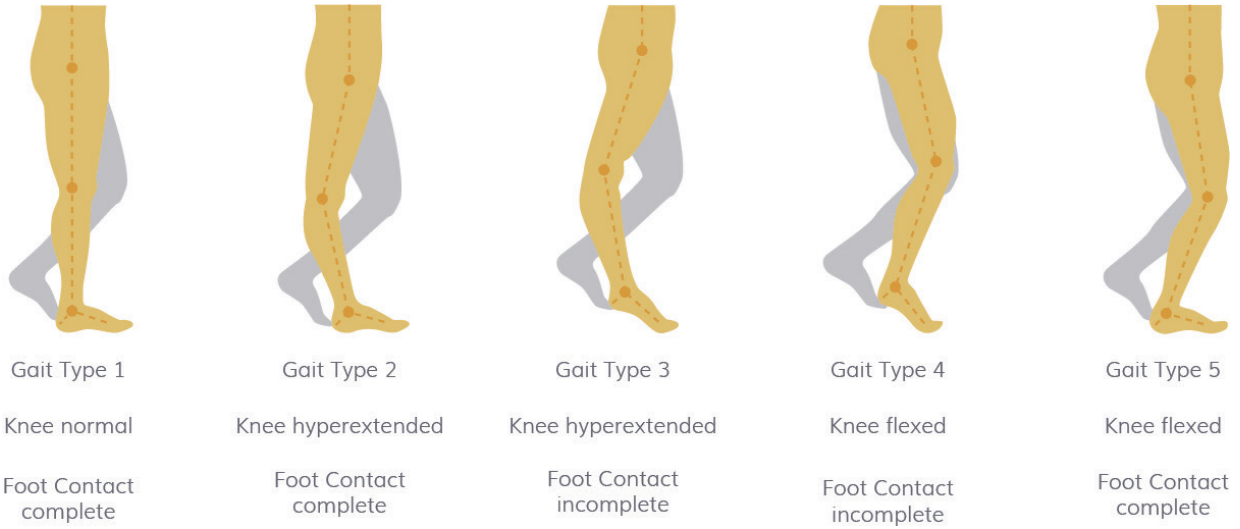

figure 7: Amsterdam gait classification

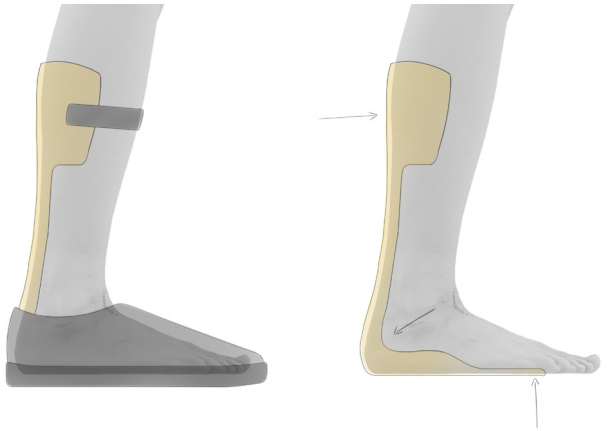

figure 8: An AFO worn with shoes and the resulting 3 point force structure exerted on the AFO during dorsiflexion

Production method

Current production method

Making a custom carbon ankle-foot orthosis consists of several steps. An orthotic device comes into view after it is established by a neurologist or rehabilitation doctor that such an aid is needed for the client's impairment. Other trajectories exist through which a person with walking troubles comes into contact with Livit or another orthopedic adviser without a referral, but these are less common. Usually, the insurance company requires the diagnosis of a specialist to cover the costs.

Livit has over 400 locations throughout the Netherlands[8]. Almost all of them consist of partnerships between local physiotherapists, health clinics, institutes, and orthopedic centers. Each of these locations has one or more orthopedic advisers who are the main contact points for the clients. The orthopedic adviser analyses the customer, takes measurements, and diagnoses the orthopedic needs. This might result in the need for an AFO, but it is not always the case, as orthopedics treat a wide variety of musculoskeletal conditions that have different available treatments such as surgery, botulinum toxin injections, physiotherapy, or occupational therapy[16], [17].

A cast of the foot and lower leg is made if an AFO is desired (*figure 9*). This cast consist of bandages impregnated with a certain soluble that hardens when it come into contact with water. This alternative method is favoured over traditional plaster due to it being considered a more pleasant experience for the customer as it makes less of a mess.

Certain measurements are made along with the cast, which are both marked on the cast and filled in on a digital data sheet. Measurements include the position of the malleoli, the navicular, the tuberosity of the 5th metatarsal, and the joints between the metatarsals and phalanges. These positions are relevant for a comfortable fit and the proper functioning of the AFO[14]. The orthopedic adviser may introduce additional modifications or markings on the cast, guided by their professional judgment. For instance, paste can be added on the medial longitudinal arch for an adjusted fit, or cork insoles can be used for an adjusted heel height.

Livit Ottobock Care currently makes these adjustments either physically on the cast or adjusts them digitally later in the process. It is therefore essential to carefully read the data sheet delivered along with the cast, as inconsistencies are prevalent along with unique requirements desired by the orthopedic advisors. Livit Ottobock Care aims to move towards a more digitized future and thus prefers requests for adjustments to be made through CAD. However, this clashes with the craftsmanship of the orthopedic advisers, resulting in an inconsistent work flow. The transition from physically oriented labour and skill towards digitalization is currently happening at Livit Ottobock Care and is also a key driver for their interest in this project.

Once all the measurements are made, the cast, along with the data, is sent to the production facility located in Dordrecht. Upon arrival, the cast is then digitized using 3D scanning equipment. All necessary adjustments are made in CAD based on the information provided on the datasheet.

The model with its adjustments is then cut out of hard foam using a CNC robot. This new positive representation of the foot is used throughout the production line for the assembly of the AFO. In the case of carbon layered orthotics, preimpregnated carbon layers are applied to the model and subsequently baked for an accurate fit.

figure 9: A cast of the lower leg and foot

Final adjustments, such as adding padding or Velcro fasteners, are made before it is sent back to the orthopedic adviser, who fits the AFO with the customer.

It is common practice to have a fitting meeting scheduled three weeks after the measurements are made. As a result the Livit Ottobock Care production centre adheres to a production timeline of 10 workdays.

An more complete overview of this production process can be found in figure 10.

(on next page) figure 10: Schematic overview of the Livit Ottobock Care work flow analysis of a carbon AFO

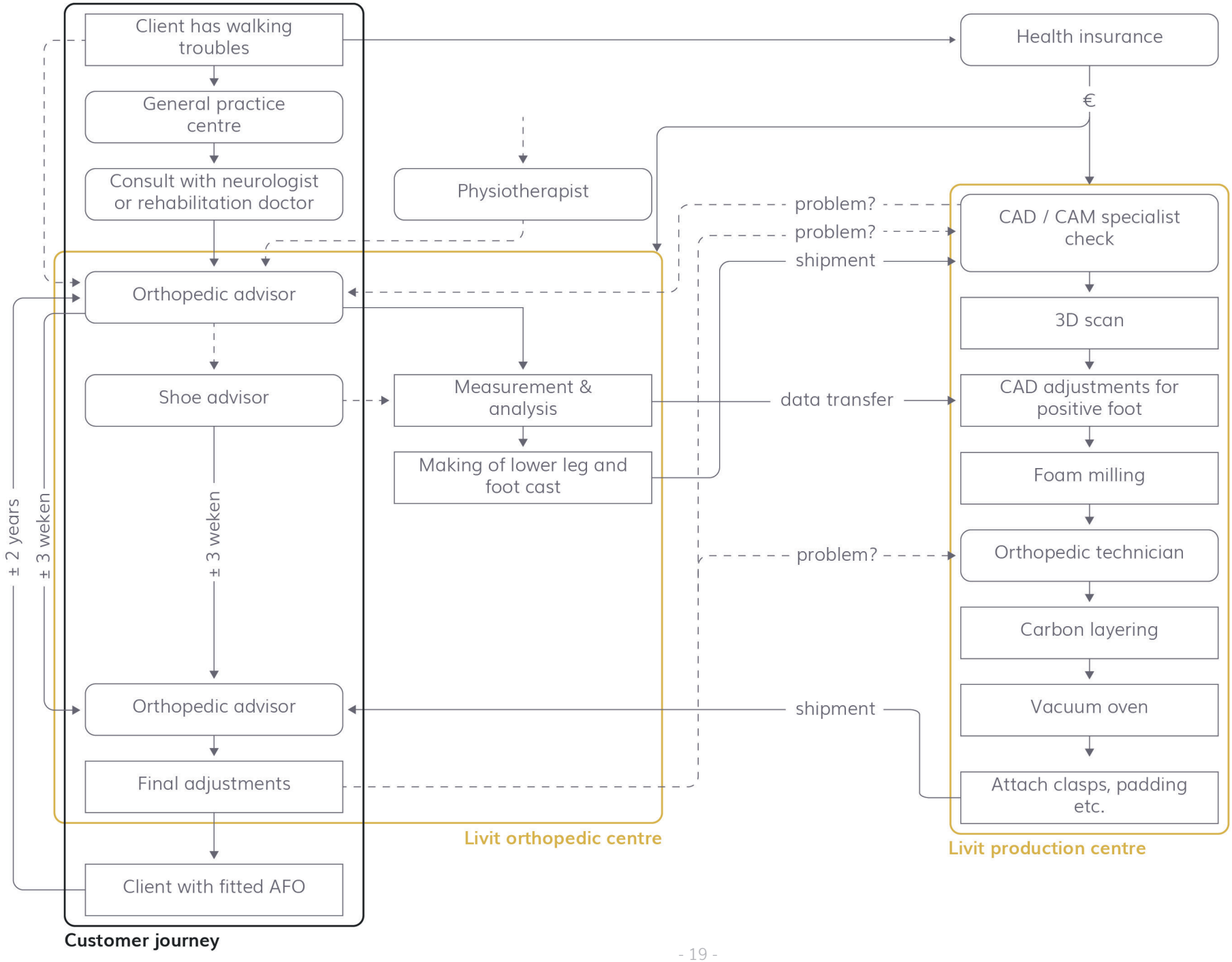
Client has walking troubles
General practice centre
Consult with neurologist or rehabilitation doctor
Physiotherapist
Orthopedic advisor
Shoe advisor
Measurement & analysis
Making of lower leg and foot cast
Orthopedic advisor
Final adjustments
Client with fitted AFO
Customer journey
± 2 years
± 3 weken
± 3 weken
Livit orthopedic centre
Health insurance
€
problem?
problem?
shipment
CAD / CAM specialist check
3D scan
CAD adjustments for positive foot
Foam milling
Orthopedic technician
Carbon layering
Vacuum oven
Attach clasps, padding etc.
data transfer
problem?
shipment
Livit production centre

Production method with Parts on Demand in the loop

This project was set up to further investigate an alternative production method for the fabrication of AFOs. Livit Ottobock Care already has a partnership with Parts on Demand, and they produce various SLS hand braces or leg prosthesis mounts (*figure 11*). The main driver behind this project is the possibility of further eliminating labour-intensive production steps and automating the production process.

During the current production process of AFOs, a CAD model is already made by scanning the casts of all clients. These are consequently digitally adjusted to ensure a better fit, as Livit has a CAD/CAM specialist team employed. These models are currently used for the CNC milling of foam-positive casts.

Having a CAD/CAM specialist team and the digital models of each client already present in their workflow makes incorporating SLS printing in the production chain easier, as fewer intrusive production measures are needed.

Outsourcing the material production to SLS-printed parts over at Parts on Demand would cut out the CNC milling, manual carbon cutting, layering and baking, creating the workflow diagram in figure 12.

With Parts on Demand in the loop, manual labour steps can be reduced, as well as material usage. However, for this option to be feasible, the timeline would ideally be as close as possible to the present one, and the SLS-printed version should have the same functions as the current carbon-layered AFO.

The bottleneck regarding time in this production chain is the shipment. First, the cast needs to be sent to the production facility of Livit Ottobock Care, where it is scanned and digitally adjusted. These digital files can then be quickly exchanged with Parts on Demand, which can produce and ship the SLS-printed parts to the Livit production facility. There, the last adjustments are made and shipped off to the orthopedic advisor on location.

This alternative has to ship the product three times instead of two. Livit Ottobock Care expressed the relevance of producing an AFO quickly to alleviate the customer from its discomfort as soon as possible.

An alternative could be to scan the casts, or better yet: the lower legs and feet of the customers at the location of the orthopedic advisors. This would make the customer information a purely digital transfer that has to be sent to the production facility. However, this is deemed unrealistic at the moment because of the high costs of accurate scanning equipment[5].

All things considered, comparing the current workflow to the proposed new workflow gives an approximation of 7 workdays for Parts on Demand to produce the SLS printed parts.

The current workflow consists of 10 workdays. Counting 1 workday for the CAD/CAM department, 1 workday for the shipment of the SLS printed parts and 1 workday for the attachment of the clasp and padding leaves 7 workdays.

REQUIREMENT

- *"The production time of the SLS printed parts should not be longer then 7 workdays"*

figure 11: A leg prothesis mount designed by Livit Ottobock Care and printed by Parts on Demand

(on next page) figure 12: Schematic overview of a possible workflow alternative with SLS printed AFO parts

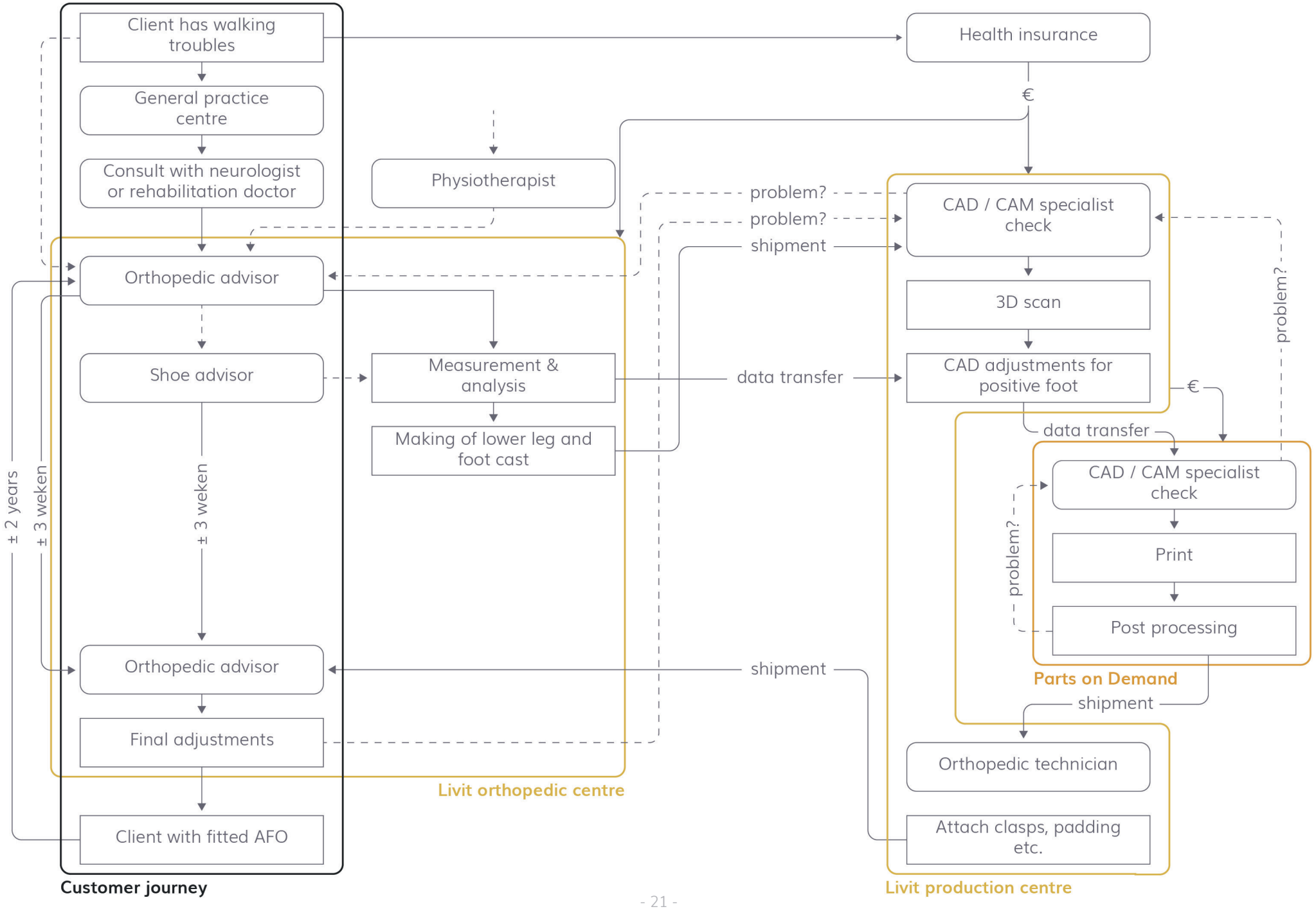
Client has walking troubles
General practice centre
Consult with neurologist or rehabilitation doctor
Orthopedic advisor
Shoe advisor
Orthopedic advisor
Final adjustments
Client with fitted AFO
Customer journey
± 2 years
± 3 weken
± 3 weken
Physiotherapist
Measurement & analysis
Making of lower leg and foot cast
Livit orthopedic centre
Health insurance
€
problem?
problem?
shipment
CAD / CAM specialist check
3D scan
CAD adjustments for positive foot
data transfer
data transfer
€
problem?
CAD / CAM specialist check
Print
Post processing
problem?
Parts on Demand
shipment
Orthopedic technician
Attach clasps, padding etc.
shipment
Livit production centre

Price

A price estimation was made to compare the SLS-printed orthoses with Parts on Demand as the manufacturer in the production workflow. Determining the exact price breakdown of the carbon dorsal leaf spring orthosis produced by Livit Ottobock Care can help determine if an SLS-printed orthosis can be a viable alternative. Price estimates were given based on a hinged carbon ankle-foot orthosis and the carbon dorsal leaf spring orthosis.

CONFIDENTIAL INFORMATION

CONFIDENTIAL INFORMATION

These prices were broken down into estimates for work hours, materials, and miscellaneous costs. The labour hours for the carbon layering process, along with the CNC and correction hours, were cross-referenced with estimated times provided by the carbon layering department[12]. Hourly rates were based on data provided by CBS[19]. Other costs were estimated.

Cost differences described

- More labour hours at the CAD/CAM department for the SLS printed orthosis as extra work is foreseen in modelling the AFO around the scanned foot.
- No labour costs for the carbon layering production step as this is replaced by SLS printing.
- No CNC handling, and processing is necessary as this production step is replaced by SLS printing.
- Less correction time is necessary as there are no carbon layers that need to be cleaned up
- No material costs for the carbon material as this is replaced by SLS printing
- There is no need to mill a positive foam model of the lower leg saving costs as well
- No storage for foam blocks and other materials is necessary. Less electricity costs are necessary as less production steps take place for Livit Ottobock Care.
- Double transport costs are billed. Once for sending the glass fibre cast from the orthopedic advisor to the production facility and once to send the SLS printed parts to the production centre.
- No vacuum carbon oven necessary, no CNC costs

The breakdown of all costs for the hinged carbon AFO can be found in appendix B. The breakdown of all costs for the carbon dorsal leaf spring orthosis can be seen in figure 13. This breakdown is partially based on the figures visible in appendix B as more data was provided for the hinged carbon foot orthosis.

Aspects marked with a green dot are price reductions beneficial to the SLS printed process as they make more money available for the printed parts. Red dots are price increases.

Comparing the current Livit Ottobock price buildup of carbon dorsal leaf spring orthoses to the price buildup replacing the carbon orthosis with SLS printed parts gives an estimated cost difference of around €290,-. This is rounded up to €300,- as the amount approximately available for Parts on Demand to create the printed components if it were to replace the carbon.

REQUIREMENT

- *"The SLS printed parts should cost no more than €300,-"*

SLS printing

Working Principle

Selective laser sintering is an additive manufacturing method and is part of the umbrella term 3D-printing. Like any other 3D-printing technique the model is built layer by layer[6]. SLS is a powder bed fusion process that uses a laser to melt and fuse the powder to form solid parts.

A powder bed is spread out and heated almost to its melting point. A laser then passes over certain sections, solidifying (sintering) certain parts[20]. A new layer is consequently smoothed over the previous layer and a laser passes again to create a solid new layer of the desired part. Repeating this process results in a final component being fully encased in powder.

A small batch takes around 24 hours to print and needs to cool down roughly the same time. The components are subsequently separated from the remaining powder through careful examination and analysis[21]. The powder is recycled for other batches and the parts are cleaned and transferred to be post-processed (if any post-processing steps were specified by the customer)

One of the most important aspects of industrial SLS printing is its possibility to pack multiple prints in one printer. 'Nesting' parts results in more products being produced at the same time (*figure 14*). This better utilizes the full volume available of each batch and makes it more cost-effective. Producing multiple parts at the same time reduces the costs per part. Parts on Demand, therefore, uses specialised software to optimize the density of a print batch.

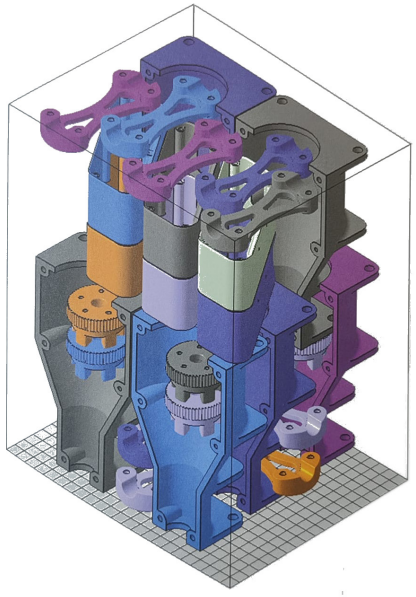

figure 14: Example of nested products in a SLS batch

Having a full batch has a second advantage concerning warping. The machine and prints are hot after when everything is printed. It is essential to evenly cool down a batch to reduce the warping of the prints[21]. Having a full batch ensures a more even distribution of areas being cooled as a batch cools from the outside towards the inside. Because of this, less deformity is present near the centre of a print batch as compared to the edges.

The desire to print a full batch is the main factor that influences delivery times for less-used materials such as TPU and CarbonLW, as several parts need to be queued before a full batch is printed.

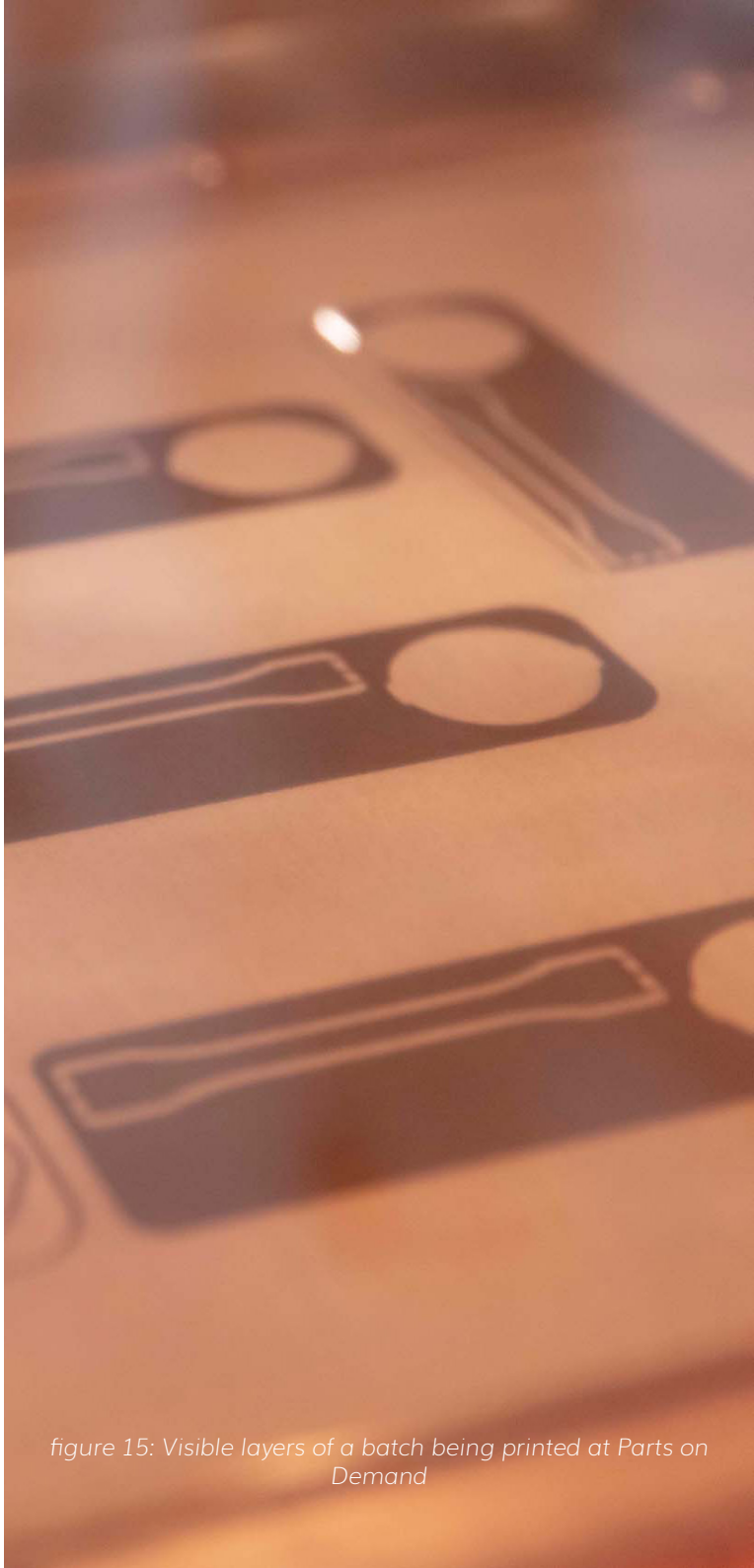

figure 15: Visible layers of a batch being printed at Parts on Demand

Design considerations

A key advantage considering SLS printing compared to other 3D-printing methods such as FDM or SLA is that the parts are surrounded by powder during printing. Designs do not require support or removal thereof for a successful print. A lot of freedom is therefore present in terms of part geometry. However, some considerations have to be kept in mind.

Dimensions

The printers themselves impose a build volume limit of 300x300x590. Parts on Demand has two print volume boxes that are being used. 300x300x290 and 300x300x590. These build volumes are interchanged depending on the demand of the material.

Less frequently utilized materials like TPU are constrained by a smaller build volume, as larger batches cannot be filled completely.

The printer used by Parts on Demand has a laser head of 0,05mm and a layer height of around 0,12mm. The particle size used for most powders is 0,06mm. The laser does not fuse just one particle but melts multiple ones together creating the solid parts. Having these dimensions combined creates a rough texture that can produce parts with a tolerance of +- 0,4mm[21].

Delivery time (work days)	10	7 (or 3~4)*	10**	7 (or 3~4)*	10		
name	PA 640-GSL	PA 2200	PA11GF Black	PA11 Nylon	TPU 1301		CFRP
Common name	Carbon LW	PA12	PA11 Black	PA11	TPU		Carbon Fibre
Color/Appearance	Dark gray	White	Black	Off white			
Density (sintered parts)	820 kg/m^3	930 kg/m^3					1500 kg/m^3
Tensile Strength (XY)	49 MPa	42 Mpa	35 MPa	51 Mpa	7 Mpa		700 Mpa
Tensile Strength (Z)	33 MPa	42 Mpa	32 MPa	47 Mpa			700 Mpa
Tensile Modulus (Youngs) (XY)	3816 MPa	1750 MPa	3450 MPa	1780 MPa			91000 Mpa
Tensile Modulus (Youngs) (Z)	1945 MPa	1650 MPa	3000 Mpa	1720 Mpa			91000 Mpa
Elongation at Break (XY)	3%	7%	9%	46%	250%		
Elongation at Break (Z)	3%	4%	5 %	41 %			
Flexural Modulus (XY)	5040 MPa	1500 Mpa		1800 MPa	60 MPa		
Flexural Modulus (Z)	4313 MPA	1500 Mpa					
Shore D hardness		75	80	72			

figure 16: Material properties of SLS printable materials at Parts on Demand

Orientation

The orientation of prints in the printer is of great influence concerning their properties. An SLS printed part is almost isotropic, meaning they have near equal strength in every direction. However, SLS printing, just like FDM printing consists of slicing each part into layers and building it atop each other. This makes the Z direction the weakest of the three.

Ensuring a stiff and rigid print would ideally have the critical parts where the most strain is present be printed in the X or Y direction of the print bed as it would result in higher strength.

Warping

As stated before, a print batch does not cool down evenly. It is recommended to have an even wall thickness throughout the model to reduce the chance of warping of the print. Having too thin walls (<1,5mm) also tends to warp depending on the height and width[21].

REQUIREMENTS

- *"The bounding box of the SLS printed parts should not exceed 300x300x590mm"*
- *"The wall thickness of the SLS printed AFO should be bigger than 1.5mm"*

Material properties

Currently, there are 5 materials commercially available to print with at Parts on Demand. These materials are PA2200 (referred to as PA12), PA 640-GSL (referred to as Carbon LW), PA11GF, PA11 Nylon (referred to as PA11) and TPU 1301 (referred to as TPU)[21].

Comparing their material properties gives the table in figure 16.

PA12

This is a thermoplastic (nylon) polymer with the formula [(C12H23NO)n. The "12" references the number of carbon atoms present in the molecule. This is the current standard at Parts on Demand and delivery times are therefore shortest[22], [23].

PA11

This is a bio-based plastic is made from castor beans, a renewable material. The name is derived from the polymerization of 11-aminoundecanoic acid, again determined by its molecular formula. The material changes colour through oxidation and is thus only available in a milky white colour unless pigment is used as a post-processing treatment[24].

Carbon LW

Carbon fibre and glass bubble reinforced PA12. The LW in the name stands for lightweight. The carbon particles present in this material are 55±30 microns. This material can not be coloured and is only available in black or dark grey[25].

PA11GF

This is the newest material currently in development by Parts on Demand. It is a PA11 reinforced with glass beads. It builds upon the sustainably sourced PA11 but has a higher strength. It is UV resistant and shrinks less, this makes colour difference less visible and makes it more resistant to wear and tear[26].

TPU

TPU 1301 is a thermoplastic polyurethane designed to be bendable and soft. It is a pliable material with a value of 86A. This makes it potentially suitable for a soft tissue like layer on the inside of the orthosis.[6]

Printed materials vs carbon fibre composite

Comparing the material properties available through printing to the current production material; the carbon fibre composite, visible in the last row of figure 16, gives a big difference in values[27]. Carbon fibre offers great stiffness and strength where the fibres carry the mechanical loads, the woven structure distributes the loads and the resin binds it all together and protects it.

Post processing

A variety of post-processing options are available for SLS printed parts at Parts on Demand. These steps are optional and take place after the desired parts have been printed. Depending on the post-processing steps required, the delivery time extends. These methods mainly influence the aesthetic look and surface finish but also come with slight material property enhancements and certain design considerations.

Shotpeening

The parts have a rough surface texture right out of the printer. Shot peening is an optional post-processing step that ensures a more even, smooth, surface and gives the parts a satin gloss finish[21]. The impact of the polybeads polishes the surface by compressing the bumps on the outside surface. Along with a smooth surface, the parts also have a slightly increased strength and any impregnated colour is more wear resistant because of the denser surface.

However, a part can not be bigger than 250x250x500mm or else it will not fit in the shot peening machine.

Premium Vapour Polishing

Premium vapour polishing (or PVP for short) is a chemical process that causes the top layer of the parts to fuse, creating a smooth surface[21]. In contrast to shot peening, PVP closes all holes and creates a non-porous surface preventing further moisture absorption, bacteria inhibition and making it easier to clean.

To mount the parts in the PVP machine an opening or eyelet is necessary to hang the part from. Also, drainage needs to be considered as the fluid should be able to drip down (*figure 17*).

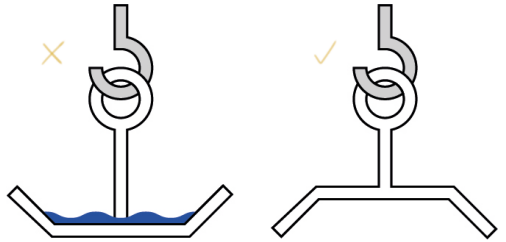

figure 17: PVP design considerations for mounting and drainage

Design considerations for this method are multitude however:

- A cavity is needed to hang the part from
- Ensure the fluid can drain from the part and not accumulate somewhere
- Parts should not be bigger than 300x570x270mm or else they will not fit in the PVP machine
- Uniform wall thickness would ideally be present as variations will lead to differences in surface finish
- Flat parts tend to warp
- The production time is extended with 1 extra workday

Colouring
Parts can also be coloured. The moisture-absorbing properties of SLS printed parts are used here by dipping them in a warm colour bath that impregnates the parts[21]. This colours the outer surface up to a depth of 100 µm to 500 µm.

As this method impregnates the parts, no wall thickness is added and does not need to be considered by looking at tolerances.

The parts can have maximum dimensions of 250x250x500mm and having a part coloured increases the production time by 1 extra workday.

REQUIREMENTS

- "All shot peened parts should not have a bounding box bigger than 250x250x500mm"
- *"All PVP parts should not have a bounding box bigger than 300x570x270mm"*
- *"All PVP parts should have a cavity to hang the part from"*

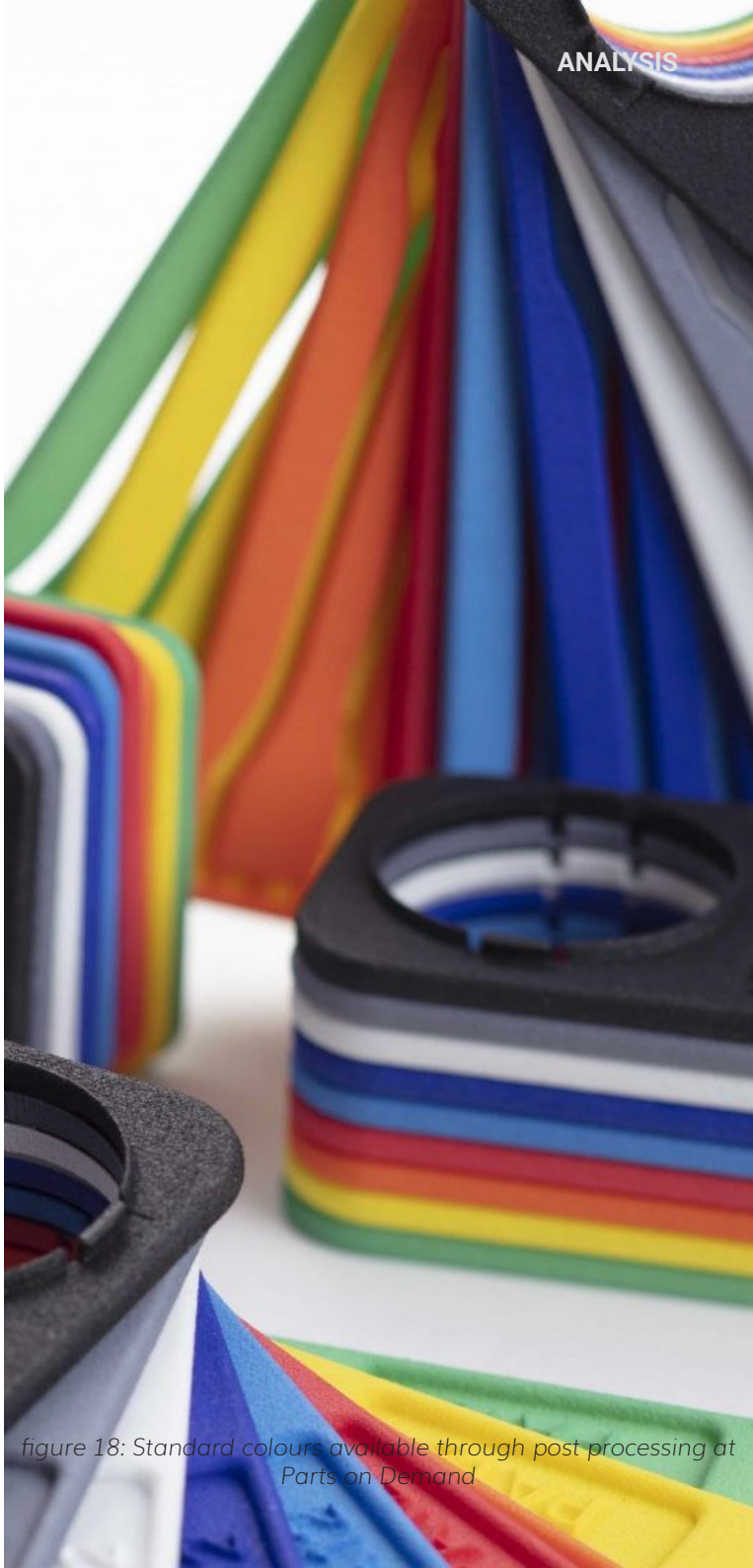

figure 18: Standard colours available through post processing at Parts on Demand

Anatomical requirements

The main consideration for prescribing a custom-made AFO is because of their better fit[14]. Studies looking into the compliance and reception of ankle-foot orthoses reveals dimensions, comfort, weight and aesthetics as the main factors influencing dissatisfaction[28],[29]. Most prominent of these is comfort in the form of concentrated pressure points on the foot, skin irritation, and rubbing of the skin.

A result from these studies also showed the preference to wear conventional shoes bought in normal shops as opposed to specially made orthopedic shoes. This taps into the factor of cosmetical acceptability. For some AFOs, specialized shoes are prescribed but this limits personal expression. This is undesirable as most AFOs can be worn inside shoes if they are designed properly.

It is an orthopedic recommendation to wear one shoe size larger than the measured shoe size for the AFO to fit inside of the shoe[8], [14]. The length with which this increases depends of the magnitude of the shoe size. This ranges from 4 to 6 mm per increment. The average value in this range is taken as a maximum thickness to which the SLS printed AFO has to comply.

Pressure points

As an AFO is worn close to the skin and for extended periods of time. A good fit is essential for user satisfaction and user compliance. In collaboration with Livit Ottobock care and other studies concerning custom-fitted AFOs, certain points of irritation were identified in figure 19[14], [15].

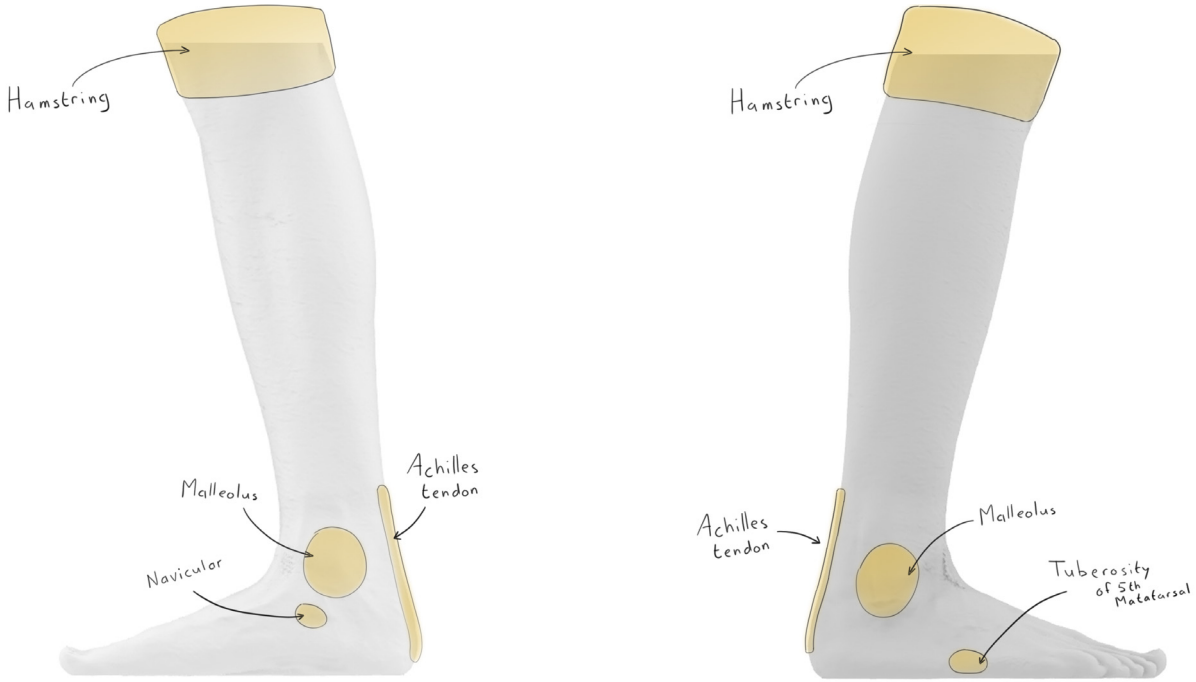

figure 19: Irritation points on foot and lower leg, to avoid direct contact in the sagital plane. Left is from the medial side, right is from the lateral side

In most of these places, bone is present close to the skin which makes applying pressure on it painful. The shape of the AFO can be adjusted taking these ergonomic aspects into mind. These points are known to Livit Ottobock and as mentioned before in the production method chapter are marked on the glass fibre cast by the orthopaedic advisor.

Livit Ottobock Care currently generates the cutlines on their model based on the malleoli positions avoiding these pressure points. For other orthoses where the design can not circumvent these points, distances are specified by the orthopedic advisor to prevent contact.

Accurate measurements and production are essential in the production through SLS printing as no to minimal adjustments can be made once printed. Common adjustments are made when the AFO is delivered to the orthopedic adviser and fitted with the client (*figure 9*). These adjustments can include adding material, for example to the lateral heel arch for more support, or removing material, for example, to better fit inside a shoe. These adjustments are common for regular thermoformed orthoses, but also impossible for carbon-made orthoses. Trimming carbon leaves splintered edges that are deemed too unsatisfactory for the final product. Special consideration is therefore taken in prescribing and measuring carbon orthoses to ensure a perfect fit. The same treatment can be applied to the SLS printed orthosis to ensure the same fit without adjustments at the end.

Range of motion

The ankle angle undergoes continuous changes during gait. In a healthy individual, this range spans from 10 to 20 degrees of dorsiflexion, extending up to 40 degrees of plantarflexion[13]. However, wearing an orthosis restricts these movements. Regardless of the ankle's rotational direction, the elastic deformation of the orthosis generates a counteracting moment opposing the rotation.

When wearing an AFO, it is not possible to achieve the maximum values mentioned above solely through ankle rotation. As explained in the AFO working principle chapter, the ankle is forced into dorsiflexion during single-limb support, and the stored energy is utilized to propel the foot off the ground. In healthy gait, the foot undergoes plantarflexion to the greatest extent possible, creating lift and acceleration. However, wearing an AFO hampers this movement due to the absence of normal muscle or nerve function, leading to a counteracting motion caused by the AFO. Consequently, AFO users experience a more restricted range of motion (ROM) compared to individuals without AFOs.

To determine the ROM while wearing an AFO, various ankle angle gait characteristics are overlapped in figure 20 to assess the ankle ranges possible whilst wearing an AFO. The data used in this figure is sourced from multiple references to provide a representable spectrum of values [15], [16], [49], [50].

It should be noted that the actual ROM is heavily influenced by step size and the stiffness of the orthosis. Larger steps result in greater angles, while a stiffer orthosis leads to reduced angles. Nevertheless, this figure provides a general idea of the typical ROM for an AFO.

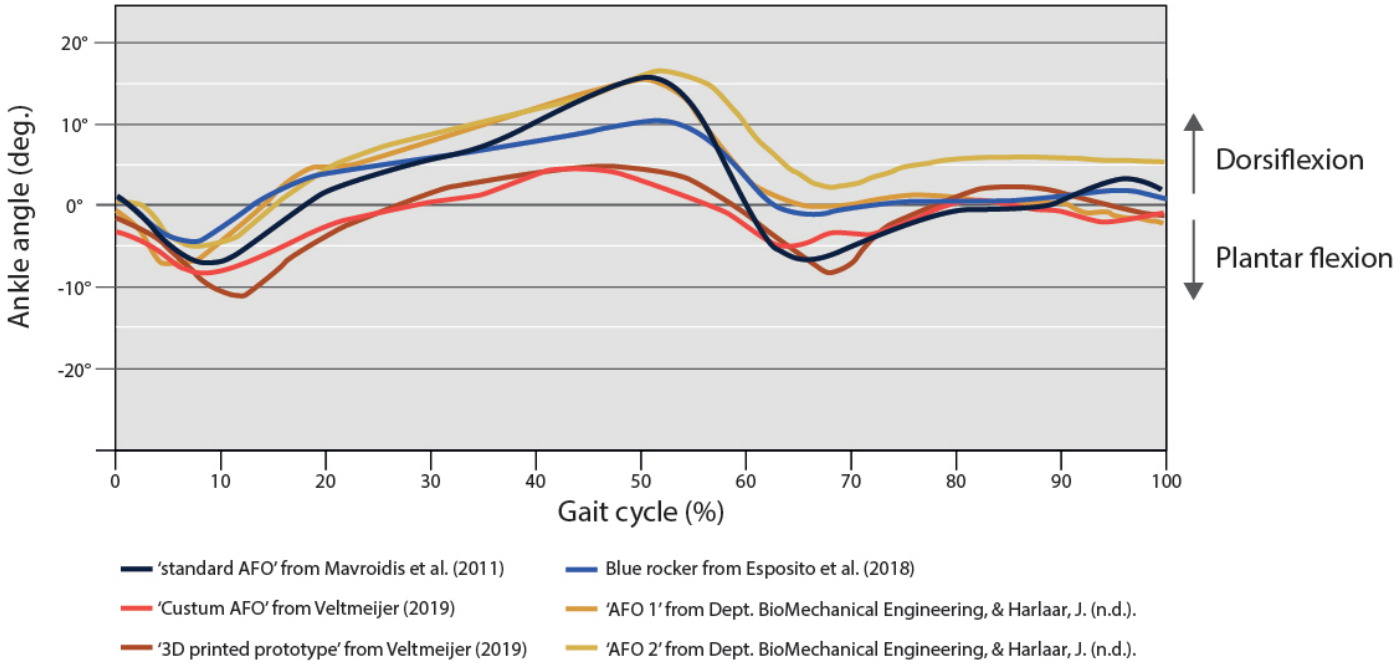

figure 20: ankle range of motion during a gait cycle of various orthoses

Based on the figure, the ROM in the dorsiflexion direction ranges from 5 to 15 degrees, and from -5 to -10 degrees in the plantar flex direction. To ensure that the AFO does not fracture during substantial deformations, a margin of 5 degrees is added to these values. Consequently, it is required that the AFO is capable of achieving 20 degrees of dorsiflexion and 15 degrees of plantarflexion without breaking.

REQUIREMENTS

- *"The AFO should not exceed 5mm thickness around the heel of the foot"*
- *"The AFO should not exert pressure on the Malleoli, navicular and tuberosity of the 5th metatarsal"*
- *"The AFO should be able to bend 15° in the plantar flex direction and 20° in the dorsiflex direction without breaking"*

Biomechanical requirements

When a PD-AFO flexes, it creates a moment. The moment, resulting from plantar flexion or dorsiflexion, can, as stated before, be an aid or impairment to the wearer depending on the magnitude and the phase in the gait cycle. The magnitude of this moment is derived from the stiffness of the AFO and the angle that the ankle makes. The stiffness also influences the achievable ankle angle; a very stiff ankle foot orthosis limits the range of motion of the wearer and thus the possible achievable ankle angle and vice versa.

During abnormal gait, different stiffness values in both positive and negative moment directions are used to time and influence the different phases of gait. It is therefore essential to consider which forces are applied and their respective effects.

Figure 21 shows the plantar flex and dorsiflex moments of various prefabricated PD-AFOs for reference[30].

Plantar flex requirements during swing phase

Plantar flexion is the extension of the ankle angle where the foot stretches. It is the motion where the toes foot points downwards.

There are two requirements for the plantar flex stiffness; it needs to be stiff enough to prevent foot drop during the swing phase but not too stiff to impede the loading response phase.

Looking at the first requirement; a dorsiflex moment prevents the toes from dragging on the ground and providing clearance by creating a force upwards (*figure 22*) through the 3-point fixation of the AFO.

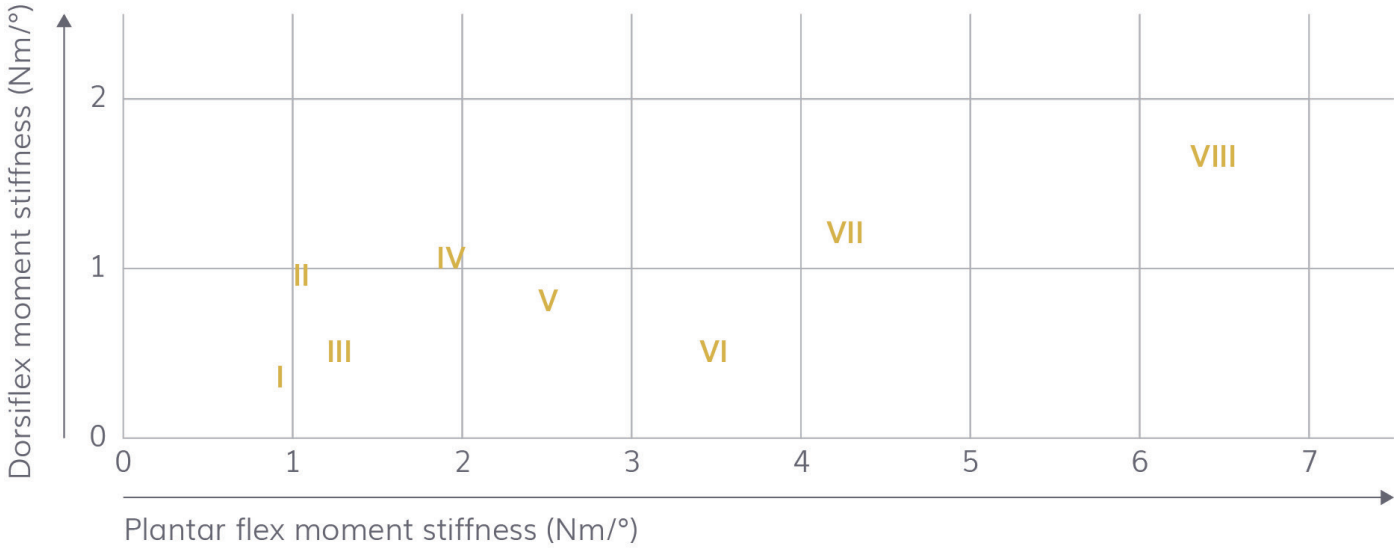

figure 21: Comparison graph of various PD-AFO's plantar flex and dorsiflex stiffness values

I **Walk on Flex**
Dorsiflex moment stiffness: 0,375Nm/°
Plantar flex moment stiffness: 0,95Nm/°

II **Spiral Matrix**
Dorsiflex moment stiffness: 0,95Nm/°
Plantar flex moment stiffness: 1,1Nm/°

III **Matrix**
Dorsiflex moment stiffness: 0,5Nm/°
Plantar flex moment stiffness: 1,3Nm/°

IV **EZ stride**
Dorsiflex moment stiffness: 1,1Nm/°
Plantar flex moment stiffness: 1,95Nm/°

V **AFO dynamic**
Dorsiflex moment stiffness: 0,8Nm/°
Plantar flex moment stiffness: 2,5Nm/°

VI **Ypsilon**
Dorsiflex moment stiffness: 0,5Nm/°
Plantar flex moment stiffness: 3,5Nm/°

VII **Walk on reaction**
Dorsiflex moment stiffness: 1,2Nm/°
Plantar flex moment stiffness: 4,25Nm/°

VIII **Blue Rocker**
Dorsiflex moment stiffness: 1,64Nm/°
Plantar flex moment stiffness: 6,4Nm/°

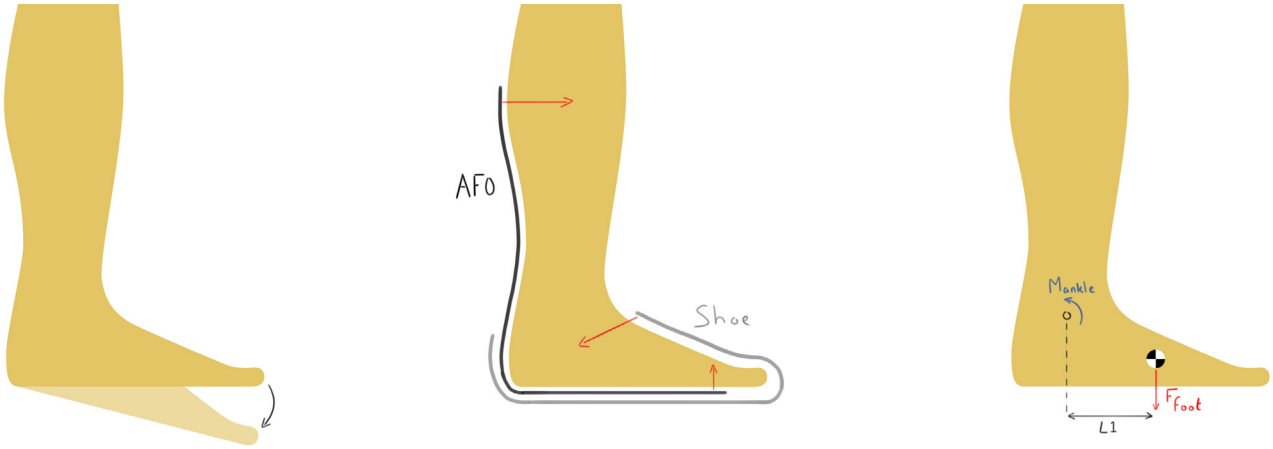

figure 22.1: foot dropping withough support and ankle function, 22.2: forces on the foot as a result from a dorsiflex moment AFO, 22.3: FBD of foot during the swing with counteracting ankle moment

Take the worst-case scenario: the AFO wearer has no muscle strength left in their ankle (*figure 22.1*) The AFO functions in combination with the shoe to provide a positive moment, preventing this from happening (*figure 22.2*). The AFO tries to keep the foot at its neutral angle by exerting forces at the top of the foot through the clamping of the shoe and a force at the sheen through the attachment of the cuff.

The AFO provides the necessary ankle moment during this phase, which can be determined by examining the free body diagram of this scenario in figure 22.3.

Averages can be taken to get a better understanding of the minimally required plantar flex moment during the swing phase to prevent drop foot. According to Plagenhoef et al. (1983)[31], the human foot averages out to around 1.43% of a male's body weight and 1,33% of a female's. Using the same literature to find the average weight of a male (73 kilograms) and female (61,99 kilogram) gives us an average foot weight of 934 grams.

Combining this with a weighted estimate shoe weight of 1kg (3 measurements) makes 1934 grams. This creates a downward force of 19,0N. The centre of mass of the foot is measured to be 1/2 of the foot length as seen from the heelside in the parasagittal plane according to Plagenhoef. Subtracting the approximated distance from heel to malleolus(1/3 foot length) gives a value of L1 of 42,5mm with an average foot length of 255mm among Dutch citizens aged 20 to 60[32]. This would give us a negative moment of 0,8Nm that needs to be counteracted. Determining that it is allowed for the toes to drop 1 cm gives us a stiffness value of 0,36Nm/° through the formula:

$$\frac{moment}{tan^{-1}(toedroplength/footlength)} = stiffness$$

It should be noted that these calculations are based on averages and estimates, and therefore, they may vary for each individual. However, they provide a general idea of the range for this value.

REQUIREMENT

- "The AFO should provide a positive moment of at least 0,36Nm/° during the swing phase"

Plantar flex requirements during initial contact

The stiffer the AFO, the more it helps in toe clearance. However, it would impede in the loading response phase if an orthosis is too stiff in the plantar flex direction. As seen in figure 23[13] the foot plantar flexes on two occasions during a stride. The first time from 0 to 7% during gait resulting in 5 degrees plantar flexion (for this individual) and the second time from 50 to 60% during gait resulting in 25 degrees plantar flexion.

The foot (and worn AFO, if that is the case) is forced into plantar flexion during the first through in the graph. The ankle is close to its neutral position, right before plantar flexion. Once the heel touches the ground, a resulting normal force is applied to the foot (*figure 24*). This normal force is not completely perpendicular to the ground. This is because a forward motion is present during a step. The angle of this ground reaction force is in reality a three-dimensional vector[13], [33]. These forces are exerted on the parasagittal (vertical force), frontal (for-aft force) and transverse plane (mediolateral force) and range in magnitude from +- 116%, 19% and 6% of the body weight. For this thesis, the decision was made to focus on the forces exerted on the vertical forces only as these are of the highest order and have to most influence on the strength and function of the orthosis. This simplification was made due to time constraints.

To better understand the forces exerted at the first through, during initial contact, an FDB was composed (*figure 24*).

The angle theta here is measured to be 99° for this specific subjec[13]. The magnitude of the ground reaction force can be determined by analysing the graph in figure 24.

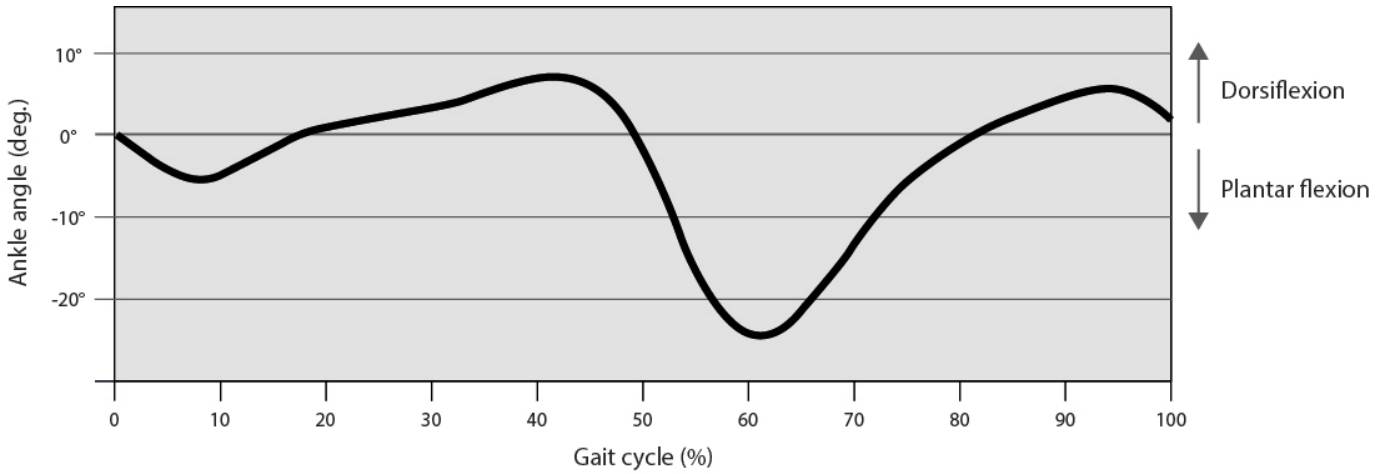

figure 23: ankle angle during a gait cycle

The ground reaction force for this specific case was measured for a step using a Bertec force plate specifically designed for gait, balance and performance analyses. The first peak in figure 24 represents the heel strike phase. This moment of impact is then followed by the first through approximately 20ms later representing weight acceptance. As seen here the ground force present at the heelstrike is bigger than the body weight multiplied by the gravitational constant. Although there is considerable variation between individuals in the magnitude of this force because of factors such as the different ways the foot can make contact with the ground, the walking speed and shoe variables such as its dampening ability, we can take this as an estimate as to what this force might roughly be as it also corresponds with magnitudes from other literature[33].

These measurements were taken with a person weighing in at around 70 kilograms with hard-heeled shoes walking fast. It can be derived from figure 25 that the reaction force can be around 1.4 times higher than just the body weight times the gravitational constant.

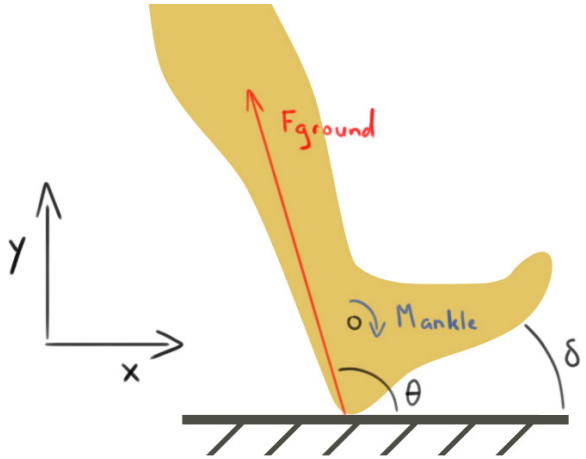

figure 24: FBD at initial contact phase in the parasagital plane

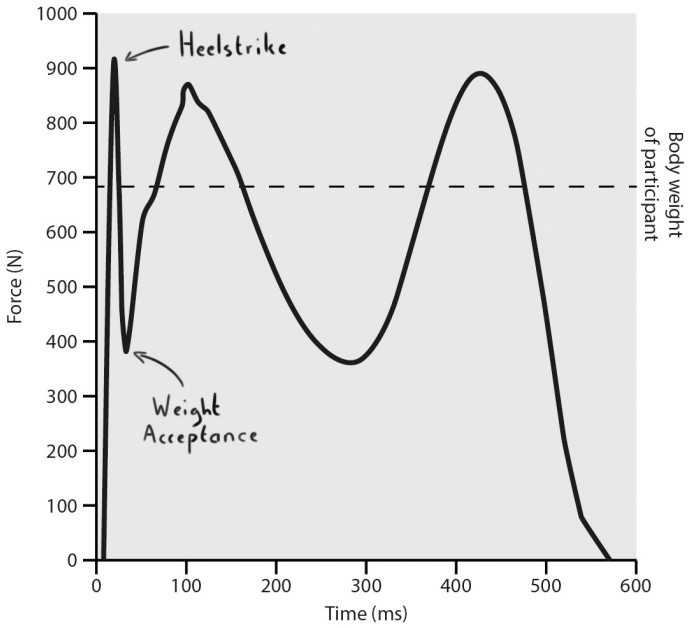

figure 25: Magnitude of ground reaction force during a full gait cycle

Knowing the force and angle the ground reaction force makes with the ground leaves us with an unknown distance from the heel to the ankle joint. This distance varies between the lateral and medial malleolus and of course, between persons. No data could be found for this measurement so an educated guess was made of 35 mm.

To translate this to the x-axis of our FBD in figure 24, the knee and hip angle needs to be known. Again, looking at the literature provided by Whittle[13] it can be read from his graphs that during initial contact the hip angle is approximately 28° and the knee angle 2°. This makes an angle of 26° for delta if the foot is held in its neutral position. This together estimates the plantar flexion angle moment to be 25,8Nm during initial contact.

During this shift, the ankle plantar flexes approximately 6° (*figure 23*) between initial contact and weight acceptance and the ground force is reduced from 900N to 380N. During normal gait, the ankle produces a counter moment to make this shift gradual instead of instantaneous. People without or with limited ankle muscle function or control will thus rely on the AFO to plantarflex 6° whilst having enough stiffness to make this a gradual shift. Therefore, looking at the weight acceptance phase where 380N ground force is present, should not be stiffer than 1.8 Nm/° through looking at the fomula:

$$\frac{\cos(26°) \cdot 0{,}035 \cdot \cos(9°) \cdot 380}{6°} = 1{,}8\ Nm/°$$

Comparing this to the dorsiflex moment values derived from other orthoses (*figure 21*) makes this plausible as no orthosis has a bigger moment than this [30].

It has to be stated here again, however, that this number is based on educated guesses and calculated for a single female aged 22 years old. The values used here differ greatly per person depending on many factors. Therefore it should be used and treated as an estimate to give an idea of what this value would roughly be.

Having a higher value than 1,8Nm/ ° in the plantar flex direction results in a later timed weight acceptance phase. This might feel to the wearer as stiff walking as the range of motion of the foot is reduced. Ideally, the AFO would not limit plantar flexion during both throughs in graph figure 25. It would therefore be ideal to stay as close as possible to the planter flex moment needed to ensure ground clearance of 0,36Nm/°.

REQUIREMENT

- "The AFO should not provide a positive moment bigger than 1,8Nm/°"

Impact requirements

The highest force exerted on the foot happens around initial contact as seen in figure 25. This force is approximately 1.4 times the weight of the wearer, depending on the gait pattern and walking speed[13], [33].
These measurements were taken using a healthy subject and comparing this to AFO users gives the insight that the forces at heel-off are higher and toe-off are lower compared to this graph[33].

As stated before the ground reaction force is in reality split into three components; the vertical force, fore-aft force and mediolateral force. During initial contact, these forces are approximately 1.16, 0.19 and 0.06 times the body weight respectively. The biggest of these is notably the vertical force and creates the biggest impact that the AFO needs to withstand.

The impact during initial contact gathers around the heel and the toes[34]. The normalized maximum vertical force ranges from around 2.5% body weight per cm^2 to 4.5% body weight per cm^2 around the heel according to Hessert et al. (2005) during healthy gait. Comparing this to the force magnitudes derived from Whittle[13] in figure 25 gives a vertical force of 797 Newton on a surface area of $26cm^2$ at the heel for a person that weights 70 kilograms through the formula:

$$\frac{1{,}16 \cdot bodyweight \cdot 9{,}81}{0{,}045 \cdot bodyweight \cdot 9{,}81} = 26\ cm^2$$

Multiplying this force by a factor of 2 to create a safety factor results in the requirement for the AFO to resist a force of 1600 Newton over an area of $26cm^2$ or $62N/cm^2$ around the heel for a person weighing 70 kilograms.

Dorsiflex requirements

Dorsiflexion is the flexion of the ankle angle where the foot contracts. It is the motion where the toes points upwards.

Dorsiflexion of the foot takes place between the loading response and heel-off phase (figure 5) during gait. The AFO deforms and stores kinetic engery in the strut during dorsiflexion as a result from the shifting of body weight in combination with gravity. This energy is then resleased at the end of the stance phase when the body weight shifts to the other foot, elevating the weight used to deform the AFO and consequently releasing its energy.

Several methods to determine the magnitude of this moment were considered based on the research available in this field[30],[48]. However, this field of study ranges wildly and is still considered to be a grey area[16], [48].

Livit Ottobock Care solves this problem by producing the carbon dorsal leaf spring orthosis with predetermined stiffness values regardless of body weight or length. This is a result of set carbon layering patterns and production experience to create a repeatable result. The custom-made orthosis focuses on the custom fit, to ensure the orthosis is comfortable to wear. A custom stiffness for the strut is not considered in the current design.

To determine if an SLS printed alternative is a viable design, it will have to be able to replicate the moments produced by the carbon dorsal leaf spring orthosis to ensure minimally the same function. Having a 3D-printed design can give advantages of custom prescribed stiffness requirements as more form freedom is present. However, as this field of study is still being explored, it is something to keep in mind for the future.

Many different factors influence this moment; stride length, body weight, leg length, foot length, and residual muscle strength. Using set values for these parameters and cross-referencing them to the literature available.

The most promising approach for this value is through measuring the metabolic effort from respiratory measurements conducted with the client. This is then concequently translated into parameter settings ideally controlling an active AFO.

As this field of study is still being explore, the decision was made to exclude it from the scope of this project. Nonetheless, the concept of custom-prescribed stiffness for individual clients should be kept in mind as it is something that is coming for the orthopedic industry and can more easily be acchieved through the use of additve manufacturing techniques such as SLS as compared to carbon layering.

REQUIREMENT

- "The AFO should be able to withstand an impact force of $62N/cm^2$ exerted vertically on the plantar surface of the AFO around the heel"

Metatarsophalangeal joints

The metatarsophalangeal joints are, as the name implies, the joints between the metatarsi and phalangeal bones of the foot[13], [14]. Each foot has 5 of each bone and consequently has 5 metatarsophalangeal joints. A line can be drawn between these joints as seen from a caudal view, commonly referred to as the metatarsophalangeal joint line, or MTP line for short (*figure 26*).

This line is relevant for dynamic orthotic design as flexing through these joints happens around the toe-off phase and helps create acceleration and lift for a healthy gait. This is the second point, next to the ankle joint, where an AFO can create a plantar flex moment to replace muscle loss or deficiency. During dorsiflexion of the toes, the AFO footplate can function as a spring, just like the strut, to store up energy that can be released to assist in lifting the foot at the very end of the toe-off phase. This is typically done by thinning out the carbon layers present around these joints en ensuring a flat surface is present there for flexing without delaminating. It is important to know which geometry is needed here for an ideal moment if the muscles lack the strength.

The current carbon dorsal leaf spring design produced by Livit Ottobock Care can be produced with 3 different stiffness values through this line. These range from very flexible to very stiff.

The stiffness of this footplate part is of great influence on the moment created in the orthosis during toe-off and is dependable on the gait condition diagnosed.

Having a stiffer foot sole ensures a longer arm is present during the toe of which in consequence creates a bigger moment. Figure 27 shows the ground reaction force during a toe-off[35].
A stiff footplate would restrict the range of motion along the MTP line. During toe off the ground force would concentrate more on the further end of the foot sole (*figure 27*). This is a longer arm for the same ground force and would thus create a bigger moment. This would be less with a flexible sole as the ROM along the MTP line is less restricted and the ground force accumulates around this spot. This has a shorter arm and thus a smaller moment.

The stiffness of the footplate is determined by the orthopedic advisors of Livit Ottobock Care and this can be done based on multiple reasons. Knee position is a key influence here as explained before on page 17. Looking at the Amsterdam Gait Classification again: a hyperextended knee needs a flexible footplate to minimize the moment forcing the knee backwards. Having a flexible footplate would place the ground reaction force closer to the ankle, reducing the moment (*figure 27*). A flexed knee would need the opposite.

Another consideration could be concerning toe walking. This is common among clients suffering from cerebral palsy. A stiff footplate would prevent the wearer from being able to walk on their toes forcing them to use the full plantar surface of the foot to make contact with the ground.

This would limit the ROM through the MTP line, but ultimately help the client have a more healthy gait. This exemplifies that AFOs are about maximizing benefits and minimizing drawbacks. There are always trade-offs to be made and it is therefore essential to carefully specify the individual clients shortcomings and goals.

REQUIREMENT

- "The AFO should be able to provide variable stiffness along the MTP line"

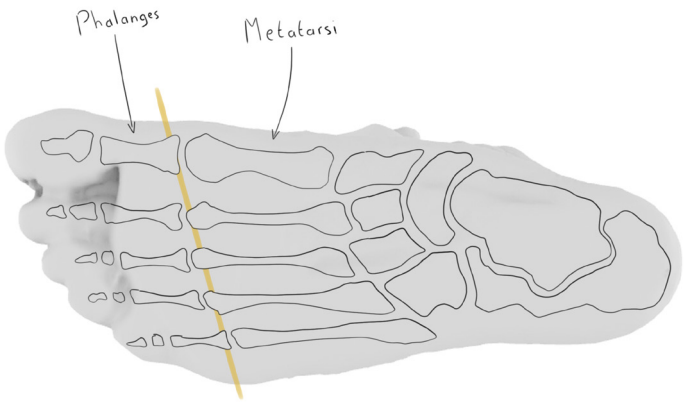

figure 26: Approximate MTP line of the right foot.

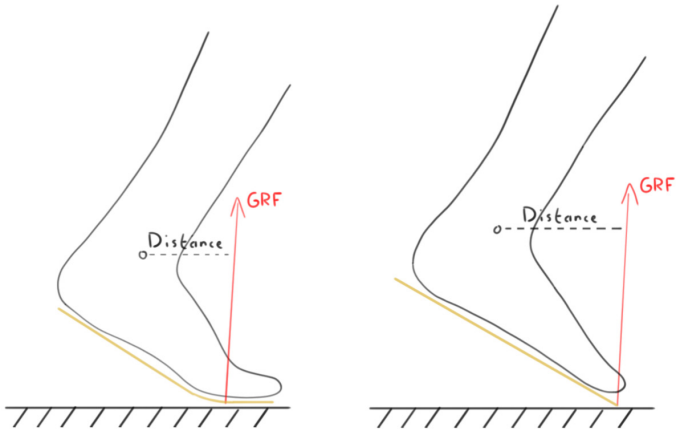

figure 27: influence of MTP stiffness. Longer distance from the ankle results in a bigger moment

Carbon dorsal leaf spring measurements

Strut measurements

Measurements were taken with a carbon dorsal leaf spring AFO provided by Livit Ottobock Care (*figure 28*). The defined main criteria that the SLS-printed AFO has to comply with is that it can deliver the same stiffness values as conventionally made carbon-layered AFOs.

Livit Ottobock Care currently does not quantify the stiffness values present in their orthoses. This is presumably true for the majority of the orthopedics industry as a whole[16]. Stiffness values are currently prescribed in the number of carbon layers necessary for the AFO being made. This is a set amount for the carbon dorsal leaf spring orthosis. This results in an AFO that is received satisfactorily.

To replicate the stiffness of this orthosis a baseline needs to be set. However, No universal standards exist for quantifiably measuring AFOs. Several setups can be found in other literature[4], [36], [37], [38] that were mimicked in a self-made comparable setup. In these setups two variables need to be measured; the displacement at the point where force is applied and the displacement at this point. Knowing the length of the sample can give us the stiffness through the formula:

$$\frac{Force \cdot Armlength}{Angle} = Stiffness\ (Nm/°)$$

This setup and its results can be found in appendix C. However, better more accurate results were generated using a device called the Bi-articular Reciprocating Universal Compliance Estimator or in short: BRUCE (*figure 29*). With lacking standardization, Prof.dr.ir. J.Harlaar from the department of biomechanical engineering, who helped in the development of this device, recommended using this device as it was specifically designed to evaluate ankle foot orthosis characteristics[37].

figure 28: Reference carbon PD-AFO provided by Livit Ottobock Care

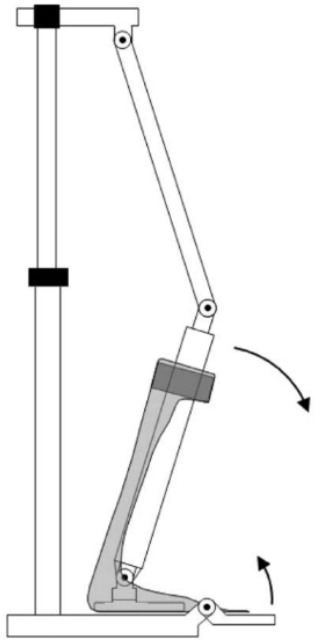

figure 29: Schematic overview depicting the working of BRUCE

Using the BRUCE to determine the stiffness of the dorsal leaf spring orthosis provided by Livit Ottobock Care gives the graph in figure 30. An average stiffness can be derived from the BRUCE measurements of 1,16Nm/°.

Only isolating the dorsiflex stiffness gives a value of 1,23Nm/° and 1,14Nm/° in the plantar flex direction. Both are almost completely linear. These are the values to aim for in the SLS printed variant.

It has to be noted that the neutral or shank vertical angle of this AFO is not 0. The BRUCE measures the angle relative to 90° from a perpendicular point to the footplate. It can be derived from the graph that the neutral angle of this specific AFO is 5,93 degrees.

REQUIREMENTS

- *"The AFO should be able to provide a linear negative moment of 1,23Nm/°"*
- *"The AFO should be able to provide a linear positive moment of 1,14Nm/°"*

MTP line measurements

The BRUCE setup is also capable of measuring the stiffness through the MTP line. However, the test conducted at the UMC in Amsterdam utilized a setup that was unable to perform these measurements. Therefore, the MTP values visible in Appendix C, obtained from measurements conducted using the home setup, were used as substitutes. These values were calculated using the same formula as previously stated:

$$\frac{Force \cdot Armlength}{Angle} = Stiffness\ (Nm/°)$$

Mapping out the calculated moment and angle values produces the graph shown in figure 31. Fitting a trendline with an R2 value of 0.963 results in the linear black line, representing the average measurements, with a stiffness coefficient of 0.24 Nm/°.

As previously mentioned, the carbon dorsal leaf spring orthosis can be manufactured with three different foot soles, each offering different levels of stiffness. The specimen provided by Livit Ottobock Care was equipped with the second stiffest MTP line, indicating the availability of a stiffer foot sole and a less stiff footplate.

Being able to achieve this stiffness also means that less stiff footplates can be manufactured by reducing its thickness. However, it has to be tested in too thin footplates would not result in fracture or plastic deformation.

REQUIREMENT

- *"The AFO should be able to provide a moment through the MTP line with a value of 0,24Nm/°"*

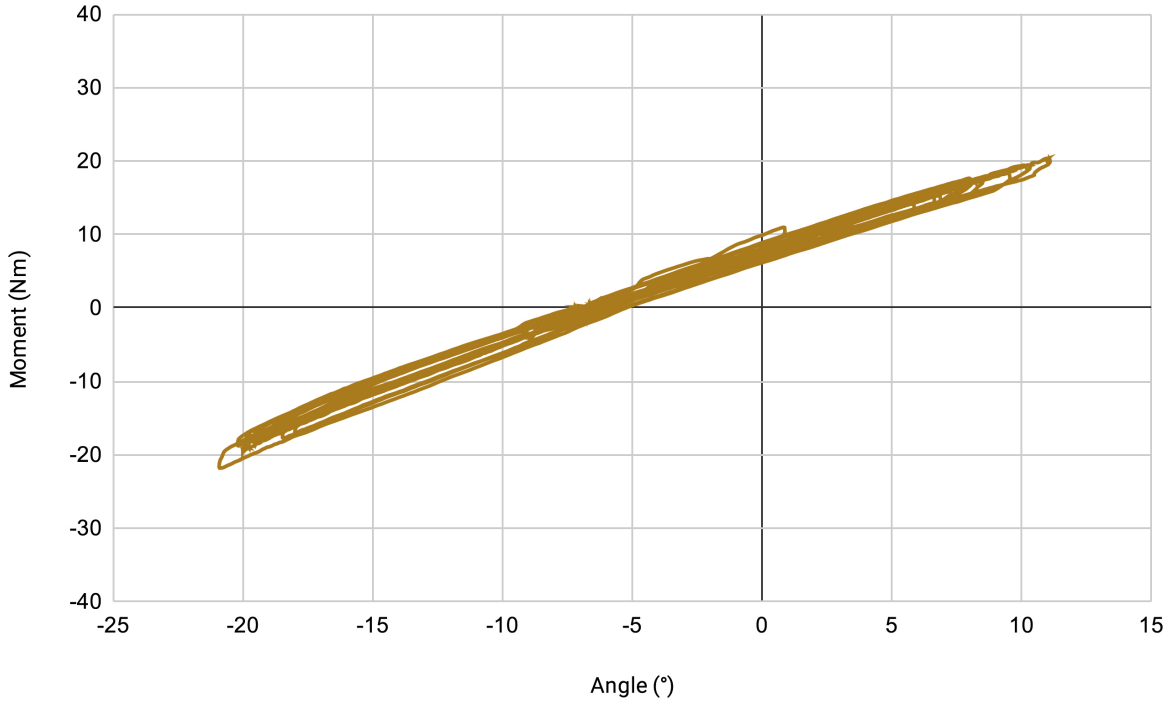

figure 30: BRUCE stiffness graph of the dorsal leaf spring AFO provided by Livit Ottobock Care

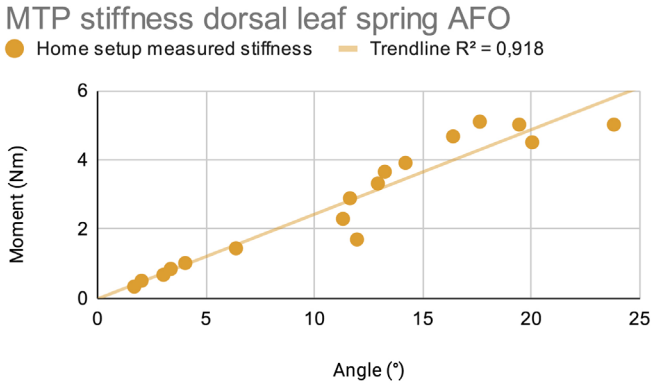

figure 31: Measured MTP stiffness dorsal leaf spring AFO

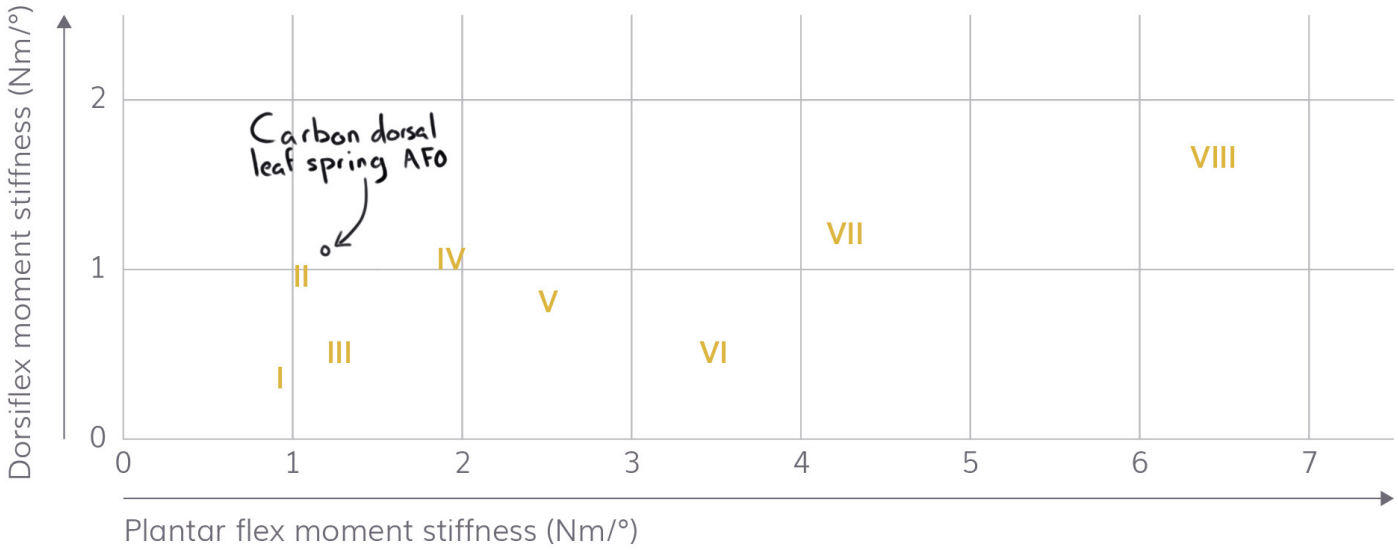

figure 32: Comparison graph of various PD-AFO's plantar flex and dorsiflex stiffness values with the carbon dorsal leaf spring AFO produced by Livit Ottobock Care

Comparing the measured stiffness of the carbon dorsal leaf spring AFO to the other passive dynamic AFOs previously documented in Figure 19 places it on the lower end of the stiffness spectrum (*figure 32*).

This outcome was expected, considering that an estimated 85% of the carbon dorsal leaf spring orthoses produced by Livit Ottobock Care are intended for children[12], [14]. Generally having a lower weight and length makes the stiffness requirements of this orthosis lower.

SLS printing orthoses requiring higher stiffness values might be achieved as a continuation of this project, but is currently not considered. Designing SLS orthoses with higher stiffness values only becomes relevant once an orthosis with lower stiffness values, such as the carbon dorsal leaf spring orthosis, is validated.

List of requirements

Key takeaways are listed in previous chapters. They are composed here in the list of design requirements to evaluate the SLS printed AFO. They also serve as starting points for the ideation phase of the project.

Mechanical

- *"The AFO should be able to provide a linear positive moment of 1,23Nm/°"*

evaluate through BRUCE measurements; results should be within 10% range

Comments This is a variable ideally tailored per person but for the carbon dorsal leaf spring orthoses a set value. Achieving this baseline evaluates if SLS-printed orthoses can be a viable alternative to carbon layer orthoses

- *"The AFO should be able to provide a linear negative moment of 1,14Nm/°*

evaluate through BRUCE measurements; results should be within 10% range

Comments This is a variable ideally tailored per person but for the carbon dorsal leaf spring orthoses a set value. Achieving this baseline evaluates if SLS-printed orthoses can be a viable alternative to carbon layer orthoses

- *"The AFO should be able to provide a moment through the MTP line with a value of 0,24Nm/°"*

evaluate through Measurements with BRUCE like testing setup. results should be within 10% range.

Comments Lower values will also have to be possible, but will most likely be more easily achievable. One stiffer value will have to be possible as well but is currently unquantifiable.

- *"The AFO should provide a negative moment of at least 0,36Nm/° and at most 1,8Nm/°"*

evaluate through BRUCE measurements; results should be within 10% range

Comments The bottom line for the AFO to measure against is a positive moment of 1,14Nm/°. However, more ideally this value would be lower if the complex geometry of SLS prints would allow it

- *"The AFO should be able to withstand an impact force of 62N/cm^2 exerted vertically on the plantar surface of the AFO around the heel"*

evaluate through Strength simulations, and user testing. Ask a participant to jump whilst wearing an SLS-printed AFO

Comments The AFO should not plastically deform during these tests, show no fracture lines or display any defects during normal use.

Ergonomical

"The AFO should not exert pressure on the malleoli, navicular and tuberosity of the 5th matatarsal"

evaluate through A user will have to be able to wear the SLS-printed AFO without expressing discomfort at these points. Avoiding these points will have to be taken into account whilst designing the AFO.

Comments These boneparts are located close to the skin. Without tissue as a cushion to distribute pressure, direct contact with an AFO will be experienced as uncomfortable

"The AFO should not exceed 5mm thickness around the heel of the foot"

evaluate through Measurements; the thickness of the orthosis 3 cm below the malleoli, is not allowed to be thicker than 5mm.

Comments Approximate 1 EU footsize difference. A bigger shoesize is considered undesirable as it will influence the fit

"The AFO should be able to bend 15° in the plantar flex direction and 20° in the dorsiflex direction without breaking"

evaluate through BRUCE measurements; reach the angle without breaking

Comments The real use case scenario will most likely not reach these angles, but the AFO should be able to make these bends without breaking as a precaution

Material

- *"The AFO should operate within its elastic deformation range"*

evaluate through FEA simulations and BRUCE displacement measurements within the range of motion of the AFO

Comments The maximum concentrated strength occurring in the orthosis will be determined using FEA and compared to the yield strength of the printable materials to determine if plastic deformation takes place

- *"The bounding box should not be bigger than 250x250x500mm for shotpeened parts and 270x300x570 for Vapour Polished parts "*

evaluate through Measure bounding box of SLS printed parts

Comments Bigger dimensions are printable in combination with these post-processing steps but come with drawbacks such as it either being done by hand or having marks for attachment in the PVP machine. This is considered undesirable by Parts on Demand and would increase the costs.

- *"The wall thickness of the SLS printed AFO should be bigger than 1.5mm"*

evaluate through Digital thickness analysis though measurements made in Solidworks

Comments A spot to carefully consider is the footplate thickness around the toes. It might require thicknesses close to this value which are prone to warping.

- *"All Vapour Polished parts should have a cavity to hang from"*

evaluate through Geometry evaluation

Comments A cavity and proper drainage is required for a vapour-polished part. It is necessary to have a spot to hang the part from which would otherwise result in markings on AFO that show where a clamp is attached

Miscellaneous

- *"The production time of the SLS printed parts should not be longer then 7 workdays"*

evaluate through Validate delivery times Parts on Demand and possibly calculate express delivery fees

Comments This is needed for the SLS orthosis to be a competitive alternative to carbon-layered custom AFOs currently produced by Livit Ottobock Care. The shorter this time is, the better

- *"The SLS printed parts should cost no more than €300,-"*

evaluate through Use costum pricing tool of Part on Demand for instant quotes on printed parts

Comments This requirement is needed for the AFO to be a competitive alternative to carbon-layered custom AFOs currently produced by Livit Ottobock Care.

SYNTHESIS

Ideation

Divergent ideas were generated based on the specified requirements for the SLS-printed AFO. These ideas explore various design directions and serve as orientation for the use of external components, shape definition or printable opportunities. These ideas emerged during the analysis phase as a result through conversations with stakeholders, mind mapping and simple 'how to'exercises.

The ideas are consequently clustered into more concrete design directions and discussed with both clients to gain insights.

For a comprehensive overview, all the ideas can be found in Appendix D.

The ideas could be categorized into several groups:

Using orthotic semi-finished products

This group consists of orthoses that combine components already in use by Livit Ottobock Care. They use various externally sourced products in their orthotic designs to provide various functions. These products include hinges, rods, or prefabricated carbon shapes.

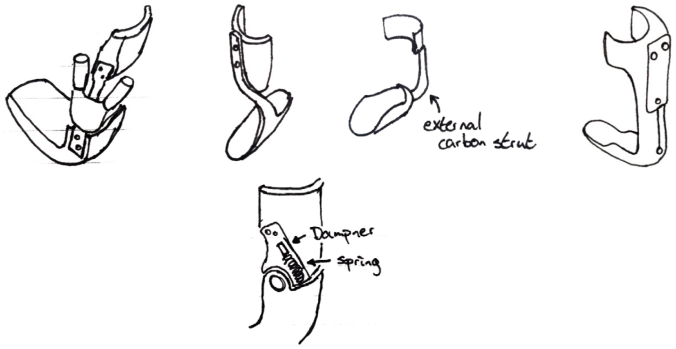

The preference was expressed during discussions with Livit Ottobock Care to avoid using prefabricated parts produced by their partners. The reason behind this concern is the manual manipulation of the attachment rods required for mounting the hinges. TThe parts supplied by external suppliers are strictly bound by contracts that state that they can only be used alongside the delivered attachment materials. While it is possible to modify this procedure, based on previous experience with carbon-layered orthoses, it was discovered that the attachment points for bolts, rivets, or other fasteners are the most critical areas where stress is concentrated. It was also notes as an issue that these connections loosen over time, causing the orthoses to rattle[39]. Using these components would give a lot of control regarding the stiffness behaviour of the orthosis as these are set and tested thoroughly by the manufacturers. The SLS printed parts would function mostly to facilitate a good fit in this scenario.

Springs

This group consists of ideas utilizing the pushing or pulling properties of springs to modify the ankle moment. These external components can aid in delivering the correct ankle moment if the material stiffness of SLS-printed parts prove to be insufficient.

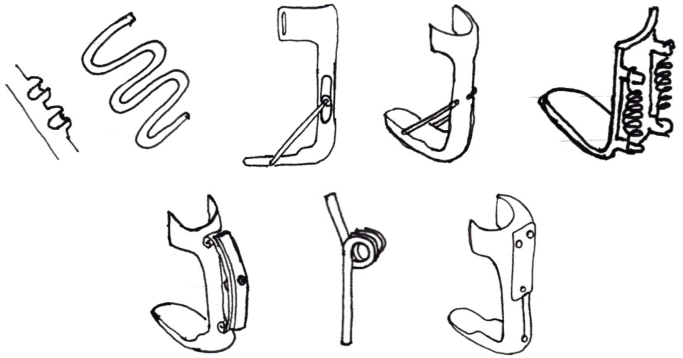

The strut of the current orthosis functions as a spring. Adding an additional spring would potentially increase the moment generated when the AFO deforms. However, it must be kept in mind that a slim and lightweight design is considered desirable. It might also prove difficult to fit a spring incorporated in the AFO inside he shoe, whilst placing it outside of the shoe might prove noticeable[15].

SLS geometry alterations

This group consists of ideas aimed at altering the stiffness of the orthosis by modifying the geometry of the SLS-printed parts.

Compared to carbon-layered orthoses, SLS-printed parts do not delaminate, providing more design freedom. Manipulating the geometry of these parts can significantly impact the stiffness of the orthosis. It is important to note here that the material properties of SLS printed materials are considerably lower compared to that ofcarbon-layered composites. Therefore, the challenge with this design direction would be to ensure the orthosis has sufficient strength to withstand deformation and deliver the required moment whilst remaining a competitive alternative to the carbon dorsal leaf spring orthosis. Using excessive material might result in increased costs, a design that cannot fit inside of a shoe or a heavy orthosis that all have to be considered.

External strut stiffness support

This group consists of combining externally sourced materials in combination with SLS prints to provide strut stiffness and consequently influence the ankle moment.

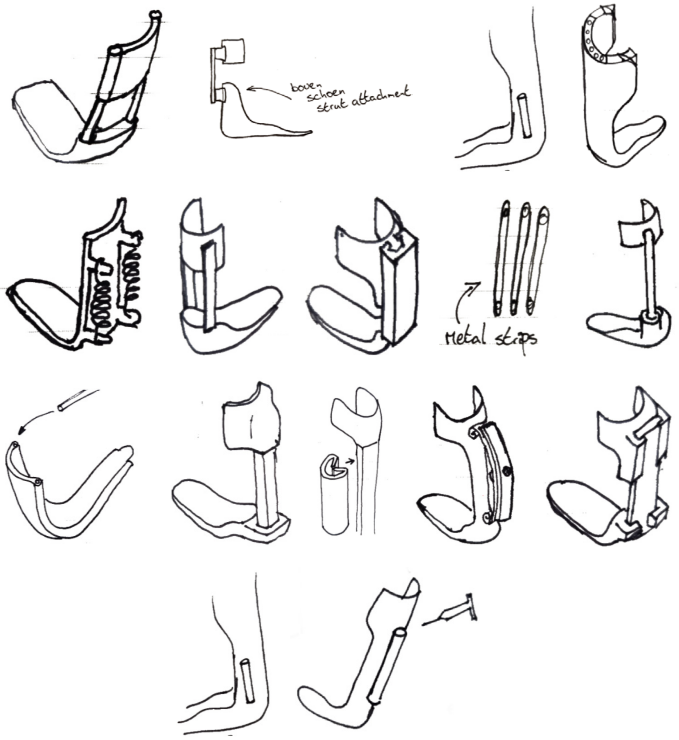

An externally produced strut could give more control over the stiffness characteristics of the AFO. The material of this component would have to be flexible and stiff, which quickly points to a carbon composite. Using external elements will likely result in connection points. It was stated as an irritation point that these connections loosen up over time, rattling the orthoses, which is deemed undesirable[39]. However, dividing the orthosis into several parts could be beneficial for the orientation of the printed parts to have the most strength.

Miscellaneous

This group consists of other ideas not easily grouped. They touch on different interesting AFO design aspects that can be interesting to keep in mind.

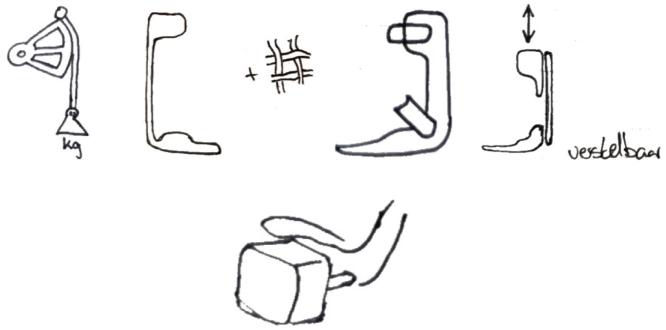

These ideas have the potential to be integrated with other ideas. They provide more radical design directions such as making an active orthosis instead of a passive orthosis or using counterweights to produce an ankle moment. These ideas provide possibilities to alternate the moment produced by the AFO independable of the SLS printing technology. However, they might be more feasible due to the bigger form freedom of SLS printing as compared to carbon layering which might facilitate the incorporation of such ideas better.

To better discuss the different ideas, three models were composed and compared to effectively communicate the various directions this project could take with Livit Ottobock Care. They expressed relevant factors to consider when fabricating an orthosis, such as costs, production time, behaviour, and longevity. These models were formed to probe which aspects were deemed most relevant and serve as conversation points to determine what could work and what would not.

The preference was expressed to keep the design as slim and light as possible without compromising the stiffness behaviour. At the same time, the connection points between parts were identified as critical areas prone to potential fracturing based on past experiences. Working with these connections would also result in increased thickness at these points, which needs to remain at a minimum.

The decision was made to focus mostly on the geometry alterations of SLS printed parts, as this could be considered a major advantage of this production technique. Emphasizing this aspect strengthens the connection between personalized orthotic design and SLS printing. This also showcases the potential of this technique, which is deemed desirable by Parts on Demand.

This could potentially result in a solid one-piece printed design requiring minimal assembly. Having it made from one piece would increase its elegance, which is expressed as important by Livit Ottobock Care.

The main concern remains whether the SLS-printed AFO would be able to provide the desired stiffness without fracturing or becoming too bulky to be considered acceptable.

Design direction 1: Prefabricated carbon layered strut with SLS printed footplate and cuff

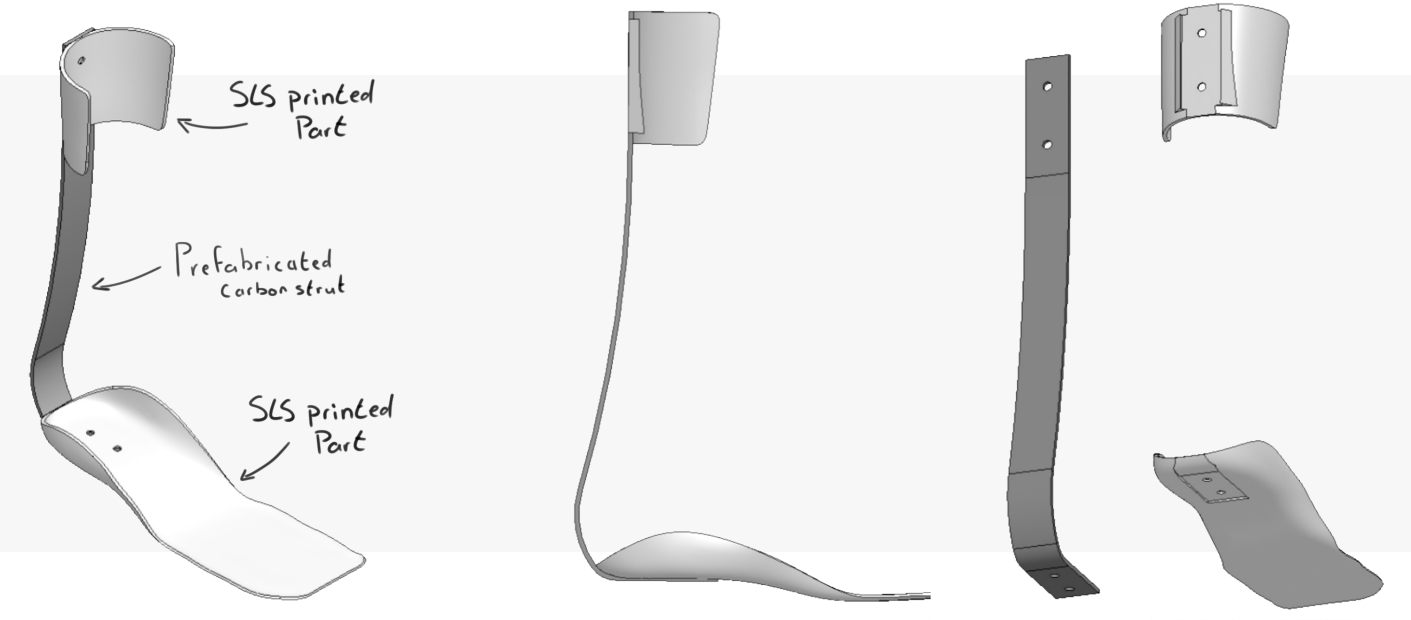

Estimated weight prints: +- 100 grams (excluding strut and connections)
Estimated price prints: +- €100,- (excluding tax, strut and connections)

Pro's
- Full stiffness control using prefabricated carbon layered strut component, available in different thicknesses produced by Ottobock[40].
- Print orientation of parts can be ideal to ensure the highest stiffness value possible
- Smaller print volume, resulting in lighter weight and costs

Con's
- Prefabricated struts are only available in 7° outwards rotation, This might not suit all wearers.
- Attachment points to the footplate SLS printed parts are under the plantar surface of the foot. This can not be thicker than 5mm, making this connection critical
- Connections that concentrate stress and can get loose

Design direction 2: SLS printed AFO consisting of multiple pieces

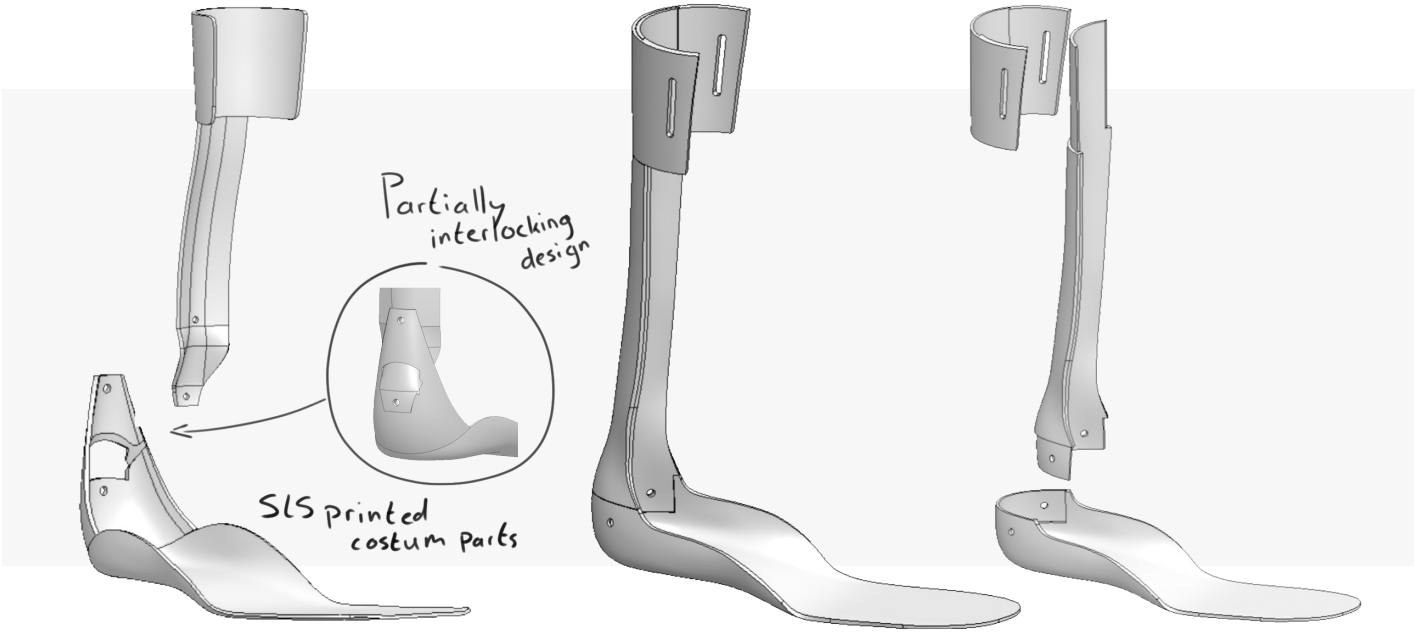

Estimated weight prints: +- 270 gram (excluding connections)
Estimated price prints: +- €150,- (excluding tax and connections)

Pro's
- Print orientation of parts can be ideal to ensure the highest stiffness value possible
- Divided over multiple parts makes it easier and quicker to print
- A part can more easily be replaced if it breaks

Con's
- Connections that concentrate stress and can get loose
- Assembly required that can result in increased production times

Design direction 3: One piece SLS print

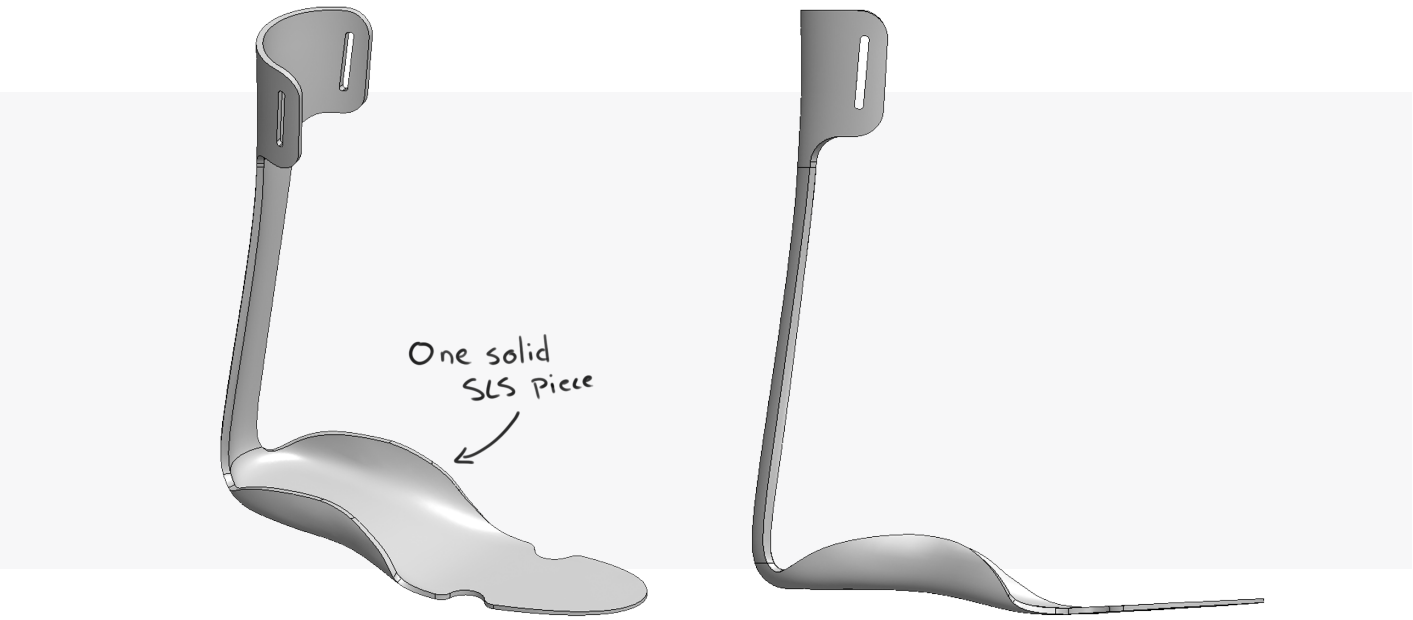

Estimated weight prints: +- 250 gram
Estimated price prints: +- €235,- (excluding tax)

Pro's
- Less concentrated stress points, forces are more equally divided over the body
- Less assembly required
- More slim, solidly perceived design

Con's
- More expensive
- In general harder to print
- Slightly less stiff around the strut due to the impossibility to orient the strut perpendicular to the X or Y axis in the printer

Form orientation

AFOs can be manufactured in all shapes and sizes. SLS-printed AFOs have the added benefit of being bound to fewer restrictions compared to carbon-layered AFOs.

A form exploration was conducted to find a desirable shape that could potentially aid in providing an ankle moment without adding too much material. These forms were drawn taking the critical irritation points, as defined on page 28, into account.

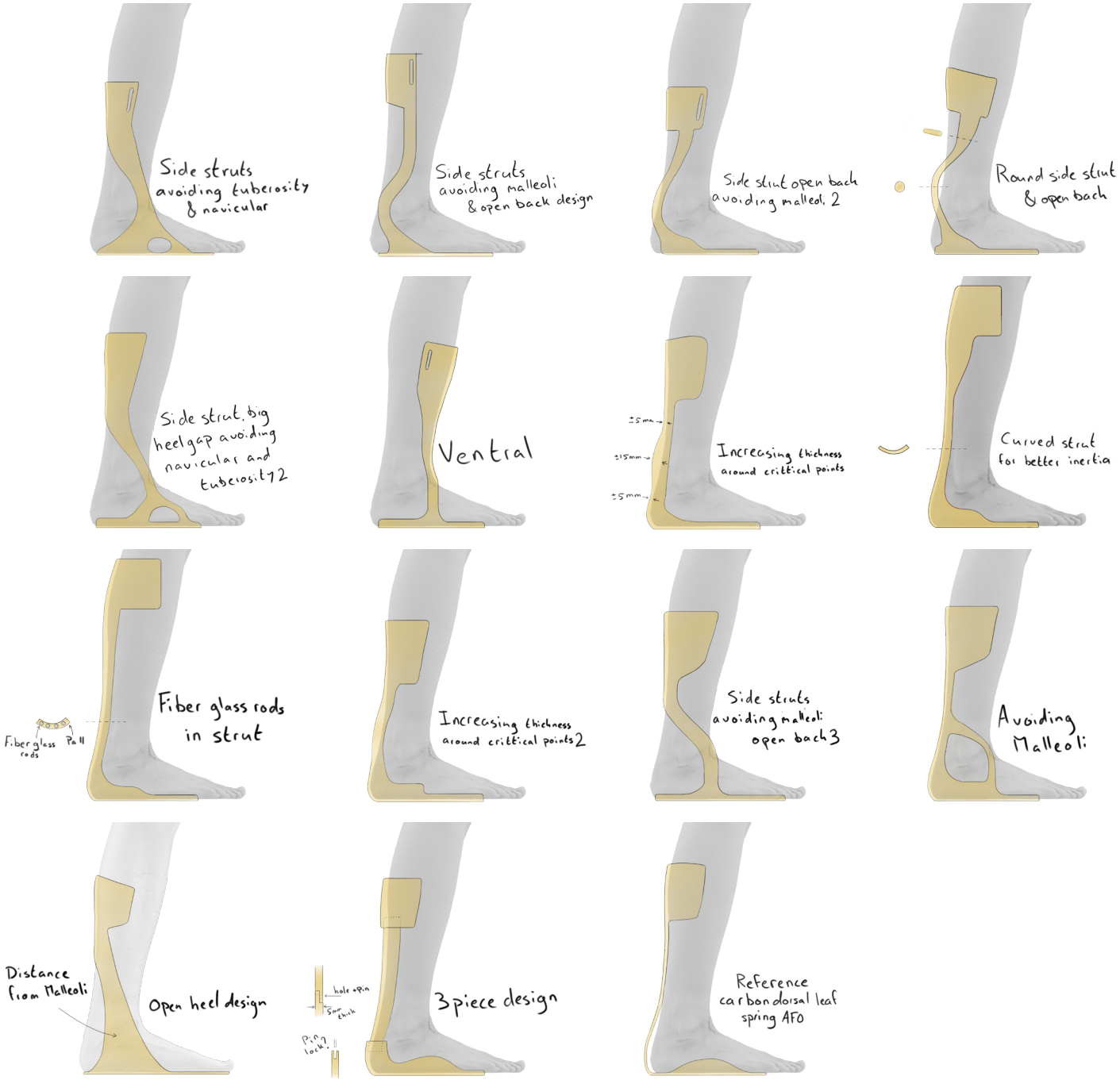

Translating these forms into simple models gave insights into their bending behaviour through conducting rudimentary finite element analysis using simulation in SOLIDWORKS[41]. More information regarding this method can be found on page 56. Some initial ideas build upon the idea of splitting the back strut into two, placing material on the lateral and medial sides of the foot instead of dorsally. However, bending these models gave quick insights into the buckling behaviour present with these structures. The AFO in the middle of Figure 33 displays different bending behaviour in dorsiflexion and plantarflexion directions. The material would also bend outwards in the middle figure during dorsiflexion, away from the foot and lower leg. However, during plantarflexion, this material would bend inwards, potentially clamping the foot and lower leg.

Another consideration was to implement an open-heel design (*figure 34*). It was experienced personally and expressed by an AFO user[39] that equipping a dorsal orthosis and putting on shoes proved difficult. Putting on the orthosis and stepping into the shoes would restrict the bending of the foot, making it difficult to put on. Alternatively, already placing the orthosis inside the foot and stepping into the orthosis and shoe at the same time would require significantly loosening up the laces to pull back the tongue as far as possible.

Placing the orthosis in the shoe and then sliding into the shoe and orthosis was experienced as easier, as more room was present for the heel. However, placing the struts on both sides of the foot showed little to no bending behaviour. The open-heel design was deemed as something to keep in mind for potential implementation in the future, while the focus remains on the stiffness behaviour for now.

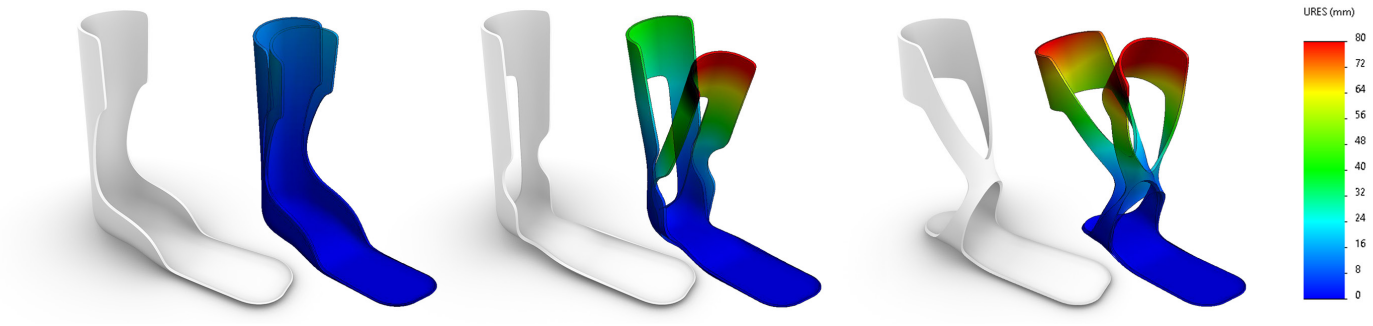

figure 33: Several shapes tested on their bending behaviour to get a better understanding of the required geometry. 60 newton was applied in both dorsiflex and plantar flex direction at the very top of their designs whilst the ground plate was fixed

figure 34: FDM fitted orthosis with side struts. Proved too stiff to function

Stiffness exploration 1

Calculations

The main criteria that the SLS-printed AFO has to comply with are that it can deliver the same stiffness values as conventionally made carbon-layered AFOs. Baseline values were measured on page 36 and 37 regarding the carbon dorsal leaf spring orthosis.

Two variables can be utilized in translating these stiffness values into orthosis geometry. A big factor contributing to the stiffness of the baseline sample is its material. Carbon composites are known for their high elasticity value. This value, also referred to as the Young's modulus, is a property of a material that states how easily it can deform when a force is applied.

A comparison between the SLS printable materials and carbon composites can be found in figure 16 on page 25. Making an orthosis printable using the facilities and materials available at Parts on Demand means working with these set values, if no external materials are added.

Another variable determining the stiffness of an object is its moment of inertia or its geometry. A thick beam is, for example, stiffer than a thinner beam made of the same material.

For example, the strut present in a PD-AFO provided by Livit Ottobock Care can be approached as a beam (*figure 35*). The stiffness of this AFO is influenced by the thickness, the length, and the width of the strut and its material composition. The carbon dorsal leaf spring orthosis produced by Livit Ottobock Care is made of a composite material consisting of woven carbon fiber sheets and a cured polymer. Its elastic modulus can be approached by taking the mean value as listed in a material database such as Ansys Granta EduPack[27].

Using a simplified FBD of the orthosis (*figure 36*), fixating the footplate similar to the BRUCE method, we can calculate the stiffness of the back strut. This uses the formula stated before where the displacement, applied force and armlength need to be known to determine its stiffness:

equation 1

$$\frac{Force \cdot Armlength}{Angle} = Stiffness\ (Nm/°)$$

The stiffness of this specific carbon dorsal leaf spring orthosis is known as it was measured before. The stiffness when dorsiflexing was measured to be 1,23 Nm/° and 1,14 when plantar flexing.

Approaching the orthosis as a beam deflecting can help determine what will happen if another material is used for the production of the orthosis. Therefore measurements were made and formulas were set up to determine the thickness of the strut when the orthosis is dorsiflexing. Having set up the formulas correctly can tell what will happen to the thickness of the strut when another material, or Young's modulus, is used.

The formulas on the next page were set up to calculate the thickness of the strut using the following measurements taken from the carbon dorsal leaf spring reference orthosis:

Elastic modulus = 91 Gpa
Dosiflexion angle = 20°
AFO length = 36 cm
Malleoli to top length = 30 cm
width of orthosis (b) = 3 cm

figure 35: Simplification of the carbon dorsal leaf spring strut as beam geometry

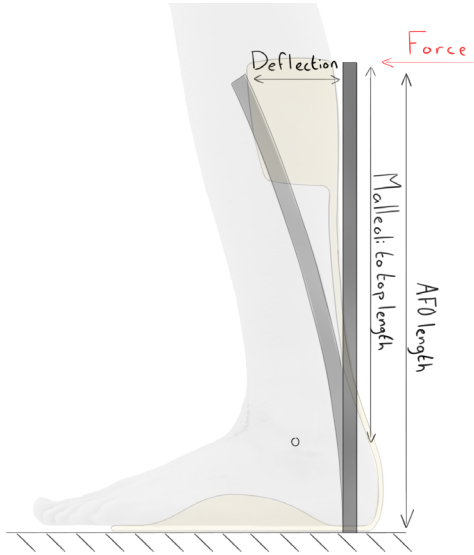

figure 36: FBD of simplified carbon dorsal leaf spring strut as a beam deflecting

The force applied around the cuff can be calculated knowing the positive moment produced by the orthosis during dorsiflexion, the length from the malleoli to the top of the cuff, and the dorsiflexion angle.

The estimated length from the malleoli to the top of the cuff is around 30 cm. The angle is defined by the maximum range of motion that the AFO needs to be able to achieve, which is 20° of dorsiflexion. The measured dorsiflexion stiffness is 1.23 Nm/°. By filling in these values, we can calculate a force of 82 N using equation 1:

$$\frac{Stiffness \cdot Angle}{malleoli\ to\ top\ length} = Force \longrightarrow \frac{1{,}23 \cdot 20}{0{,}3} = Force$$

The thickness of the beam can be calculated using the formula for a fixed loaded beam[42] and the formula for the moment of inertia of a rectangular shape:

equation 2 $$\frac{Force \cdot AFO\ length^3}{3 \cdot E \cdot I} = deflection$$

equation 3 $$\frac{b \cdot h^3}{12} = I$$

The combination of these formulas can be used to calculate the thickness of the strut. However, for equation 2, the deflection needs to be known. This can be calculated using trigonometry, which gives us a deflection of 13.1 cm through the formula:

equation 4 $$tan(angle) \cdot AFO\ length = deflection$$

Taking the elastic modulus value of 91 Gpa for a carbon composite[27] gives us a moment of inertia of $1{,}07 \cdot 10^{-10}$ through filling in equation2:

$$\frac{Force \cdot AFO\ length^3}{3 \cdot E \cdot Deflection} = I \longrightarrow \frac{82 \cdot 0{,}36^3}{3 \cdot 91 \cdot 10^9 \cdot 0{,}131} = I$$

Knowing the width of the strut, b = 3 cm, we can solve the thickness by filling in equation 3:

$$\frac{b \cdot h^3}{12} = I \longrightarrow \frac{0{,}03 \cdot h^3}{12} = 1{,}07 \cdot 10^{-10}$$

The calculated strut thickness of 3.5 mm closely corresponds to the measured thickness of 3.3 mm. This provides validation for the mathematical calculations, which can then be applied to other materials and geometries.

By changing only the elastic modulus values to those of the SLS printable materials in these formulas while retaining the same geometry, we can estimate the resulting orthosis strut thicknesses if printable materials are used.

Filling in the respective values of 3.816 GPa for CarbonLW, 1.75 GPa for PA12, 3.45 GPa for PA11GF, and 1.78 GPa for PA11 (*taken from figure 16*) gives calculated strut thicknesses of:

CarbonLW = 11 mm
PA12 = 14.5 mm
PA11GF = 11.3 mm
PA11 = 14mm

Measurements

To better give insights into the material behaviour, test prints were produced both to validate the math and to measure if the SLS printed materials would be elastic enough to refrain from breaking when deflecting.

A prototype was modelled and manufactured consisting of 3 SLS printed parts (*figure 37*). This model was made to have interchangeable struts to save on printing costs and reduce manufacturing time.

Four struts were printed using the available four SLS printable materials with thicknesses calculated using the formulas as depicted on the previous pages (*figure 39*).

The 'cuff' and 'foot piece' were printed using 5mm thick PA11, chosen for its high elongation capability to ensure durability during testing, minimising the risk of fracture for these parts.

The four different struts were mounted in the orthosis and BRUCE stiffness measurements were conducted to visualise their bending behaviour and to see if the values would be similar to the measurements conducted with the carbon dorsal leaf spring AFO.

The values can be found in the graphs depicted in figure 40 to 43. The Pa11GF strut was not measured in these tests due to human forgetfulness. These tests were conducted in the UMC in Amsterdam with time constraints and Pa11GF was in haste forgotten. It can be concluded from the other test results that the stiffness would be most likely within a 15% deviation range from the stiffness values measured with the carbon dorsal leaf spring orthosis.

The stiffness values derived from these graphs are somewhat similar to the values of the carbon dorsal leaf spring orthosis. What can be seen in the test results is that the negative moments of the SLS 3-part orthosis are larger than the positive moments. This is because the PA11 footplate and cuff pieces were not stiff enough and showed defective behaviour as well as the struts. Whilst dorsiflexing the walls around the heel would fan out, reducing its stiffness.

It can be seen in figure 41 that the carbonLW strut broke during dorsiflexing. The breaking was exactly at the point where the bolt was attached (*figure 38*). This was to be expected as it was hypothesised that these points would be the most critical as stress due to concentrated stress. It was also logical that the carbonLW sample broke as this material is the most porous and least flexible (*figure 16*).

figure 37: 3 piece strut testing SLS printed model

figure 38: breakline of carbonLW strut during measurments

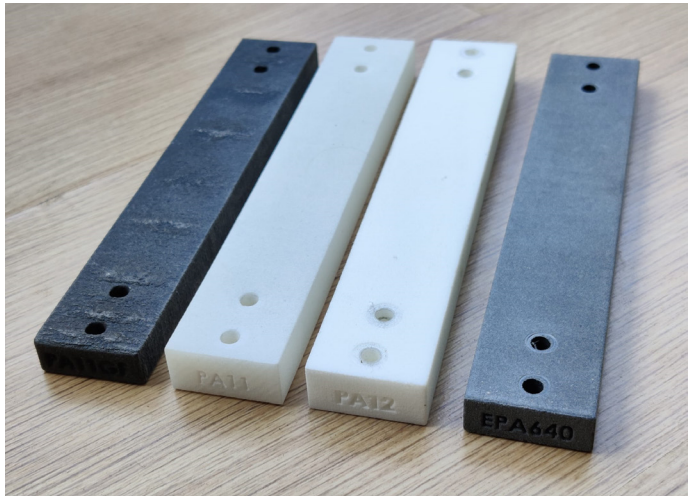

figure 39: interchangeable struts. Carbon LW 11.0mm, Pa12 14.0mm, Pa11GF 11.3mm, Pa11 14mm

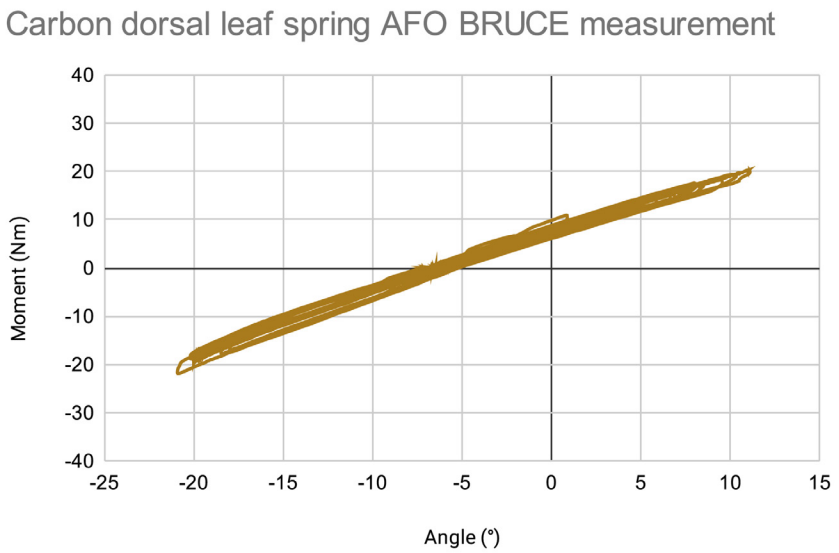

figure 40: average stiffness of 1.16Nm/°, positive moment of 1,23Nm/°, negative moment of 1.14Nm/°

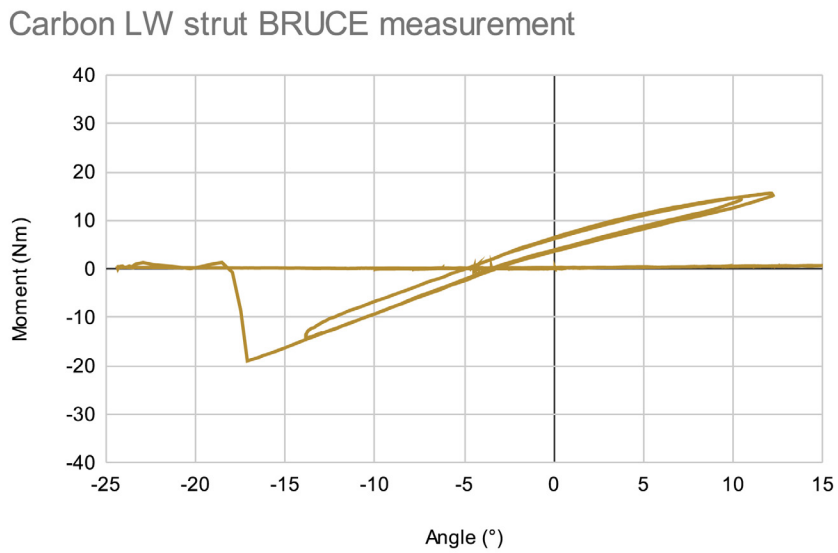

figure 41: average stiffness of 1.09Nm/°, positive moment of 1.04Nm/°, negative moment of 1.47Nm/°

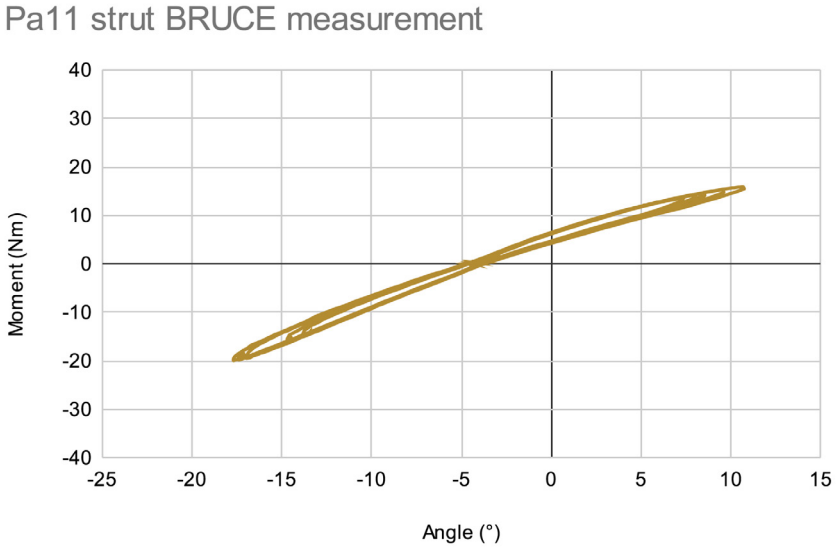

figure 42: average stiffness of 1.31Nm/°, positive moment of 1.26Nm/°, negative moment of 1.40Nm/°

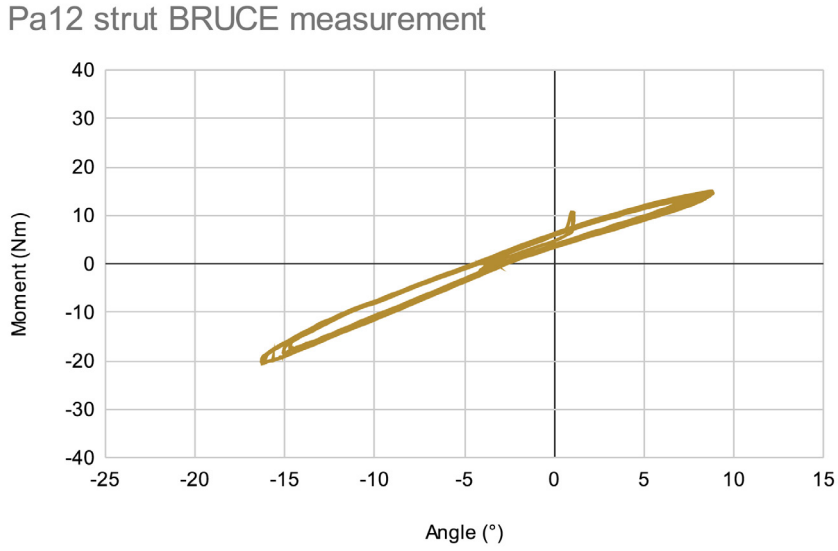

figure 43: average stiffness of 1.27Nm/°, positive moment of 1.33Nm/°, negative moment of 1.62Nm/°

Material evaluation

The results from these tests emphasised the porosity of CarbonLW. The high stiffness can be a good fit for the production of orthosis, but the low flexibility results in a shorter life of use. As stated before, the AFO needs to at least have a range of motion of 15 degrees plantarflexion and 20 degrees dorsiflexion. The achieved ROM is dependent on the client, but the AFO will need to provide the possibility to reach these angles without breaking or plastically deforming.

Carbon LW will most likely be incapable of reaching these angles and thus a decision was made regarding the material most suitable for the production of the orthosis (*figure 44*) regarding material and AFO criteria. Comparing these qualities gives a slight advantage to PA11. This material will therefore be used further on for tests.

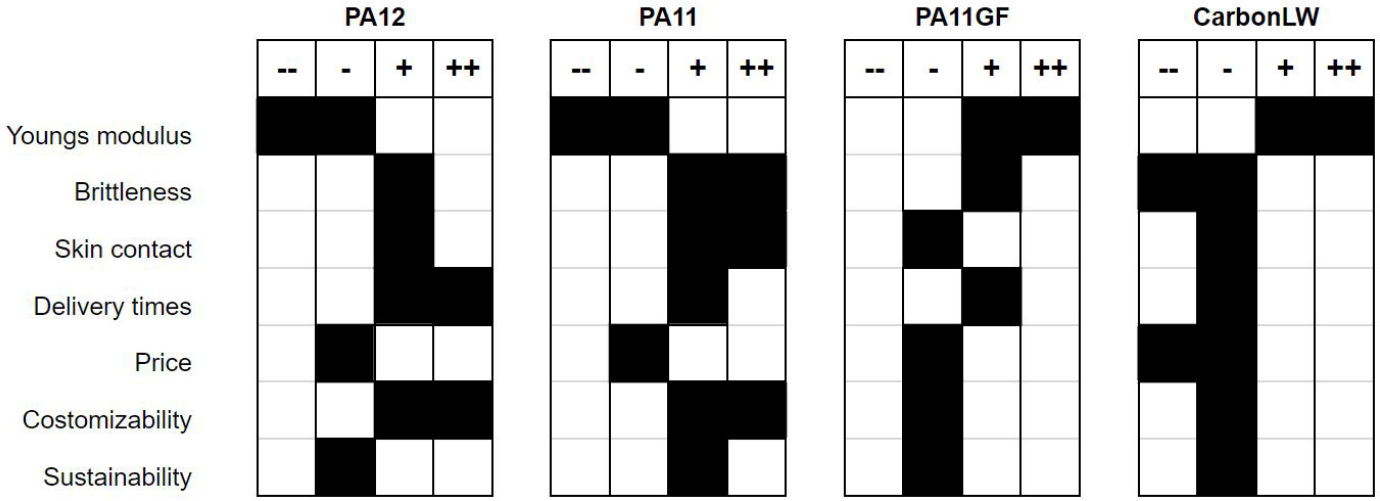

figure 44: Harris profile concerning material choice

Youngs modulus
The elastic modulus was assessed on its magnitude. The higher this value, the thinner the orthosis can most likely be produced resulting in a slimmer, lighter, cheaper and overall more desirable design.

Brittleness
The brittleness was assessed on its flexible behaviour as a result of its tensile strength, elongation at break and flexural modulus values as listed in figure 16.

Skin contact
The AFO will not directly come into contact with the skin but Livit Ottobock Care has expressed the desire to have a skin-contact-approved ankle foot orthosis to guarantee a safe product. Parts on Demand can use the premium vapour polishing treatment on all materials that fuse the surface making it more smooth and thus preventing rubbing of the skin. However, glass and carbon fibres present in the printed material still give concern.
PA11 would be the most suitable here as Parts on Demand has it certified to be skin contact approved and even food safe with the appropriate treatments.

Delivery Times
This is again a measurement based on the data in figure 16. Materials are allocated to printers based on the demand for the materials. Currently, PA12 is by far in the greatest demand with TPU and CarbonLW the least. However Parts on Demand are predicting an increase in PA11 orders, as this is still a relatively new material similar to PA12, but with increased properties and other advantages.

Price
A quote was determined for an AFO model and prices were determined for each of the materials[43].
Each material is priced the same except for CarbonLW which is approximately 15% more expensive.

Customizability
85% of the carbon dorsal leaf spring orthoses are produced for kids[12]. It was noted that almost all kids expressed the desire to have a customized AFO through the use of a print that is added over the orthosis. Parts on Demand can not add prints to their products but can colour them. This is not feasible for PA11GF and CarbonLW prints, as they emerge from the printer in a black colour and thus do not adequately absorb lighter pigments[21].

Sustainability
Only PA11 is made from a sustainable source: caster oil and thus has a lower sustainable impact[44].
Carbon LW and PA11GF are composites while PA12 consist of a single material.

Stiffness exploration 2

Ankle trimline simulations

The stiffness tests conducted with the 3 piece orthosis gave insights into the material choice, thicknesses and geometry behaviour. Calculating the cross-section of the beams approached the stiffness values aimed for by the carbon dorsal leaf spring orthosis, but resulted in limiting the AFO strut to a rudimentary beam design too thick to be worn inside of a shoe. Making a Pa11 AFO with a strut shaped like a beam results in a product thickness of 14mm if it was the same width as the carbon dorsal leaf spring orthosis. This exceeds the design requirement of having a maximum of 5mm thickness around the heel and thus another design solution is necessary.

The strut is flat and approximately 3,3mm thick in the dorsal leaf spring AFO made by Livit Ottobock Care. This piece of carbon is flat as this shape divides the stress better over its length. This is beneficial for the carbon composite as it decreases the chance of delamination[45]. This also places the force perpendicular to the web of fibres. As seen in figure 45.1, the force is evenly distributed when the strut is flat. In figure, 45.2 a semicircle beam is used. The stress is concentrated at the edges of the beam and not perpendicular to the layers of the carbon fibres. This can create shear cracks at these spots which will, in due time, result in delamination. Thus Livit Ottobock Care ensures the strut is flat to prevent this from happening[12].

SLS printed materials, on the other hand, do not delaminate and are near isotropic[21]. This means that more geometric freedom is available in general, but also in the cross-section of the AFO through the transverse plane as the stress exerted on the strut does not have to be divided equally along its width.

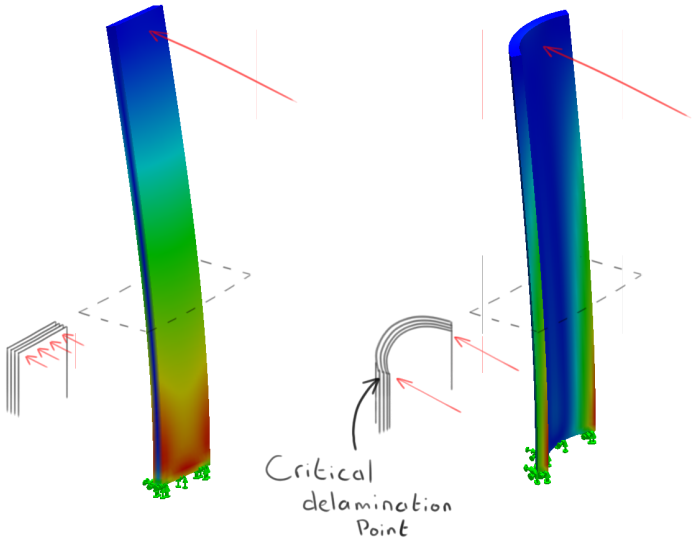

figure 45.1: stress distribution of a rectangular beam, 45.2: a semicircle made out of layered carbon composite

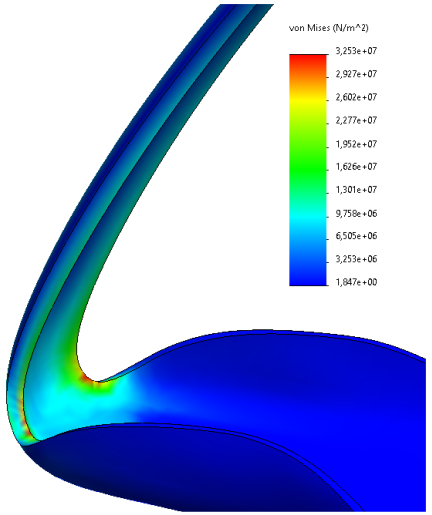

figure 46: vonMisses stress concentration through FEA

Because of this, a shape is possible that follows the curvature of the leg more closely, such as the shape in figure 45.2.

This shape, unlike the rectangle, will not bend symmetrically. The axis of revolution as a result of the force applied and the direction will result in different behaviour on either side. Because of this, the shape will bend outwards when force is applied from the curved side, as also seen around the heel of the foot in the three-piece interchangeable strut prototype. This is no direct problem for the fitting as it bends away from the leg and thus does not pinch it, but it also results in different stiffness values for the plantar flex en dorsiflex moments.

Only using this shape for the strut does not result in enough stiffness whilst staying under the 5mm thickness requirement around the heel. Simulations using finite element analysis were made in Solidworks[41] to more closely determine what is happening when forces are applied to more complex shapes. This can be approached mathematically, as done before in the previous chapter, but is considerably more complex. Therefore the decision was made to simulate the bending behaviour.

For this setup, the footplate is fixed, as close to the mounting method of the BRUCE setup as possible, and 60N is applied at a height of 300 mm in the dorsiflex direction divided over the surface of the cuff. The large displacement option is used to provide more accurate results and the true scale deflection is shown to better evaluate its results.

The FEA method of SolidWorks can simulate the deformation and displacement that occur in the model and thus the stiffness can be calculated. Also, the stress concentration can be visualised to better see what is happing with the model (*figure 46*). It becomes evident when looking at this figure that the stress concentrates at the critical point around the heel. This is considered the weakest point according to the FEA. This means that increasing the moment of inertia in this specific place would yield the biggest increase in stiffness.

Consequent FEA models were made and calculated (*figure 47*). Applying more material around the foot in this area results in less displacement and consequently more stiffness.

This gives a design parameter that can be used to influence the stiffness values of the strut; increasing the surface area around the heel (*figure 48*). This is also an aspect of the AFO that would not have been possible for the carbon fibre variant as it would most likely delaminate around these edges as stress is concentrated in these places.

It has to be kept in mind however that stress will concentrate in this place. The tensile strength of Pa11 is around 50Mpa. Exceeding this threshold will result in plastic deformation. This is something that has to be regarded closely when increasing or decreasing the ankle trimline to see what the vonMisses stress concentration is. It will also have to be closely regarded that the geometry here will not come into contact with the malleoli, which would create irritation points.

figure 48 Design opportunity; increasing AFO surface area around the heel increases stiffness

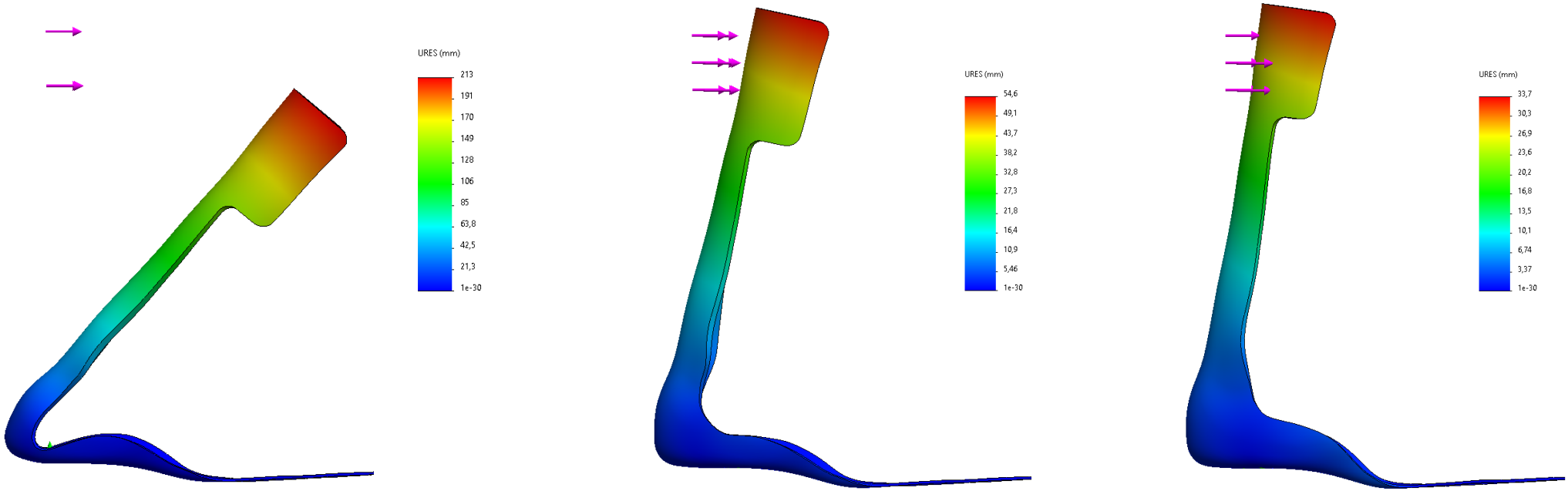

figure 47: 60N applied, 44.1; low ankle trimline, 44.2: medium ankle trimline, 44.3: high ankle trimline

Thickness simulations

The thickness of the AFO shell remains important for the stiffness of the orthosis. A key factor to consider here is the prescribed maximum thickness around the heel requirement (point D in figure 49).The thickness of the orthosis cannot be bigger than 5mm for the AFO to fit inside a shoe. This applies to points A to D in figure 49. These points will have to stay below this value and ideally be as low as possible for a slim design. Point A and B are of great influence on the stiffness around the MTP line, and page 68 and 69 will further look into this.

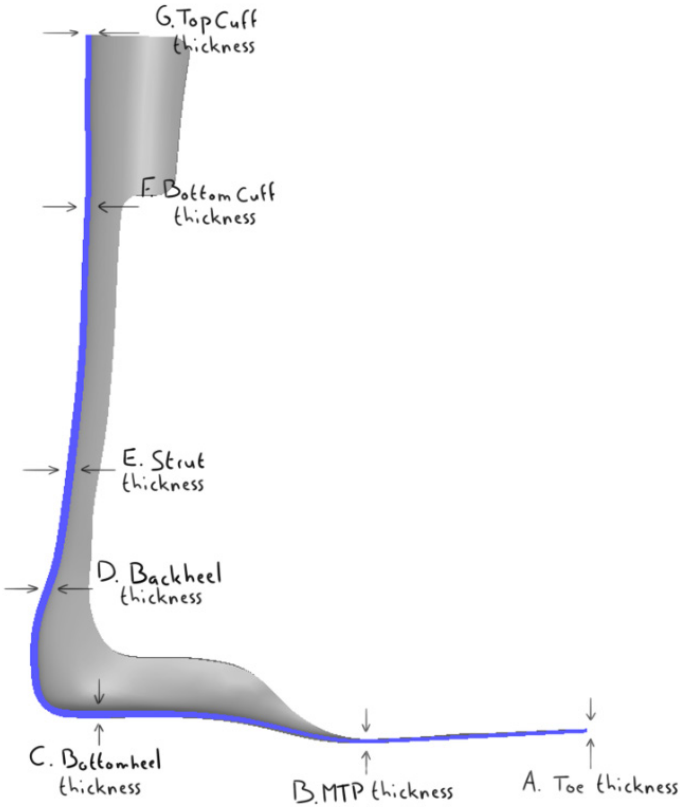

figure 49: Cross section of AFO in parasagital plane

To determine the relevance of the other points, FEA simulations were conducted. These simulations mainly focused on points C to E as these points experience the most stress. Their relevance is mapped out in figure 50.

These values were calculated by increasing or decreasing the thickness of the orthosis at these points and measuring the displacement difference when a load of 50 Newtons is applied (Appendix E).

It can be seen in figure 50 that increasing the thickness at point E has the biggest impact on the stiffness of the orthosis compared to points D or C. This is due to the geometric shape, which has a larger moment of inertia at points C and D compared to E (*figure 51*). Thus, a balance between these two factors has to be found to create the appropriate stiffness.

At points C and D, the orthosis cannot be too thick, or else it will not fit inside a shoe. The cross-section shape at point D cannot extend too far beside the foot as it will come into contact with either malleolus, which is undesirable.

Multiple FEA simulations were conducted, tweaking the thicknesses and geometry at these points to approach the desired plantar flex and dorsiflex stiffness values of 1.23 Nm/° and 1.14 Nm/°.

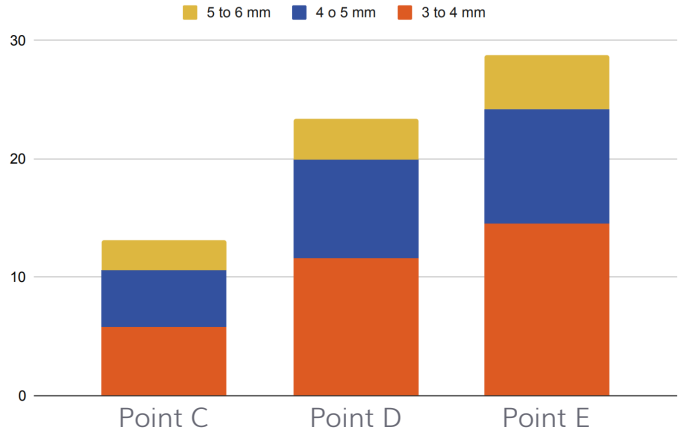

figure 50: relevance of increasing thickness at points C, D and E

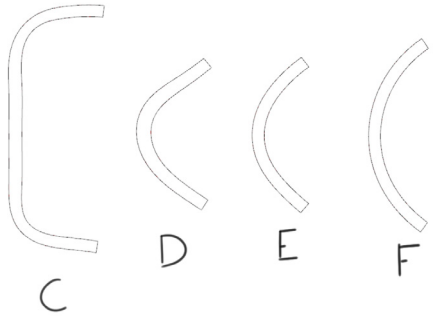

figure 51: thickness cross-section at point C, D, E and F generated using a foot model provided by Livit Ottobock Care

Simulated stiffness in relation to BRUCE stiffness

A comparison between the values generated through finite element analysis, the home measurement values and BRUCE measurements were made to validate if the FEA stiffness values were accurate. This was done using the 3 piece prototype as the data of all three measurement methods was available. The offset angle of the BRUCE measurements was set to 0 in figure 52 to create a more even comparison.

What can be seen in figure 52 is that the stiffness values of the BRUCE measurements are considerably lower than that of the simulated measurements and home measurements. Mapping out the difference between BRUCE measurements and simulated measurements gives figure 53. It is this difference that needs to be accounted for when simulating a model. What can be seen is that this is not a linear difference. Especially in the plantarflex direction it can be seen that this is an exponentially increasing difference. Therefore a polynomial line, with an R2 value of 0,995, was fitted to the data[46] which generated the difference quadratic formula of:

$$-0{,}015 \cdot angle^2 + 0{,}657 \cdot angle + 0{,}54 = \Delta moment\ (Nm)$$

This formula does not fit perfectly as there is not much data available. This is currently based on two datasets; the BRUCE measurements and the simulated stiffness of a single prototype. However, it can for now be used to better predict the difference between these two measurements.

The data used in figure 52 and 53 can be found in appendix F. The BRUCE data was omitted as it contained over 4500 entries.

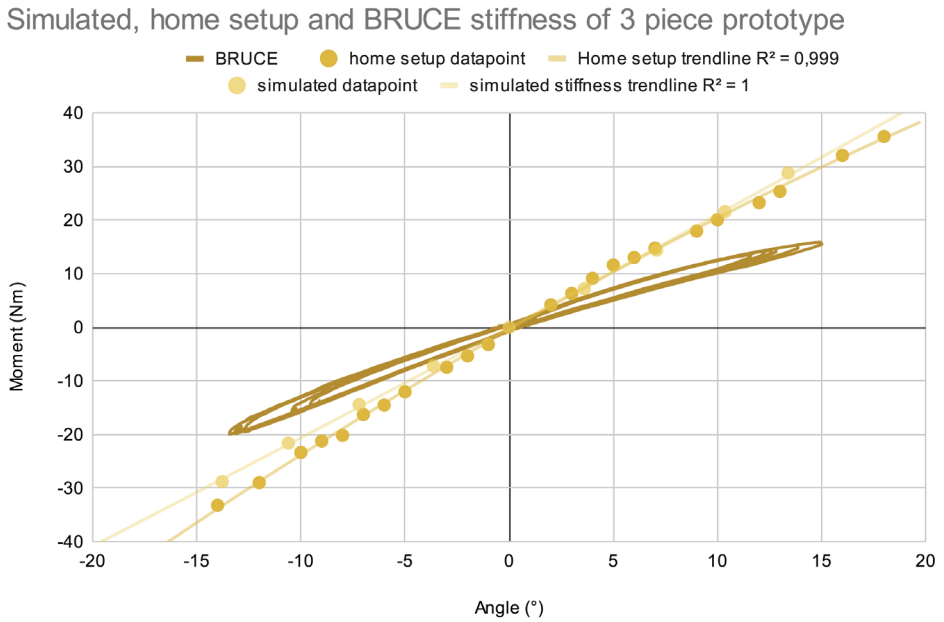

figure 52: Simulated stiffness, home measurements and BRUCE measurements of 3 part prototype

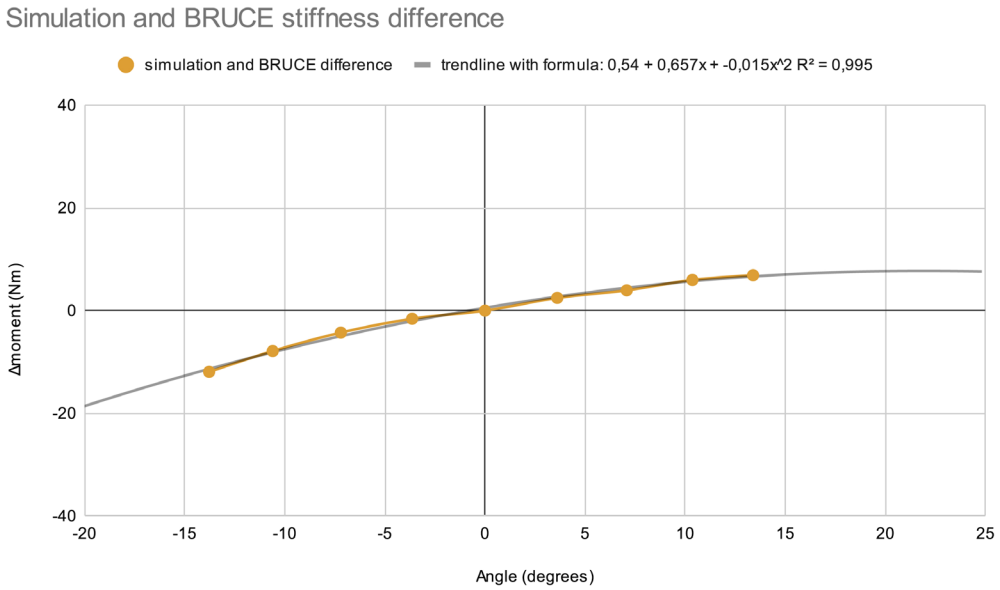

figure 53: difference between simulated stiffness and BRUCE measurements with fitted trendline

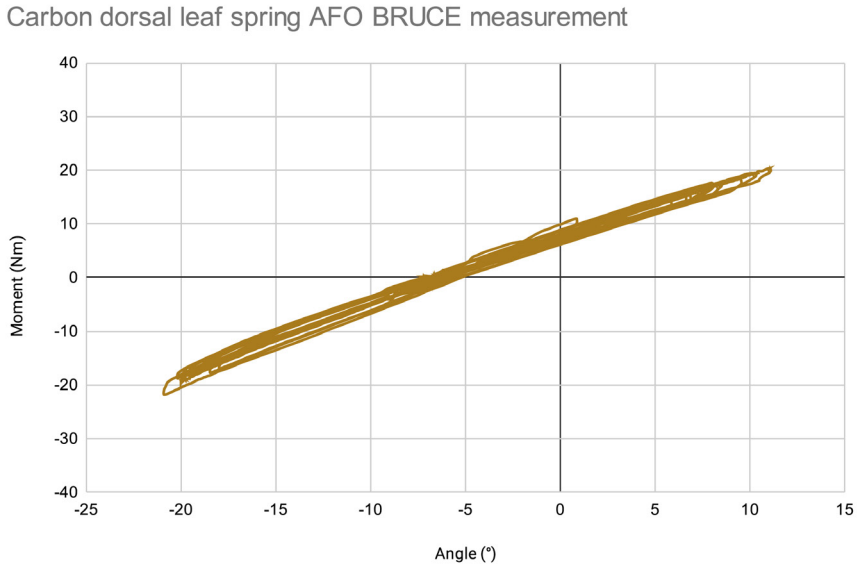

figure 54: BRUCE stiffness graph of the dorsal leaf spring AFO provided by Livit Ottobock Care

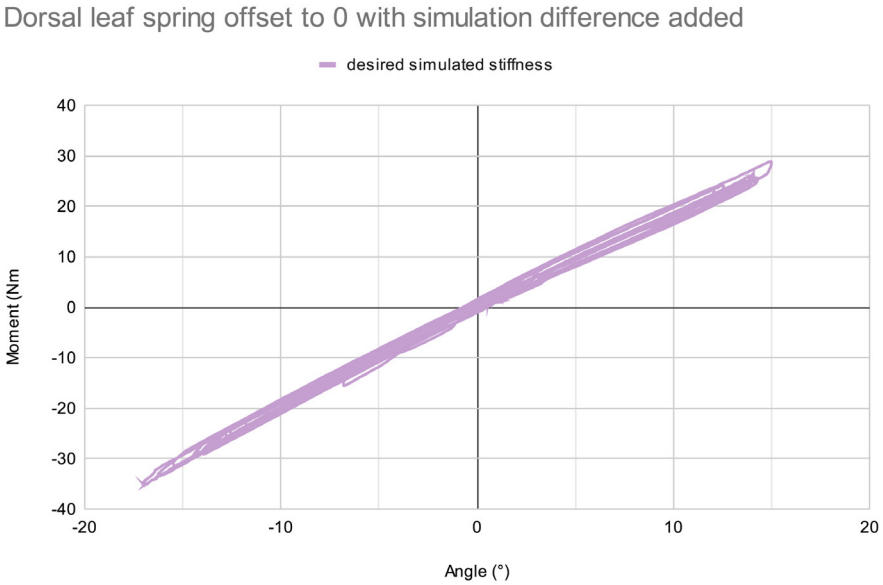

figure 55: BRUCE measurements of carbon dorsal leaf spring orthosis translated into desired FEA stiffness behaviour

Using this formula on the desired stiffness behaviour measured using the BRUCE setup of the carbon dorsal leaf spring orthosis (*figure 54*) creates figure 55. In this figure the SVA is offset to 0 and the stiffness is calculated using:

BRUCE measured moment + Δmoment
= desired simulated moment

This translates the BRUCE measurements conducted with the carbon dorsal leaf spring AFO to approximate FEA simulated stiffness values.

Having a rough idea of how the simulated stiffness translates into BRUCE-measured stiffness, a new model can be made by iterating on the different thickness values depicted in points A to G in figure 49. This resulted in an AFO model visible in figure 57. This model was made using a strut, 5,5 cm wide and 2 cm deep (*figure 58*). The model was made to closely represent the carbon dorsal leaf spring orthosis and thus has the same footplate length and cuff height of 24 cm and 36 cm. The simulated stiffness compared to the desired simulated stiffness can be found in figure 56.

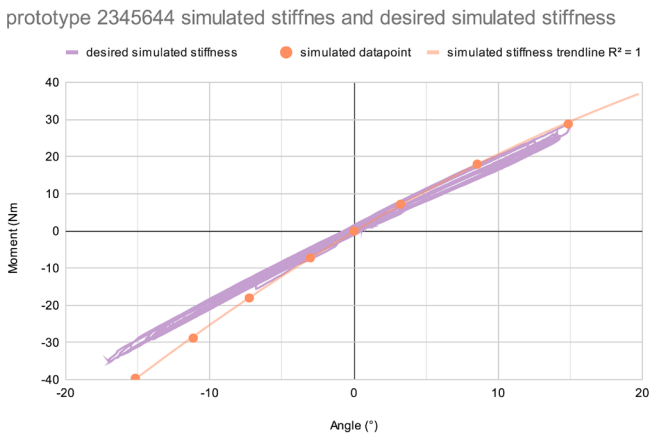

figure 56: Simulated stiffness of new prototype compared to desired simulated stiffness

Averaging out the stiffness when dorsiflexing approximates the desired simulated stiffness. However, in the plantarflexion direction, the stiffness of this prototype is significantly higher. A compromise had to be made in this prototype as attempts to decrease the stiffness in the plantar flex direction also decreased the stiffness in the dorsiflex direction. The decision was made to focus on the dorsiflex stiffness in this prototype and later iterate on the design to also correct the plantarflex stiffness.

This model was SLS printed in one piece with a PVP post-processing treatment to best represent the final orthosis.

The thicknesses at points A through G were 2mm, 3mm, 4mm, 5mm, 6mm, 4mm, and 4mm, respectively. Hence, this prototype was named prototype 2345644.

These thicknesses and this geometry were based on the simulated behavior depicted by the model during finite element analysis. The measurements and data of these simulations can be found in Figure 56. From this data, it can be derived that the average simulated stiffness is calculated to be 2.27 Nm/°. The average positive moment is 2.03 Nm/°, and the average negative moment is 2.51 Nm/°.

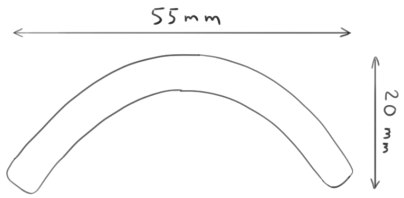

figure 58: cross section measurements of the strut at 10 cm height

figure 57: CAD model and SLS print of prototype 2345644

Stiffness evaluation of prototype 2345644

The stiffness characteristics of the prototype were evaluated using two different methods: a home setup, resembling the setup used for the MTP stiffness measurements of the carbon dorsal leaf spring orthosis (Appendix C), and the BRUCE setup. The stiffness of the strut was measured in both the plantarflexion and dorsiflexion directions.

Due to the orthosis exhibiting nonlinear behavior, the stiffness in the dorsiflexion direction was measured three times with the home setup. The combined data, along with the BRUCE measurements, is presented in figure 59.

Both of these methods were used and compared using the same prototype to validate if the home setup would be accurate and precise enough to provide reliable results. Having a dedicated setup within reach would speed up the process of conducting stiffness tests and result in quicker iterations.

However, as can be seen in figure 59, the stiffness measurements between the home setup and BRUCE setup differ greatly. The home setup measured a positive moment of 1.35 Nm/° and an average negative moment of 2.41 Nm/°, with an overall average stiffness of 1.69 Nm/°. The BRUCE setup measured a positive moment of 0.7 Nm/° and an average negative moment of 1.04 Nm/°, with an overall average stiffness of 0.87 Nm/°.

The most significant outcome derived from these tests regards the breakage of the prototype during plantar flexion at approximately -12 degrees (shifting the neutral angle to 0) while conducting the BRUCE measurements. This result is undesirable considering that the AFO should be capable of reaching an angle of -15°, as documented in the list of requirements.

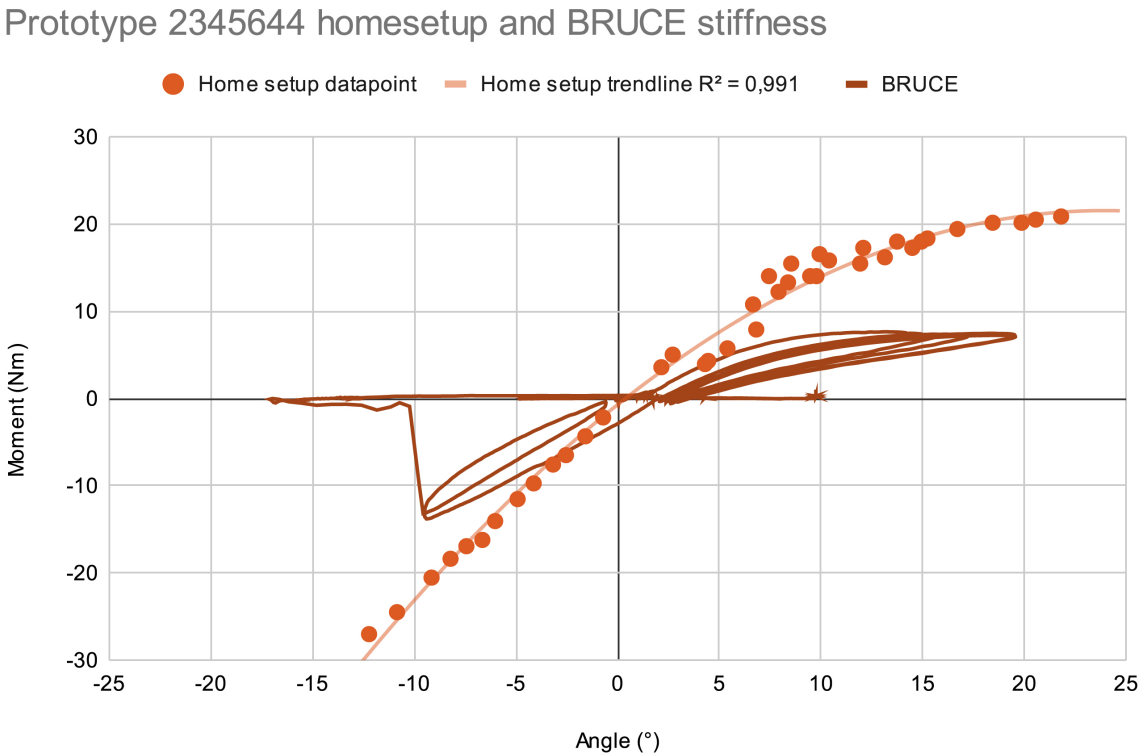

figure 59: home setup stiffness compared to BRUCE measurements of prototype 2345644

Next to the breakage of the orthosis, there are several other things that can be concluded from figure 59:

- The prototype did not exhibit linear behaviour in the dorsiflex direction, thereby the value of these averages.
- The home setup does not produce similar results compared to the BRUCE measurements.
- The prototype displayed excessively high stiffness values in the home setup measurements and excessively low stiffness values in the BRUCE measurements.

figure 60: fractured prototype 2345644

Fracture resistance

Addressing the most important finding: the breakage of the prototype. It was already identified in the chapter concerning the ankle trim line that stress is concentrated around the edge of the prototype and that it is not evenly distributed. It is predicted that the 2345644 prototype broke due to stress concentrated around the heel. This fracture occurred precisely at the location where stress concentration was identified through FEA, as can be seen in figure 64. This location was also roughly predicted by other sources such as Raj et al. (2022a)[4] and Marques et al. (2010)[51].

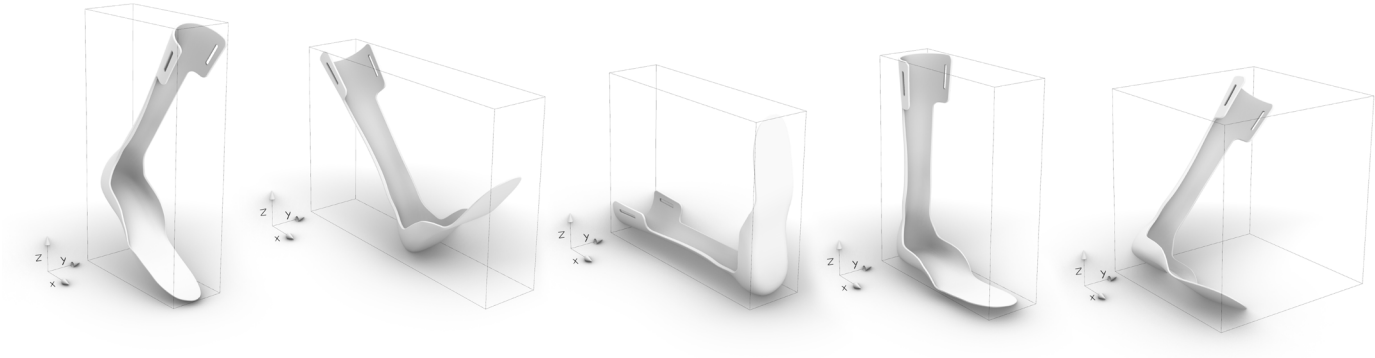

figure 61: print orientations and bouding boxes; 61.1: 230x100x440mm; 61.2: 440x100x230mm; 61.3: 355x100x280mm 61.4: 280x100x355mm; 61.5: 280x300x320mm

An important factor contributing to the fracture of prototype 2345644 was its print orientation. Although SLS printing is known for its near-isotropic properties, it is not entirely the case. The tensile strength of PA11, the material used for the prototype, is 51 MPa in the X and Y directions, while it measures 47 MPa in the Z direction[24]. This difference may be perceived as negligible on paper, but the engineers at Parts on Demand experience a more substantial difference between these directions and advise altering the print orientation for increased strength at this specific point.[36]

Prototype 2345644 was printed using the orientation visible in figure 61.1. This orientation places the print lines in the Z direction directly along the fracture line of prototype 2345644 (*figure 62.1*). Altering the print orientation would change these lines and potentially make them more resistant to fracture.

The current print orientation was influenced by the other prints included in this specific batch. The part was oriented using specialized software to optimize the parts included in the batch. The print orientation was not specified for this prototype, so no consideration was made for its orientation.

Some print orientations were considered for next iterations of the AFO. The ideal orientation of placing the lines perpendicular to the fracture line can be seen in figure 61.2. This would potentially resist fracturing the most but is not a realistic option. As listed before, the printers over at Parts on Demand have a maximum print volume of 300x300x570. The bounding box of the carbon dorsal leaf spring orthoses are estimated to range from 300x200x80 to 500x290x110 and thus cannot be printed in every orientation. This makes the bounding boxes visible in figure 61.2 and 61.3 too large to be printed in their orientations.

What is possible is to rotate the print in the frontal plane resulting in figure 61.5. Printing in this orientation will result in Z axis lines visible in figure 62.2. It is predicted this will increase its resistance to fracture at these concentrated stress points as the Z lines point in different directions and are longer from these stress points. A preference for print orientation can be specified to Parts on Demand where it will be considered.

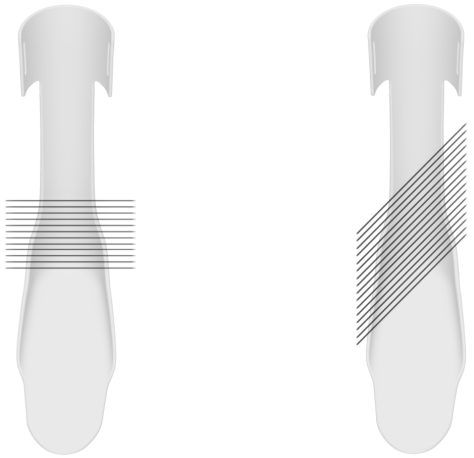

figure 62.1: alignment of Z axis lines in prototype 2345644 62.2 longer Z axis lines in print orientation 59.5

Another consideration to reduce concentrated stress at the area around the heel is to even out the stress area. The stress currently collect in a kink around the heel. The stress reaches a high magnitude as it is concentrated in such a small area. Distributing it over a bigger area and smoothing out this curve could potentially reduce the stress.

An interesting paper regarding beam theory by a Taylor et al. (2011)[52] introduces a more variable slope instead of a constant radius to a shape similar to the strut of an orthosis (figure 63). The variable slope distributes the force more evenly over the shape and thus reduces its magnitude.

Applying this principle to the AFO gives promising results through FEA (figure 64). By adjusting the curve present in the heel arch to this more gradual slope reduces the stress by +- 40% from 1,3e^7 N/m^2 to 0,8e^7 N/m^2. This will most likely help to reduce the change of fracture and should be implemented for the next prototype.

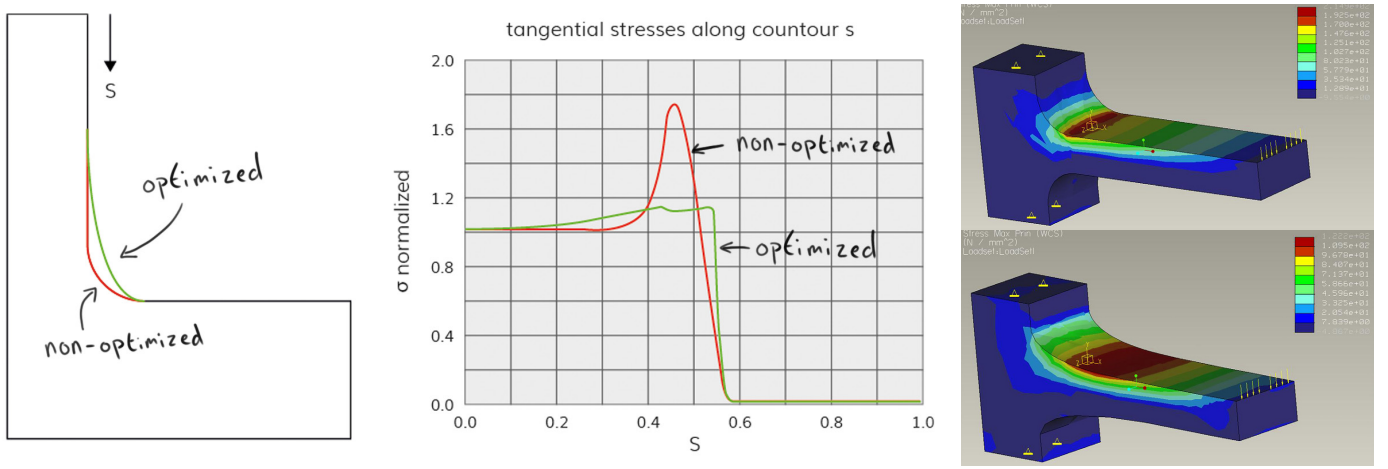

figure 63: stress accuring in a shape with filleted radius (non optimized) vs gradual slope (optimized). Fixed on one side and loaded in tension at the top edge

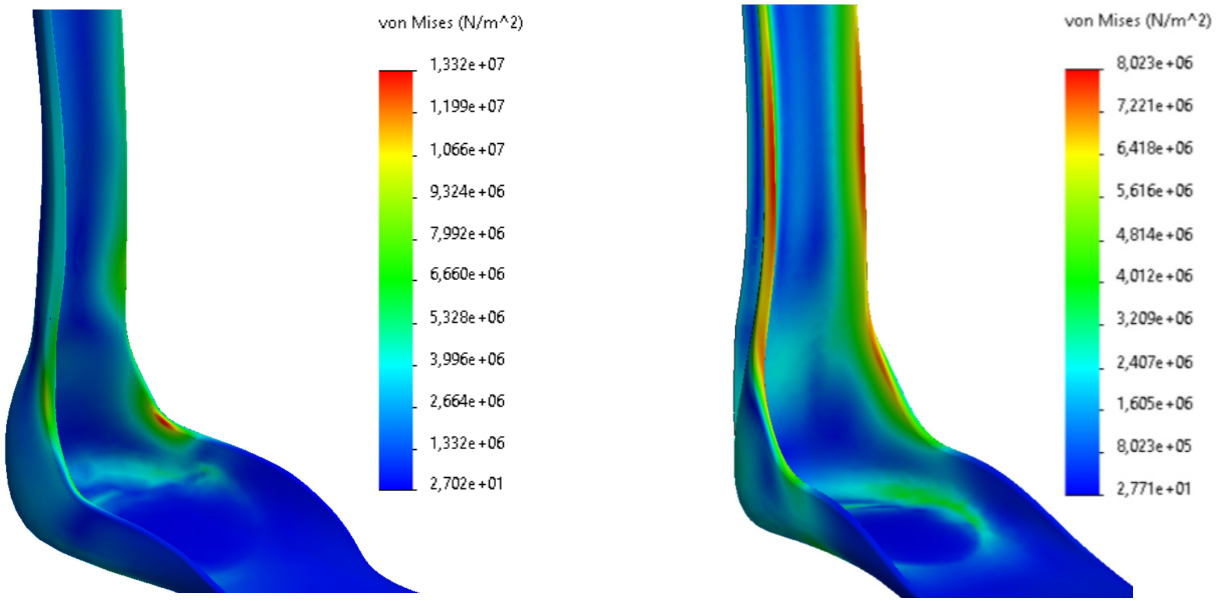

figure 64: on the left; stress concentrated around the heel in prototype 2345644 with a rounded heel arch and on the right; stress concentrated at the strut in a new prototype with a gradual sloped heel arch

Buckling prevention

More closely examining the stiffness behaviour of the orthosis reveals that it loses its stiffness in the dorsiflexion direction due to buckling around the heel.

This makes the stiffness behaviour of the 2345644 different in the plantar flex and dorsiflex direction whilst the carbon dorsal leaf spring AFO has a near linear behaviour.

Implementing the gradual slope heel arch already solves some of this problem as it places the stress higher up the strut, flexing the strut more instead of the heel arch. The gradual slope adds more material around the heel, strengthening this part as well.

To further address this issue, the decision was made to increase the thickness around the heel from 4 mm to 4.5 mm. This would still be below the maximum requirement of 5 mm, as listed in the design requirements.

It can be stated that the orthosis will have slightly greater stiffness when dorsiflexing in a real-use scenario. If an inner shoe is attached to the bridge of the orthosis and/or a shoe is worn over the orthosis, the force fanning out from the heel to the sides is counteracted. However, considering how pliable most shoes are, this will likely have minimal effect.

It is predicted that these adjustments will provide some improvement but will not completely eliminate buckling. Although they provide some insights, both the FEA method and the home setup stiffness measurements have proven to be inaccurate. Therefore, a trial-and-error approach is being used for this optimization.

With a better understanding of this problem and a more accurate estimate of how the geometry influences the measured stiffness, a new model can be created to further iterate on the design and closely resemble the stiffness behavior of the carbon dorsal leaf spring orthosis.

One aspect to consider regarding the buckling of the orthosis that has to be kept in mind is that the sideways forces will likely translate into pressure exerted on the top of the wearer's foot (*figure 66*). This raises the question of how comfortable it will be to wear an orthosis exhibiting this behaviour and should be tested.

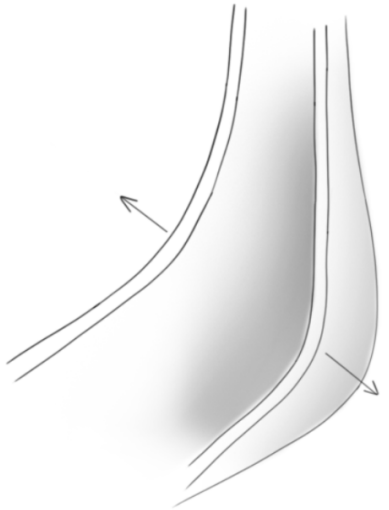

figure 65: buckling around the heel

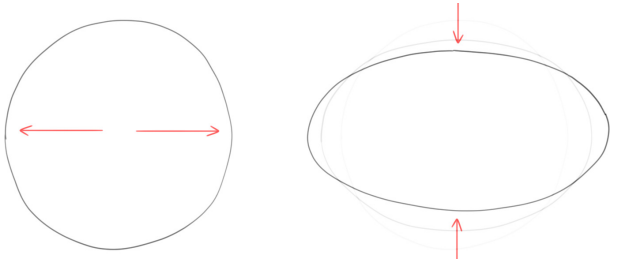

figure 66: fanning out material from the heel may translate into stress pointing down and clamping the foot when wearing an inner shoe or shoe around the orthosis

Stiffness exploration 3

Moment of inertia shapes

The moment of inertia of prototype 2345644 was more closely regarded to better understand how the difference between the moment in the plantar flex and dorsiflex direction could be more reduced.

The current shape of the strut is made in such a way as to offer great resistance to deformation in one direction and less resistance in the other direction (*figure 68*). During dorsiflexion, the shape buckles, while it provides additional resistance in the plantar flexion direction. This is not the case for the carbon dorsal leaf spring orthosis as the strut has a more symmetrical shape (*figure 67.1*). Having this shape translated to the SLS AFO results in a thick design, as used in the 3 piece prototype struts. However, the curved thin shape used in prototype 2345644 can also be made symmetrical resulting in the shape visible in figure 67.4.

Using this symmetrical shape throughout the entire backside of the strut is not feasible as the increased thickness would prevent it from fitting inside the shoe. However, this geometry can be utilized above the shoe line.

Efforts were made to model and simulate more symmetrical strut designs to assess their effects (appendix G). Although the FEA simulations do not provide exact stiffness values, they help determine the stiffness difference between dorsiflexion and plantar flexion. Ridge-like structures were modelled to facilitate easy modification and alteration of their designs and volumes.

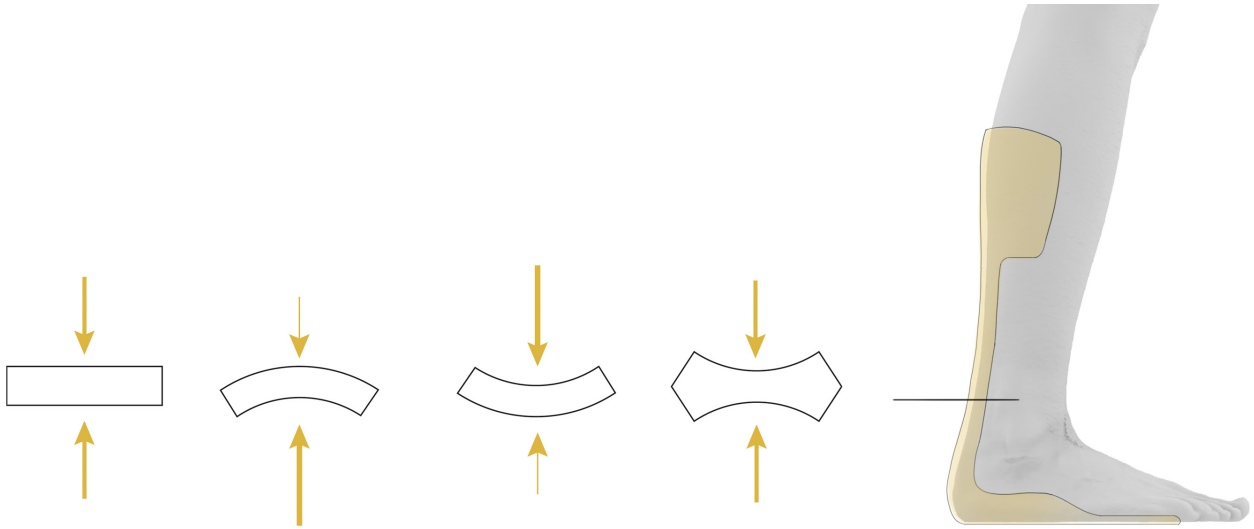

figure 67.1: squared flat symmetrical shape, 67.2: positive curve offering great resistance for forces pointing upwards, 67.3: negative curve offering great resistance for forces pointing downwards, 67.4: blend of negative and positive curve resulting in symmetry

The models in Appendix G were not simulated with the same strut width and thus do not present accurate stiffness values. To evaluate the effectiveness of the designs, a score was assigned, which is the positive moment divided by the negative moment. This score represents the ratio between the two values. A higher score indicates less stiffness in the plantar flexion direction and higher stiffness in the dorsiflexion direction.

Based on these tests, the two best ridge designs were identified (*figure 69 and figure 70*). The decision was made to proceed with the design in figure 70, considering the material used in the design. Less material results in reduced weight, which is perceived as more comfortable and cost-effective. Additionally, having thinner parts in the design is preferable for the PVP and color treatment, as it ensures more even impregnation, resulting in a smoother surface and uniform coloration of the part[21].

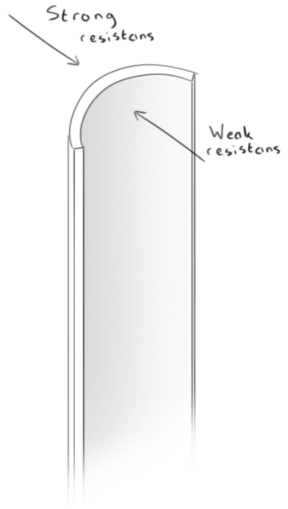

figure 68: the U shape of the strut has more resistance to bend in one direction and less in the other direction

figure 69.1: More symmetrical strut shape for more even stiffness in plantarflex and dorsiflex direction

figure 69.2 Cross section of strut at point E

Anti-curve design attached to the strut for a more symmetrical moment of inertia.

weight: 247 gram
negative moment: 1,88Nm/deg
positive moment: 1,75Nm/deg
positive moment / negative moment = 0,931

figure 70.1: Two fins fanning out shape for more even stiffness in plantarflex and dorsiflex direction

figure 70.2 Cross section of strut at point E

Filleted, dissolving fins attached to the strut for a curved dog bone-like moment of inertia

weight: 218 gram
negative moment: 1,83Nm/deg
positive moment: 1,72Nm/deg
positive moment / negative moment = 0,940

The width of the strut can be reduced compared to prototype 2345644 to decrease its plantar flex stiffness. Additionally, the width, height, length, and position values of the ridges can be adjusted to increase the dorsiflexion stiffness.

The inclusion of ridges in the model introduces another set of parameters that are used in the design of the orthosis. To better explain which parameters are used to tweak the stiffness of the orthosis, a detailed overview of how the current model is built is necessary which can be found on page 74 to 77.

By incorporating the sloped heel arch in this design, the stress is distributed higher up the strut. As a result, the strut undergoes more elastic deformation compared to the previous prototype. In the previous design, the heel arch experienced more buckling, whereas in the current design, the strut buckles to a greater extent indicating the pressure is more present here hopefully reducing the chance of fracture.

MTP stiffness

In prototype 2345644 the MTP stiffness was excluded as a simplification. Some tests were conducted to examine the thickness of the footplate and its resulting moment, aiming to determine the required thickness to achieve the same moment as the carbon dorsal leaf spring orthosis.

Samples were designed with estimated thicknesses based on the formulas described on pages 51 and 52. For the MTP samples, the FBD in figure 71 was used with a length value of 9,5 cm and a footplate width of 7,2 cm.

The FBD was derived from the method used to measure the MTP line in the dorsal leaf spring orthosis, as illustrated in appendix C.

Calculations

The stiffness along the MTP line of the carbon dorsal leaf spring orthosis was calculated through

$$\frac{Force \cdot Armlength}{Angle} = Stiffness\ (Nm/°)$$

Which resulted in a value of 0.24 Nm/°, as explained on page 37. This value can be used as a starting point for determining the required thickness of the footplate to achieve a similar flexible behavior while using a different material.

Again, looking at the simplified FBD in figure 71, equation 1 can be used, with any angle, for example 20, to determine the ground force at that point:

equation 1 $\quad \frac{Force \cdot Armlength}{Angle} = Stiffness\ (Nm/°)$

$$\frac{Stiffness \cdot Angle}{Armlength} = Force \longrightarrow \frac{0{,}24 \cdot 20}{0{,}095} = 50{,}53\ N$$

The deflection can be calculated knowing the deflection angle and the length of the beam through:

equation 4 $\quad tan(angle) \cdot Armlength = deflection$

$$tan(20) \cdot 0{,}095 = 0{,}035\ m$$

The moment of inertia can be calculated knowing the force, the deflection, arm length and material (Pa11, $1{,}78e^{9}$ Pa) through:

equation 2 $\quad \frac{Force \cdot Armlength^3}{3 \cdot E \cdot I} = deflection$

$$\frac{Force \cdot Armlength^3}{3 \cdot E \cdot deflection} = I \longrightarrow \frac{50{,}53 \cdot 0{,}095^3}{3 \cdot 1{,}78e^{9} \cdot 0{,}035} = 2{,}32e^{-10}$$

Using the moment of inertia, the new footplate thickness is calculated through:

equation 3 $\quad \frac{b \cdot h^3}{12} = I \longrightarrow \frac{0{,}072 \cdot h^3}{12} = 2{,}32e^{-10}$

This results in a thickness of 3,38 mm.

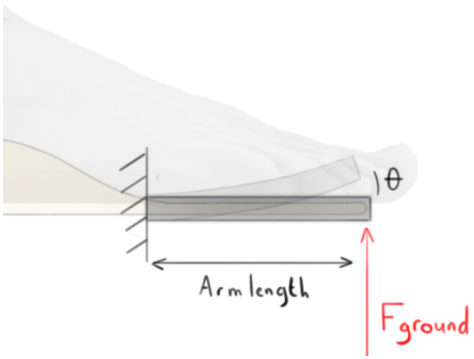

figure 71: Simplified FBD around the metatarsophalangeal joints

Measurements

To verify the accuracy of the calculations, small-scale samples were printed and tested. Two variables were measured: the displacement at the point where force is applied and the corresponding force at that point. By knowing the length of the sample, we can calculate the stiffness using the formula used for determining the thickness:

$$\frac{Force \cdot Armlength}{Displacement} = Stiffness\ (Nm/°)$$

The test setup used for measuring the stiffness of the samples is illustrated in Figure 73. Further details and information about these tests can be found in Appendix H.

SLS printed samples were measured to approach the aimed for value of 0,24 Nm/°. These samples mimicked the shape of the foot with variable thicknesses and were used in the same test setup to measure their stiffness.

It can be derived from these measurements that the thickness of the sole will likely have to increase to approximately 3,5 mm compared to the measured 2,2mm of the carbon dorsal leaf spring footplate. The current AFO is used in combination with an inlay sole that sits between the AFO footplate and the sock of the user. Increasing the footplate thickness would have to be counteracted by a reduction of the thickness of this foot sole. These soles are currently produced by Livit Ottobock Care themselves through CNC milling. These foot soles cannot be produced too thinly or else they will lose their rigidity underneath the CNC machine and would fail.

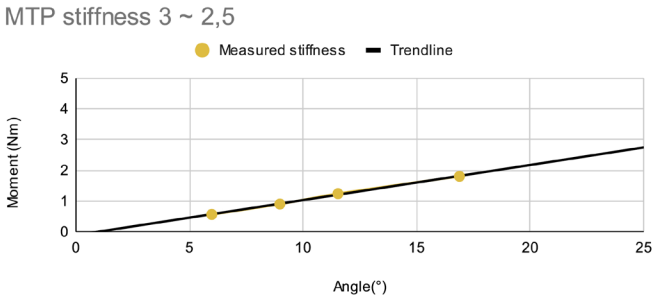

figure 72.1: average stiffness: 0,102 Nm/°

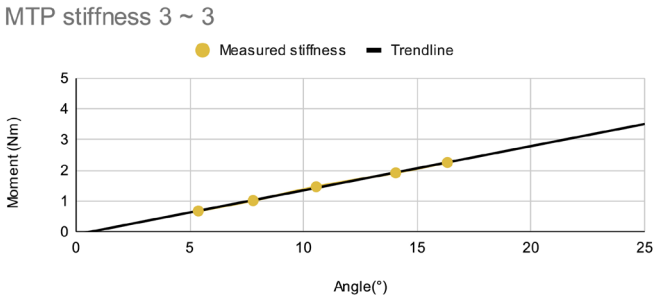

figure 72.2: average stiffness: 0,134 Nm/°

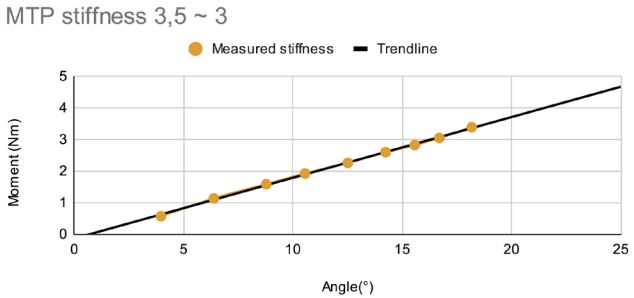

figure 72.3: average stiffness: 0,177 Nm/°

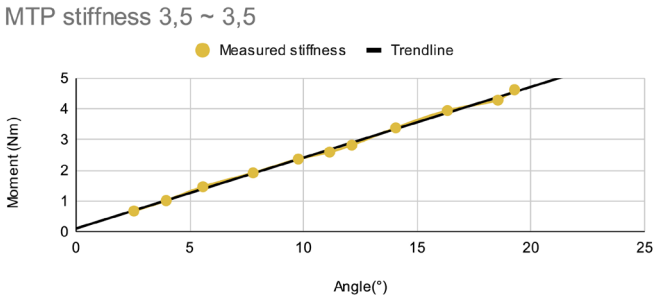

figure 72.4: average stiffness: 0,245 Nm/°

Exploring the potential influence on the production of the foot soles would be a valuable aspect to consider in the continuation of this project. Further investigation is needed to determine how adjustments to the footplate thickness would affect the production process of the foot soles.

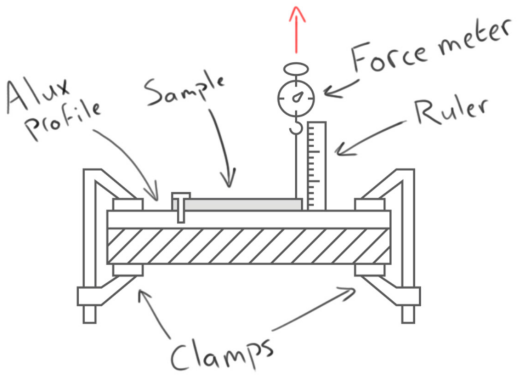

figure 73: Schematic overview of test setup

Resulting Ridge prototype

The knowledge collected so far is combined into a new prototype. This prototype was dubbed the Ridge prototype due to the inclusion of ridge-like structures on the back of the strut.

Comparing the ridge prototype to the 2345644 prototype gives the following differences:

- The thickness around the heel is increased to 4,5mm (point C in figure 46) compared to 4.
- The thickness of the strut is reduced to 5mm (point E in figure 46) compared to 6mm
- The thickness at the MTP and tip point of the footplate are increased to 3,5mm (point A and B in figure 46) compared to 2 and 3mm.
- The shape of the heel arch has been adjusted to be a gradual slope instead of an even fillet
- Ridges are present at the back of the strut placed 4 mm from the edges of the strut, 7mm wide and protruding 6mm.
- The strut has been reduced in width from 60 mm to 53 mm as the most stiffness now derives from the ridges
- The CAD model has been tweaked to be more symmetrica and 'clean'
- The model weights in at 235 grams compared to the 215 grams of prototype 2345644
- The model costs €260,- to print compared to the €240,- of prototype 2345644 (both excluding tax)

This prototype, just like the 2345644 prototype has been printed using PA11 and vapour polished to prevent moisture absorption and to smooth out the surface. The decision was made to dye this prototype blue for a more clear distinction between the two.

Stiffness evaluation of the ridge prototype

BRUCE measurements were conducted to measure its actual stiffness. The home setup measurements proved unreliable so none were conducted for this prototype. The data regarding the BRUCE measurements can be found in Appendix I.

During the BRUCE measurements, an average negative moment of 1.54 Nm/° and an average positive moment of 1.00 Nm/° were recorded.

A comparison between the measurements obtained from the ridge model and those conducted with the 2345644 prototype is presented in figure 74. To facilitate a more accurate comparison, the neutral angle of both orthoses was offset to 0.

It is evident from this figure that the stiffness has increased in both the plantar flex and dorsiflex directions. Although the dorsiflex direction still exhibits some buckling, it is significantly reduced compared to the previous prototype. Additionally, figure 74 demonstrates that the ridge prototype can withstand a greater plantar flex angle without fracturing.

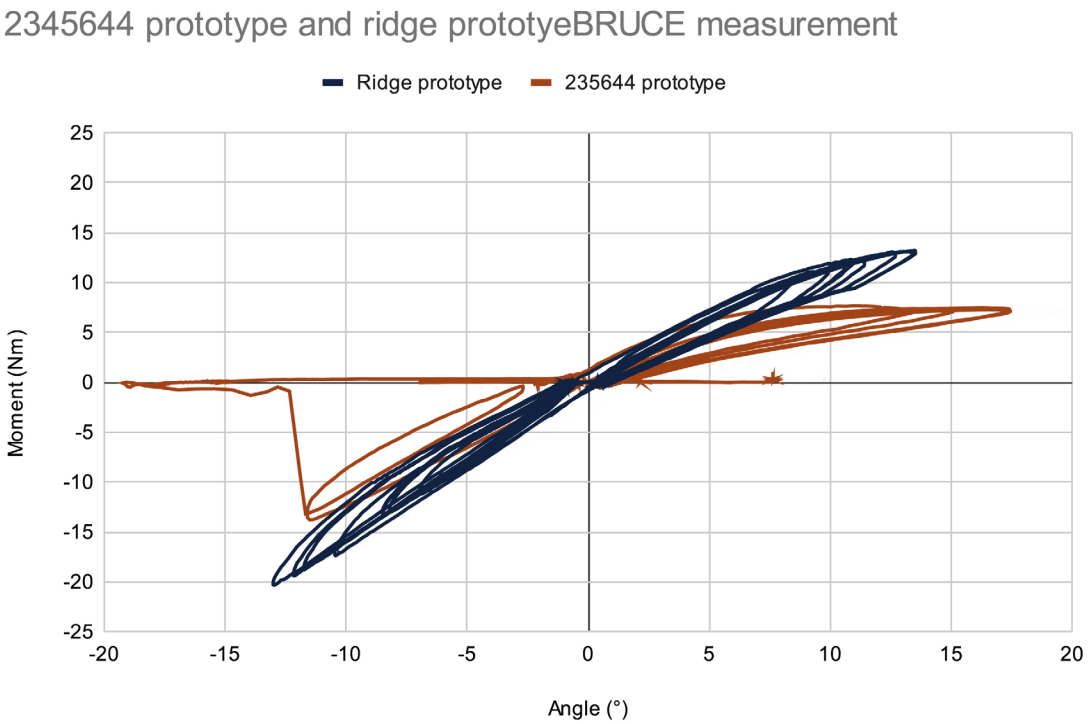

figure 74: BRUCE stiffness comparison between prototype 2345644 and the ridge prototype

Figure 75 shows the comparison between the ridge prototype and the carbon dorsal leaf spring measurements. The data shows some deviations between the ridge prototype and the carbon dorsal leaf spring AFO:

- The dorsal leaf spring AFO shows more linear stiffness behaviour than the ridge model
- The ridge prototype is slightly stiffer than the dorsal leaf spring orthosis in the plantar flex direction
- The ridge prototype is slightly less stiff than the dorsal leaf spring orthosis in the dorsiflex direction
- The ridge prototype buckles in the dorsiflex direction

What can also be seen in Figure 75 is that the carbon dorsal leaf spring AFO was measured using larger angles. This is due to how the BRUCE setup used by the Amsterdam Medical Centre operates, as the data measured during the test is in volts. The current setup can only convert these values afterward into the correct angle and moment. Therefore, the magnitude of the angle was indeterminable while conducting the test, and estimates were used.

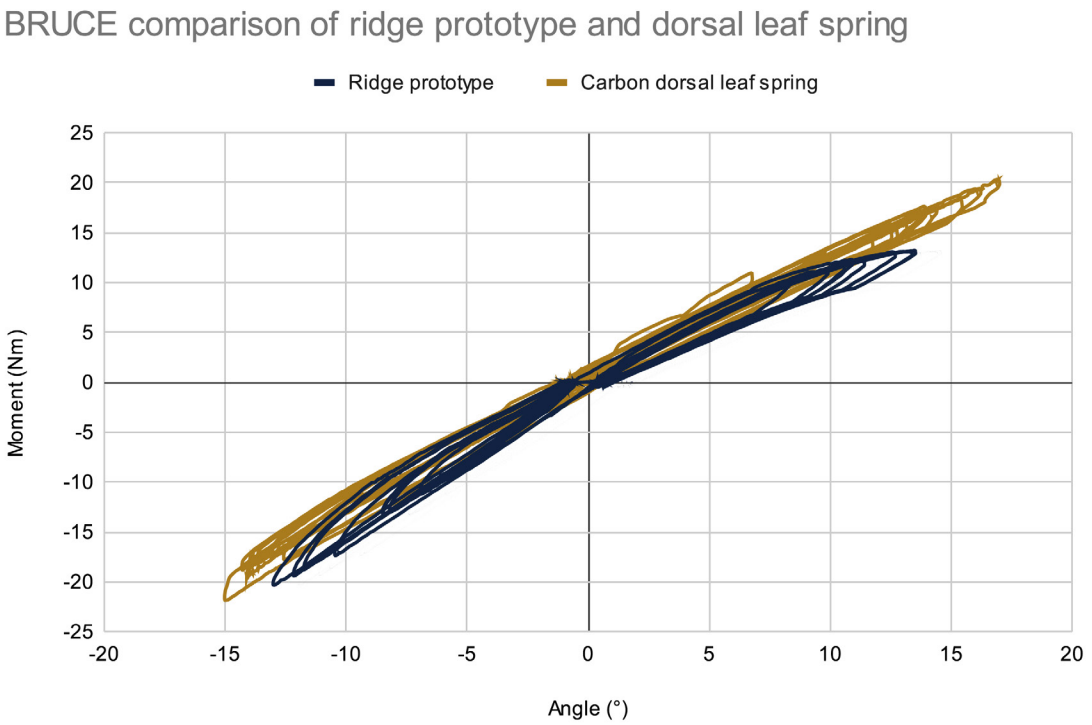

figure 75: BRUCE stiffness comparison between the ridge prototype and the carbon dorsal leaf spring orthosis

MTP stiffness evaluation

A home setup was used to evaluate the MTP stiffness of the footplate. Ideally, the BRUCE setup was also used to validate the characteristics of the MTP line. Unfortunately, the BRUCE setup employed by the UMC in Amsterdam was still unable to measure the stiffness around the MTP joints.

However, since the stiffness through this line was also measured using the home setup with the carbon dorsal leaf spring orthosis, using the same setup again for the Ridge orthosis will provide high precision but possibly low accuracy. It will, at least, indicate if it behaves comparatively to the MTP behaviour of the carbon dorsal leaf spring.

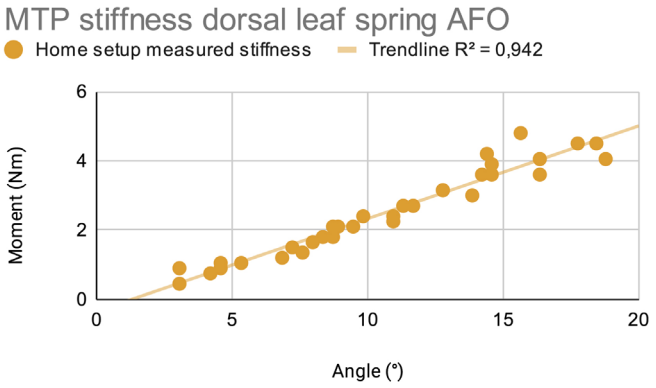

figure 76: Homestup measurements of MTP stiffness in the Ridge prototype

The data for the ridge prototype MTP measurements can be found in Appendix J. This data can be used to generate the graph in figure 76, which consists of three different measurements combined. A trendline is fitted to the data to better visualize its average stiffness. The calculated stiffness is 0.22 Nm/°, which is considered very comparable to the target value of 0.24 Nm/°.

According to the experts at Livit Ottobock Care[14], the ridge prototype featured an exceptionally long footplate tip. It was suggested that the flanks on either side of the footplate, which provide mediolateral stability and prevent the footplate from bending, should have been extended further towards the MTP joint line (*figure 77*). Implementing this change would increase the stiffness by reducing the length of the arm. Consequently, it would be possible to decrease the thickness of the footplate to a value below the current 3.5 mm, while still achieving the desired stiffness of 0.24 Nm/°. This modification should be considered for the next iteration.

The footplate of the carbon dorsal leaf spring orthosis can be fabricated using three different stiffness values, as explained on page 37. The current SLS printed prototype is based on the medium stiffness value. It should be noted that there are stiffer and more flexible footplates available, although their quantified stiffness values were not provided for this project.

The more flexible footplate will most likely not prove difficult as Pa11 is a very flexible material as proved by the footplate of prototype 2345644 (*figure 78*). This footplate was at the tip 2 mm thick and at the MTP line 3mm thick. This footplate proved to be extremely flexible without breaking. Therefore, it is highly probable that an SLS printed orthosis can be manufactured with a more flexible footplate.

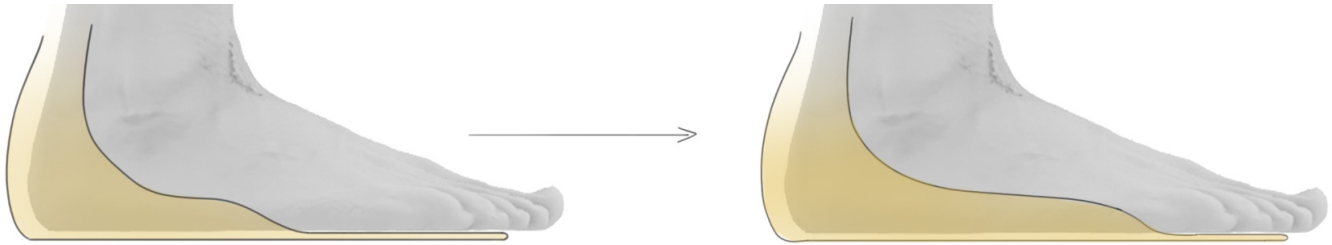

figure 77: footplate without side support should have been closer to the MTP line

However, creating a stiffer, rigid footplate may pose challenges. Increasing the footplate thickness would result in clamping the toes against the roof of the shoe, causing discomfort. An alternative solution needs to be explored if an SLS printed orthosis with a stiffer footplate, similar to the carbon dorsal leaf spring orthosis, is desired. One possibility is to incorporate a stiffer external material, such as a carbon plate, into the footplate of the orthosis to provide additional stiffness (*figure 79*). However, the feasibility of this approach using SLS printed materials has not been validated and requires further research.

figure 78 The more flexible SLS printed footplate of prototype 2345644

figure 79: An external ridged material such as a thin carbon plate can potentially be added to the SLS orthosis to create a more stiff footplate

Model buildup

The current prototype does not display the same stiffness behaviour as observed in the carbon dorsal leaf spring orthosis. However, it does approach the same stiffness characteristics. More iterations on the design are necessary to close the gap between the two.

Due to the time constraints of this project, no further iterations are made in this thesis. However, to facilitate future development and design enhancements, including iterative improvements and adaptations for different foot models, a generative model was developed and explained in this chapter.

Input parameters

The AFO is custom-made for each individual client. To streamline the design process, a model was created that can efficiently convert the orthopedic advisor's parametric input into a printable model.

It is essential to keep an overview of the input needed for designing an orthosis and how this influences the final design.

Some of the parameters currently defined by the orthopedic advisor are listed in figure 80. Other parameters incorporated in the adjusted CAD model are:

- AFO height
- Fixation circumference
- Medial malleolus distance
- Medial longitudinal arch
- Lateral malleolus distance
- Lateral longitudinal arch
- (os) Navicular distance
- 5th metatarsal distance

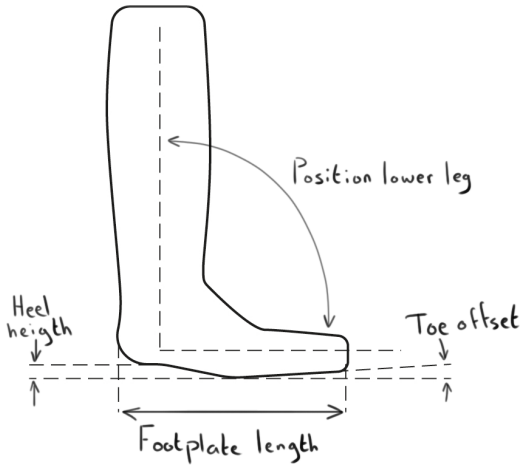

figure 80: foot measurements taken to make an AFO fit

The production facility of Livit Ottobock Care only functions as an executive practitioner and follows the predefined parameters in the production of the orthosis. This approach was also followed in generating the model used for the SLS AFO.

The current workflow at Livit Ottobock Care already involves creating a CAD model of the lower leg and foot. This is done by making a cast on the location of the orthopedic advisor and sending this cast to the production facility. The cast is then scanned and stitched together digitally, resulting in a 3D representation of the lower leg (*the top image in figure 81*).

The model is digitally adjusted to incorporate most of the input parameters, resulting in a cleaned up model (*bottom image in figure 81*). The mesh is modified to achieve streamlined geometry, including a flat foot sole, smooth surfaces, and inflated areas to accommodate padding or create distance between the AFO and the malleoli for example.

figure 81: From 3D scan, to cleaned up model

figure 82: From 3D scan, to SLS AFO

Livit Ottobock Care incorporates all the relevant parameters digitally into the model before milling it out of foam. The foam model is then used as a base to apply carbon layers and create the AFO. While their custom in-house software is capable of generating features, manual adjustments are often necessary.

The proposed workflow described on page 20 and 21 aims to eliminate the need for milling a foam model, resulting in changes to certain CAD steps. Since Livit Ottobock Care already includes most parameters and generates adjusted CAD models, the decision was made to base the SLS printable model on these existing models.

Therefore, this report will not delve deeper into the scanning of the leg, measurements, and required distances, as well as the digital adjustments made in CAD for model cleaning and achieving the desired shank vertical angle (the combined angle of the lower leg position and heel height).

Instead, the SLS AFO can be automatically generated on top of the cleaned-up adjusted model (*bottom image in figure 82*).

To achieve accurate results and provide design freedom for the orthosis modeling, other input parameters become relevant. These parameters allow for precise adjustments and offer control over variable stiffness, as well as customization in the shape of the AFO for an optimal fit.

These tweakable parameters include:

Fitting
- The position of all points in the X, Y and Z direction of the trim lines
- The fillet radius of the cuff
- The fillet radius around the toes

Thickness
- The position of thickness points
- The AFO thickness at these points

Backridges
- The width of the back ridges
- The length of the back ridges
- The depth of the back ridges
- The distance from the strut edge of the back ridges
- The slope of the back ridges

The model was built using the Rhino[53] software with the Grasshopper plugin as these programs specialise in parametric modelling. An attempt was made to create a rudimentary interface using this software for easy manipulation of these values and faster iteration. This could in the future be modified for easier use. This interface can be found in Appendix K.

The automatic steps that the Grasshopper model uses to generate the orthosis are broken down on the following pages to break down the model and make it easier to understand. A near complete overview of the Grasshopper code can be found in Appendix L. An attempt was made to structure the program and thus groups were made. In total, the Grasshopper code can be divided into 15 steps, where the 16th step is executed in Solidwords as this proved easier. The model is capable of generating an orthosis in 8 seconds. It has to be said that this model was composed with great help from various sources. In particular, the thesis of van Leijsen, L. (2020)[56] was useful as well as guidance and tips from Anne van den Dool.

Step by step breakdown of the Grasshopper model

1

The cleaned and adjusted mesh is imported into Rhino and opened in Grasshopper

2

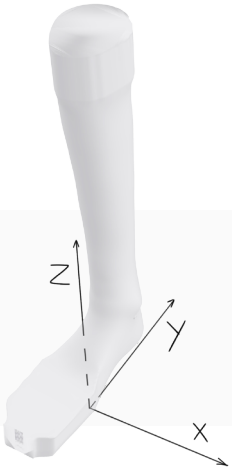

The model is aligned with the XY plane

3

A cross-section is made in the caudal plane of the foot and divided into points. A line is then fitted to this collection of points to find the average axis along the foot

4

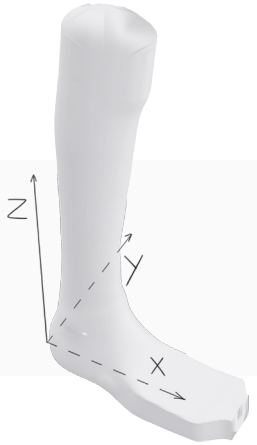

This line is fitted parallel to the X axis to orient the model at the origin

5

A cross section is made in the XZ plane and a curve is generated at the boundaries of the model. This is then divided into points

6

The points along the plantar surface of the foot, around the heel and the back of the leg are extracted and cross sections at an angle are generated from these points

7

A loft is generate from these cross-sections

8

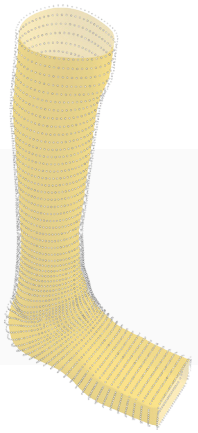

The curves are divided into points and variably offset along the normal vectors of the surface to create the desired thickness

9

A second surface is constructed from these points and the surfaces are stitched together

10

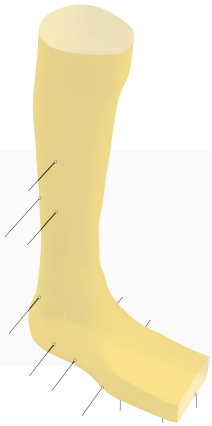

Points are generated on the surface using moveable intersecting lines to generate the trim lines of the AFO

11

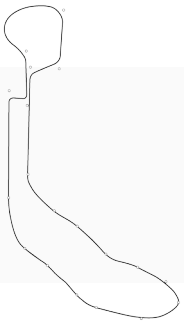

A curve is generated following the inner surface of the AFO through these points

12

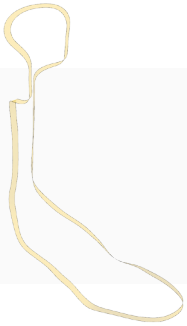

The curve is offset along the normals of the AFO surface and a surface is generated between these curves

13

The AFO shell is split with the surfaces of the AFO cut lines to make the main shape of the AFO

14

Ridge surfaces are generated at the back of the orthosis using the straight trim lines on either side of the strut as a basis. These surfaces are then lofted together

15

Everything is merged and stitched together to create a solid boundary representation

16

Holes are extrude for the attachment of the cuff and fillets are added using Solidworks

VALIDATE

User testing

The SLS-printed orthosis has been quantifiably validated in an attempt to mimic the stiffness of the carbon dorsal leaf spring orthosis. The main focus of this thesis was to validate whether SLS-printed orthoses can achieve the same stiffness behaviour as carbon orthoses, while remaining intact and serving as a competitive alternative in terms of price, weight, and design. The function of the orthosis has thus far only been validated theoretically without having a user directly involved.

Participant

A suitable participant, willing to take part in this test, was found through the help of Livit Ottobock Care. The participant was required to have prescribed carbon dorsal leaf spring orthoses and experience walking with them for an extended period of time.

The participant in question has treated Spina Bifida with prescribed dorsal leaf spring AFOs for both of his feet based on his diagnosed gait. For the best AFO function, inner shoes are attached to his orthosis for a better fit and function (figure 85). These inner shoes can be worn inside of regular shoes and are attached with rivets to the footplate of the orthosis to provide a snug fit, securing the foot soundly and exerting extra pressure on the top of the foot for an increased 3-point pressure (*figure 8*). It is common to prescribe a carbon dorsal leaf spring AFO with an attached inner shoe[14]. The decision was therefore made to attach an inner shoe to the SLS printed design as well to provide a more realistic scenario and even comparison to the carbon orthosis by providing the same function.

Production

To validate the final ridge design, two prototype orthoses were manufactured using the input parameters as described on pages 74 and 75, along with the scanned CAD models of the participant.

These models (*figure 83*) were produced well in advance of the user test. As a result, not all design considerations are present in these prototypes, as they were queued in production before the final design was determined. Therefore, these prototypes do feature the ridges introduced in the ridge prototype, but do not have all the adjustments in place to reduce the chance of fracture. They are printed in the improved print direction (figure 61.5) but does not feature the gradual slope present in the heel arch.

The stiffness of these models was based on FEA simulations that aimed to achieve the desired simulated stiffness behaviour introduced on page 60 (figure 84).

Although these prints are based on older data, the test would still provide valuable insights into the influence of the SLS-printed orthoses on gait and the overall reception of these orthoses.

The inner shoes were produced by the tailors at Livit Ottobock Care. Padding and clasps were also added by Livit for comfort. The rsult demonstrate how an orthosis could look like when it was produced through a collaboration between the two involved parties.

This resulted in the prototypes seen in figure 85.

figure 83: 3D models generated for the right and left foot of the participant

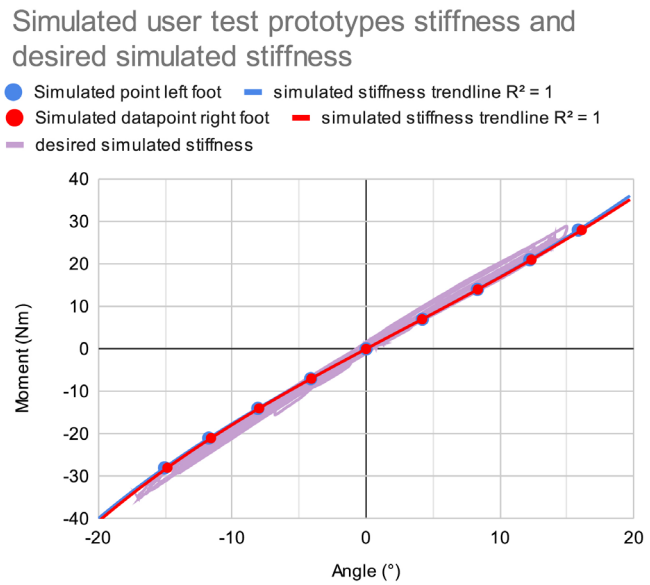

figure 84: simulated stiffness of user test prototypes compared to desired simulated stiffness behaviour

Test setup
The full test setup document and consent form can be found in appendix M.

This test aimed to determine if the SLS printed orthoses would depict similar behaviour compared to the carbon dorsal leaf spring orthosis and have a positive effect on the gait of the participant. The tests were conducted at the medical centre Blixembosch in Eindhoven, with the presence of an orthopedic advisor from Livit Ottobock Care (Chantal Engel) to assist in the tests.

The participant would conduct three rounds of gait analysis: once walking a trajectory without any aid, once walking the same trajectory with the carbon dorsal leaf spring orthosis and once the same trajectory with the SLS printed orthosis, all on a treadmill.

These trajectories were carefully recorded using trackers placed on the participant's joints, specifically capturing the ankle angle and lower leg position. The full extent of this test and its results can be found in appendix N.

The participant was asked several questions during and after these tests regarding his experience and perception of the SLS-printed orthoses.

Finally, the participant was asked to perform some everyday activities whilst wearing the SLS-printed orthoses, such as walking outside, walking on a slope, walking up and down a set of stairs and even running and sprinting on a patch of grass, as he enjoys playing soccer while wearing his orthoses. (*figure 87*)

Results
All the results and analysis can be found in appendix N.

The ankle angle of the participant was tracked in the sagittal plane and can be found in figure 86, along with the ankle angles present when not wearing any orthosis and ankle angles present for a normal gait pattern as defined by Whittle[13].

It was established that the participant needed to wear his orthoses as he is unable to plantarflex. This can be seen by looking at the blue line in figure 86, which almost does not plantarflex. The heel-off phase is delayed because of this, and the ankle only really plantarflexes between initial contact and the weight acceptance phase.

The orthosis did not break and the participant expressed that the orthoses felt good during the everyday testing such as walking around, walking stairs and running. He had the idea that they were slightly stiffer initially, as it made him stand more upright, but after some time, he expressed that they felt similar.

Interpretation and implications
Comparing the effect of the carbon orthosis to the SLS-printed orthoses reveals minimal differences when analyzing figure 86. Both smooth out the plantarflexion between initial contact and weight acceptance and reduce the degree of dorsiflexion by the participant. It is possible that the SLS orthosis is slightly stiffer in the dorsiflexion direction compared to the carbon orthosis, thus limiting the degree of dorsiflexion slightly more. It was noted that the SLS orthoses felt slightly more rigid or stiff, but this might also be due to it being a new orthosis with still stiff leather as well.

figure 85: Prototypes used for the user test

It was established during the conduct of these tests that the main reason why this participant wears AFOs is to stabilize himself while standing still. During standstill, the participant would lean forward, having his knees very flexed and hanging in the orthoses, relying on their stiffness to provide a positive moment, keeping him balanced. Both the carbon orthosis and SLS orthosis worked well, according to him, to provide this moment.

To further explore the behaviour of the AFO during normal use, the participant was asked to walk around and perform various tests. It was stated during these tests that they felt different, but not in a bad way. They felt good and similar in function to the carbon dorsal leaf spring orthoses. The participant stated to be very positive about the fit and function of the orthosis and showed interest in a potential follow-up study to wear the AFOs for an extended period.

The most important insight was that the participant was able to walk around with the orthosis, walk stairs and even run without the orthoses breaking. These tests were only brief and not repeatedly done, but they demonstrated the potential of SLS orthoses.

Caveats and limitations

A clear caveat is that the stiffness values of these orthoses were not accurately measured. More insights and design considerations were explored after producing these prototypes, which could have improved their behaviour, had they been implemented.

Another factor influencing this test is the exclusion of an important design consideration when making the intermediate model (middle image in figure 82). Usually, the model is inflated around the legs to make room for the padding of the AFO. This was however missing in the printed model, requiring the removal of the padding for the orthoses to fit. Fortunately, the participant wore high thick socks underneath ensuring enough cushioning was present for the AFOs to fit comfortably. He did not report any discomfort or skin rubbing, despite the padding being removed.

It was also discovered during testing that the carbon orthosis the participant wore had the highest stiffness value through the MTP line instead of the middling stiffness value of 0.24 Nm/°. As his knees flexed extensively a stiffer footplate would have helped to provide a bigger counteracting moment. Interestingly this did not have a lot of effect on his gait. This could be attributed to the potentially stiffer strut of the SLS orthosis, which limited knee flexion.

However, the most important limitation of this test is that it involved only a single pair of SLS-printed orthoses for a single participant. To draw better conclusions, further tests need to be conducted with larger participant groups and over extended periods.

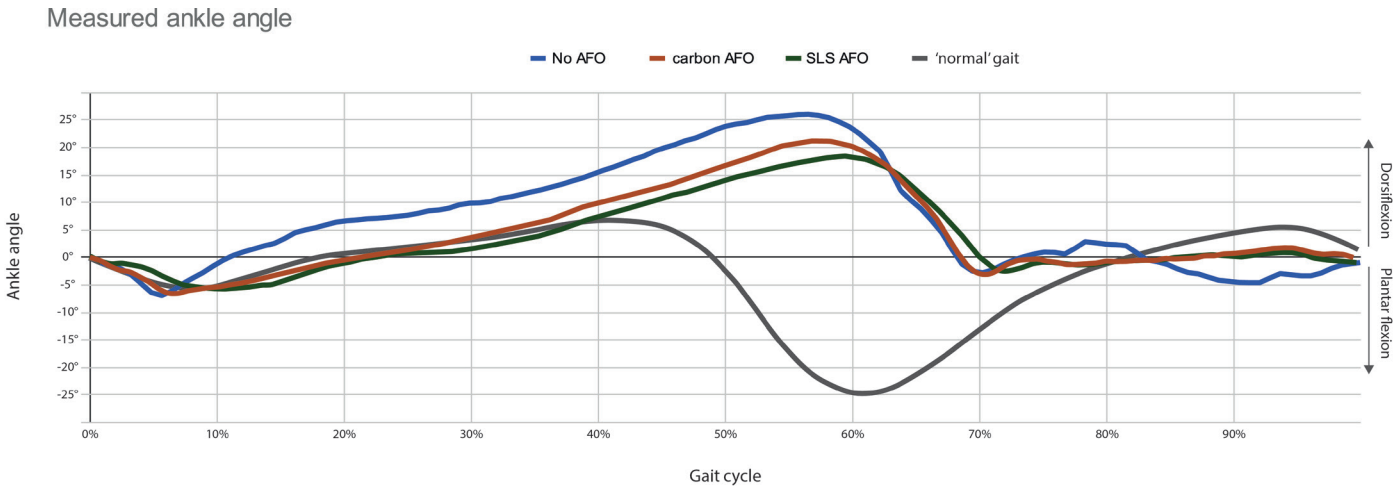

figure 86: ankle angle during a full gait cycle of the participant when no AFOs are worn, when carbon AFOs are worn, when SLS printed AFOs are worn and a 'normal' gait cycle as depicted by Whittle[13]

figure 87: The participant was asked to walk around, climb stairs and run whilst wearing the SLS AFO

Requirements

Some requirements were addressed in the preceding chapters, but for better comprehension, an overview is presented here. The final result closely aligns with most of the requirements listed on pages 39 to 42, but not all of them are fully met. This chapter aims to validate the extent to which the identified requirements have been achieved.

Mechanical

"The AFO should be able to provide a linear positive moment of 1,23Nm/°"

The positive moment of the ridge prototype measures 1.00 Nm/°. Figure 75 illustrates that this moment does not exhibit linear behaviour. While this value falls within a 20% range of the targeted value, it does not meet the desired 10% accuracy.

The user test showed that extensive dorsiflex flexure can be present in the orthosis, theoretically reducing the moment as the positive moment decreases when it is exposed to greater angles. This did not have a significant effect on the gait of the participant who partook in the research but might have on others.

The influence of the orthosis decreasing in stiffness is something to closely regard in the case of continuing this project, especially qualitatively. It is currently undocumented what influence the attachment of an inner shoe has on this moment and how significant this moment is exactly when the AFO is worn.

"The AFO should be able to provide a linear negative moment of 1,14Nm/°

The positive moment of the ridge prototype measures 1.54 Nm/°. While this value can be considered linear, it falls within a 35% range of the targeted value, which does not meet the desired 10% accuracy.

Lowering this value though altering geometry may also decrease the positive moment. One possible solution is to adjust the ridge parameters, which can increase the positive moment to a greater extent while having a lesser impact on the negative moment. By tweaking these parameters, it may be possible to improve the performance and achieve a more desirable positive moment within the desired range without compromising the positive moment too much.

"The AFO should be able to provide a moment through the MTP line with a value of 0,24Nm/°"

As indicated on pages 72 and 73, the current MTP value for the ridge prototype is measured to be 0.22 Nm/°. This measurement meets the desired 10% accuracy requirement. However, it is important to note that this measurement was not conducted using the BRUCE setup.

"The AFO should provide a negative moment of at least 0,36Nm/° and at most 1,8Nm/°"

The positive moment of the ridge prototype was 1.54 Nm/°, which falls within the aimed for range. Ideally, this value would be lower.

"The AFO should be able to withstand an impact force of 62N/cm² exerted vertically on the plantar surface of the AFO around the heel"

An FEA simulation was conducted to assess the ability of the SLS-printed AFO to withstand the applied force (*see figure 88*). However, it is important to note that this simulation does not fully replicate the actual scenario. In reality, a shoe is worn over the orthosis, which distributes some forces, and a foot with a sock on is placed directly inside the orthosis, along with an insole that also helps distribute forces. In the simulation, a force of 1600N was applied to a round surface area of 26cm² on the plantar surface of the foot.

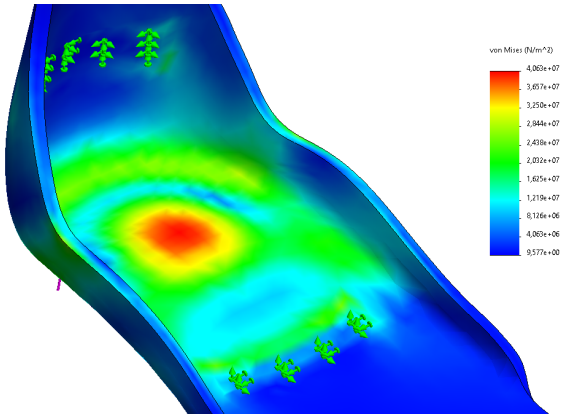

figure 88: FEA vonMisses stress results of 1600N impact force on 26cm² around the heel of the AFO on the plantar surface of the foot.

The simulation resulted in an 8mm displacement, which would be perceptible to the wearer. It is estimated that this value would be lower in reality as the afore mentioned shoe, sock and insole will distribute most of the force. At the red centre in figure 88, a pressure of 40.6 MPa is present. This pressure is close to the tensile strength of 51 MPa (as stated in the material table in figure 16) and is highly dependent on the fixation method used in this study. Currently, the AFO is fixed 5 centimetres away from the loaded surface.

Based on the available data, it is deemed plausible that the AFO is able to withstand this force.

Ergonomical

"The AFO should not exert pressure on the malleoli, navicular and tuberosity of the 5th matatarsal"

Careful consideration is made to avoid exerting pressure at these points while designing the orthosis. The archline stops before the malleoli and navicular while maintaining a distance from the tuberosity of the 5th metatarsal by inflating the intermediate CAD model (*middle image in figure 82*) to ensure proper spacing within the orthosis.

The participant did not express any discomfort at these points during the user test and stated that the AFOs fit well. The participant in question did however have numb feet, being unable to feel anything at these points. This should therefore be cross-referenced with other user tests to see if the AFOs would still be considered comfortable.

"The AFO should not exceed 5mm thickness around the heel of the foot"

A digital measurement was conducted using Solidworks to determine the final thickness around the heel (*figure 89*). The overall thickness is below 5mm, but the ridges protrude slightly over 10mm. These ridges could be pressed into the cushioning material of the shoe and did not pose any problems during the user test. This can however depend highly on the type of shoes worn by the user.

To potentially reduce the thickness of the orthosis around the heel, the ridges could start at a higher point. The parameter that influences this has been included in the Grasshopper model for further adjustments. The effect of this parameter has not been explored however.

"The AFO should be able to bend 15° in the plantar flex direction and 20° in the dorsiflex direction without breaking"

During BRUCE testing, the ridge orthosis was subjected to 13,15° in the plantar flex direction and 13,65° in the dorsiflex direction. In the user tests, the orthoses were exposed to 7,00° in the plantar flex direction and 18,90° in the dorsiflex direction.

It is estimated that the orthosis was exposed to bigger angles during the running exercises conducted whilst wearing the AFOs, but these specific angles were not documented.

It is noteworthy that the AFOs did not fracture or break when exposed to these angles.

To obtain more accurate results, BRUCE measurements with higher angles need to be conducted with different specimens to fully validate of an AFO can bend to such extreme values. Consequently, users should wear the orthosis for longer periods of time to see if they hold up.

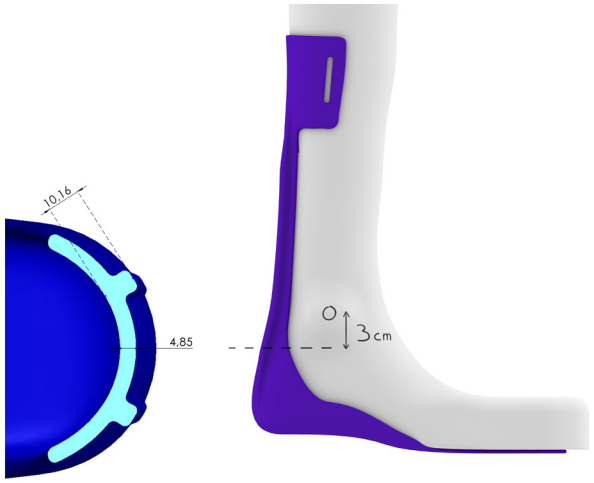

figure 89: Thickness measurements in Solidworks of the ridge prototype, 3 cm below the malleoli

Material

"The AFO should operate within its elastic deformation range"

The yield strength of the Pa11 material used by Parts on Demand is currently unknown. However, the tensile strength in the XY direction is 51 MPa, and in the Z direction, it is 47 MPa. Pa11 is considered to be the most flexible material, next to TPU, printable by Parts on Demand.

To estimate its yield strength, an average value from competitive SLS printing companies capable of printing Pa11 is used, which is approximately 36.7 MPa[54],[55].

Using this estimated yield strength value, FEA simulations were conducted to estimate the point at which the AFO would start to experience plastic deformation. The simulations indicate that the AFO would begin to deform plastically when bent beyond 25.3° in the dorsiflexion direction and 22.4° in the plantarflexion direction (*figure 90*), calculated using the formula:

$$Tan^{-1}(Displacement/Armlength) = Angle$$

These angles are above the expected range of motion and the AFO would therefore theoretically not plastically deform. However, in the case of dorsiflexion, the angles approached those observed during the user tests. It is therefore, again, advised to further evaluate this with BRUCE measurements and physical examination to see how the AFO behaves when exposed to these angles.

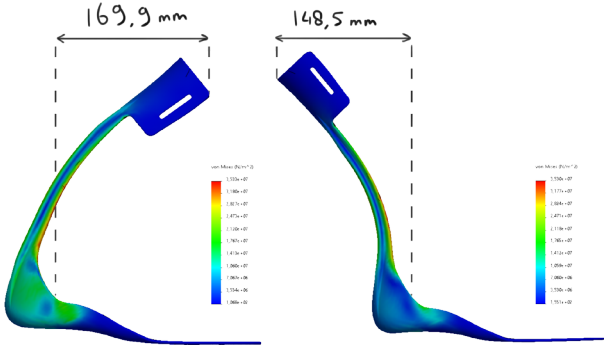

figure 90: Displacement in dorsiflex direction and plantar flex direction before the material starts to plastically deform

"The bounding box should not be bigger than 250x250x500mm for shotpeened parts and 270x300x570 for Vapour Polished parts "

A bounding box is digitally drawn over the Ridge prototype (*figure 91*). The orthosis should be vapour polished in the end, so the bounding box should not exceed the dimensions of 270x300x570.

Based on estimations, the height of the orthosis is not expected to exceed 500 mm. The length from the plantar surface of the foot to the hamstring is on average 467 mm and can extend up to 534 mm to accommodate 95% of the Dutch population aged 20 to 60[32]. The orthosis will be mounted well below this point and these values will likely be lower as this orthosis is also mainly prescribed to children (85%)[12].

It is also estimated that the length of the orthosis will not exceed 300 mm. The length from the heel until the toes of Dutch citizens aged 20 to 60 is on average 253 mm and can go up to 286mm to fit 95% of the population[32]. It is therefore unlikely that the length of the orthosis will ever excel 300 mm.

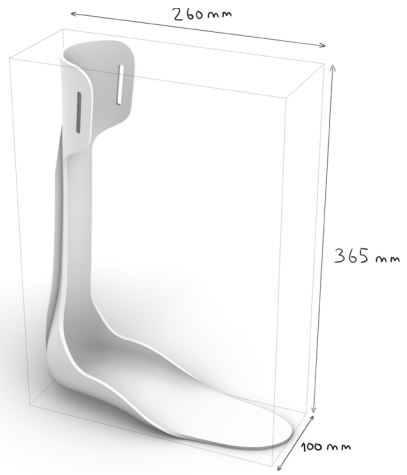

figure 91: Bounding box measurments of the ridge prototype

It is also estimated that the width of the orthosis will most likely not exceed 120 mm. Again using the same database, the average foot width is 96mm and can go up to 108mm to fit 95% of the population.

"The wall thickness of the SLS printed AFO should be bigger than 1.5mm"

The thinnest part of the AFO is located at the toes. This has to be around 3.5mm to facilitate the right stiffness for the MTP joints. The orthosis therefore does comply with this requirement which should reduce the chance of warping.

"All Vapour Polished parts should have a cavity to hang from"

The orthoses currently feature slits at the top for the mounting of the cuff. The current carbon dorsal leaf spring orthosis uses a hole in this place, also to mount the cuff. The hole can serve as a convenient attachment point for suspending the orthosis, ensuring optimal access and coverage during the vapour polishing treatment.

Miscellaneous

"The production time of the SLS printed parts should not be longer then 7 workdays"

The production time of Pa11 is 7 workdays[21]. However, this time does not include the vapour polish treatment and colouring of the orthosis. Parts on Demand officially add 1 extra workday for each post-processing step resulting in a production time of 9 workdays. This exceeds the required 7 workdays and would produce the following timeline:

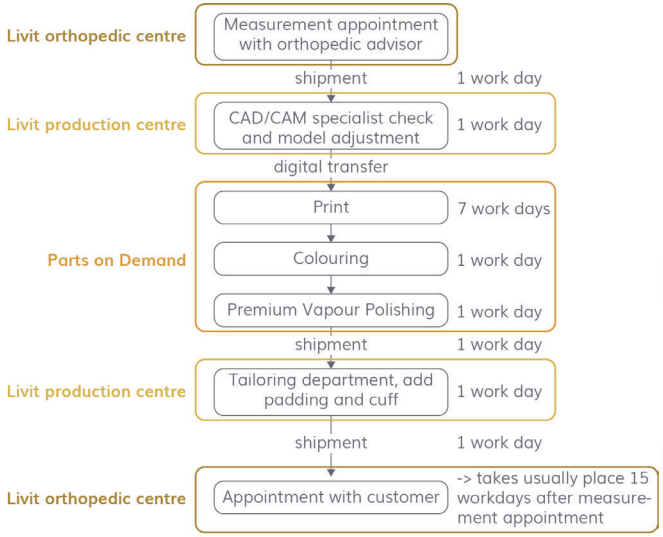

figure 92: Production timeline if production of the printed parts would take 9 workdays

This would make achieving the desired appointment date with the customer very tight. It is possible to accelerate the SLS print production time if the prints are given higher priority. This can potentially be arranged through negotiations between the two involved parties which is not uncommon for Parts on Demand.

It is anticipated that the production time for Pa11 parts will decrease over time as the material continues to be developed and allocated to multiple printers. With the availability of more printers capable of printing this material, it is foreseeable that express delivery times of 3 to 4 workdays will be achievable in the future. This improvement in production efficiency will contribute to faster turnaround times for manufacturing Pa11 orthoses but will probably come with a higher price.

"The SLS printed parts should cost no more than €300,-"

The prices of the following orthoses are measured using the custom pricing tool from partsondemand.eu[6]:

Prototype 2345644
€239,60 ex. tax
€289,92 incl. tax
215 gram

Ridge prototype
€259,41 ex. tax
€313,89 incl. tax
235 gram

Left foot user test prototype
€244,48 ex. tax
€295,82 incl. tax
209 gram

Right foot user test prototype
€241,37 ex. tax
€292,06 incl. tax
208 gram

These prices are considered to provide a competitive price point for the carbon dorsal leaf spring orthosis. These orthoses ranged from 35 to 37 cm in height and 24 to 27 cm in length. An orthosis measuring in at 45 cm high and 28 cm in length was generated to calculate how expensive an orthosis would be for a very large leg and foot:

Theoretical large prototype
€278,26 ex. tax
€336,69 incl. tax
? gram

The price increases for bigger feet, but not by an exceptionally large amount.

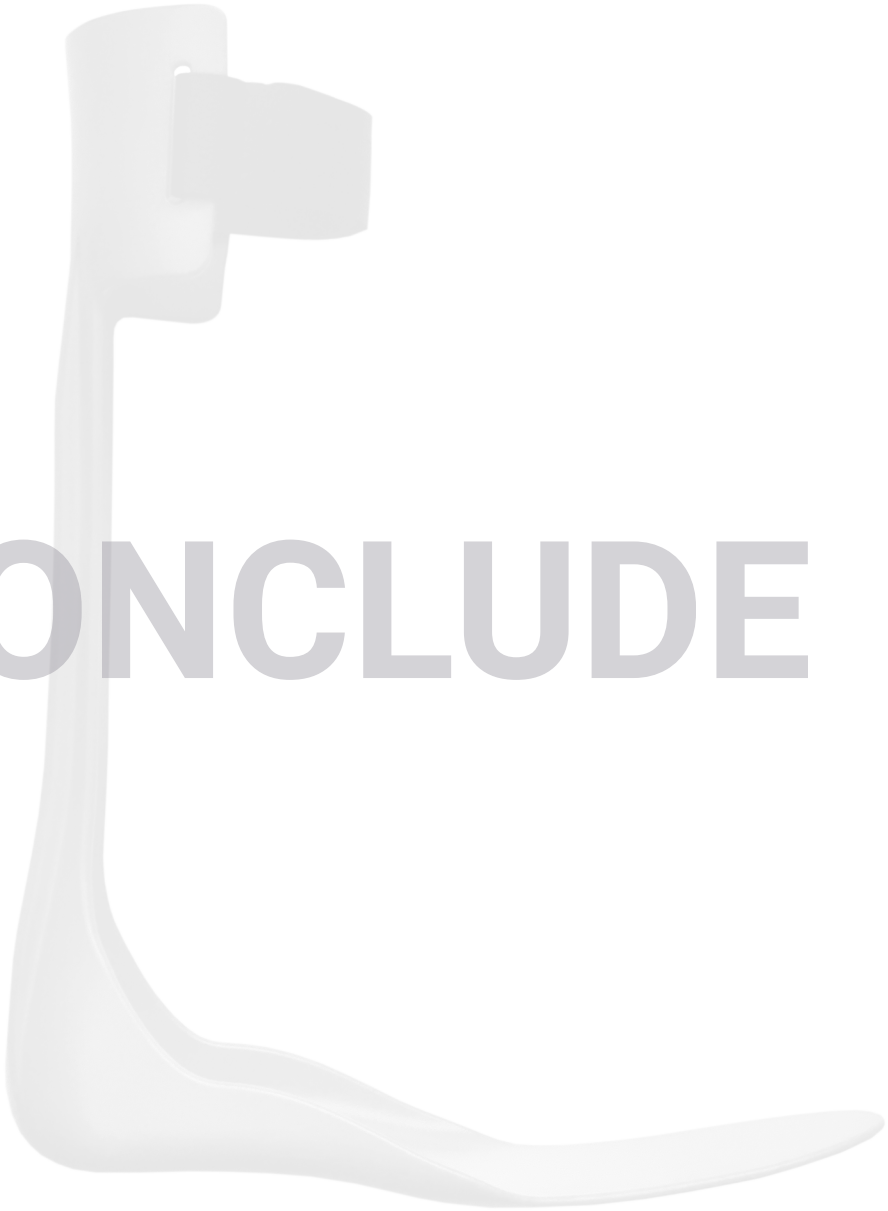

CONCLUDE

Discussion

Should we SLS print a carbon dorsal leaf spring orthosis?
The challenge of this thesis was to create a printable design. This resulted in a prototypes that showed promise on some fronts, but trade-offs on others. To answer the above-posed question, a comparison was made assessing the advantages and disadvantages of the current state of the design compared to the carbon dorsal leaf spring orthosis.

Figure 92 depicts a comparison regarding some important aspects of both types of orthoses. The carbon dorsal leaf spring orthosis is the better option regarding most of these quantified aspects as the material properties of the composite remain superior to the printable materials. Because of this, it can be lighter whilst displaying the same stiffness behaviour.

The moments of the SLS printed orthosis diverge from those of the carbon dorsal leaf spring orthosis in the current design. This however did not have significant effects on the gait correction capabilities of the device as seen in the user test chapter depicted on pages 79 to 81.

SLS printed orthosis

Carbon dorsal leaf spring orthosis

Weight	± 225g (excluding padding, cuff etc.)	147g (excluding padding, cuff etc.)
Price	± €270,- (excluding tax.)	± €300,- (excluding tax.)
Production time	± 12 workdays	10 workdays
Positive moment	1,00 Nm/°, non-linear	1,23 Nm/°, linear
Negative moment	1,54 Nm/°, linear	1,14 Nm/°, linear
Sole thickness	± 3,5 mm	± 2,2 mm

figure 92: data comparison between the current SLS printable design and the carbon dorsal leaf spring orthosis

It is important to note that this study was a single case study conducted over a short period of time and that the SLS printed designs remain prototypes and no final products. Although the SLS orthoses exhibited similar behaviour to the carbon orthoses for this specific test case, they had different moments. To make the step from prototypes to end products the printed orthoses will need to be closer to the aimed for moments. Refining the ridge designs, general geometry or other features unique to SLS printing will result in roughly the same stiffness characteristics of the carbon dorsal leaf spring orthosis if necessary for other users.

The SLS-printed orthosis is currently heavier and thicker than the carbon dorsal leaf spring orthosis. SLS printing and its form freedom capabilities might optimize the design of the AFO by removing unnecessary material. Page 91 will further explore these possibilities. Utilizing this aspect could potentially reduce the weight of the orthosis, theoretically enhancing its comfort. However, reducing the thickness of the orthosis may prove challenging as the moment of inertia plays a crucial role to provide its stiffness.

A bottleneck for the SLS printed orthosis can be its production time. The AFO must be produced promptly to restore mobility and function to the client as soon as possible. Pa11 is still being tweaked and scaled up and is predicted to become the standard material of Parts on Demand but it is not quite there yet. The lead times for Pa11 printed parts may decrease over time, or express delivery and high-priority orders can be arranged through collaboration. However, considering the current state and adhering to prescribed production times, meeting customer demands for a fitting appointment three weeks after the measurement appointment would be a close call.

There are however some advantages that SLS printing orthoses will bring that carbon orthoses cannot. SLS printing excels at automation compared to carbon layering. Once a model has been generated, no human labour is necessary for producing the general AFO shape. This can save up to an estimated 8 hours of human labour[12] also eliminating human error. Reproduction is even better as it just requires a press of a button if an AFO breaks due to unforeseen circumstances.

SLS-printed designs can also fit closer to the skin compared to carbon designs. The carbon composite strut for example needs to bend in a flat plane to prevent delamination whilst this does not count for SLS printed orthosis (*figure 93*). This makes it potentially more comfortable due to more evenly distributed pressure but has not been validated.

Determining whether SLS printing an orthosis is a viable alternative to the current production method remains challenging. The primary concern in this regard is the functionality. The customer is vital when regarding medical aids and thus the device should aid minimally just as well as the current carbon orthosis.

Initial tests yielded promising results in terms of their reception and function. Furthermore, it is believed that the design can still be enhanced to increase both of these factors. Follow-up research is recommended to further validate the design with the main concern being its function over time which will be addressed in the next chapter.

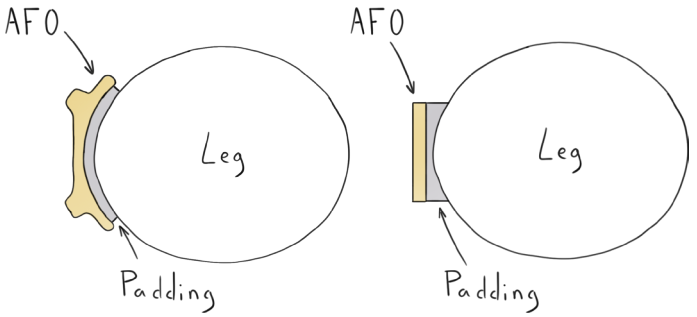

figure 93: On the left, the SLS AFO with more evenly compressed padding, on the right the carbon dorsal leaf spring AFO with more compressed padding in the middle

Recommendations

If this project were to continue, several recommendation are prescribed as to possible follow up steps.

Function
The final prototypes displayed desirable behaviour during the user test. However, further iteration steps are necessary to better approach the desired stiffness and be able to predict it in case other users are in need of it. To continue this research, a tweakable model was developed as a basis to continue or learn from. It is predicted that by adjusting the ridges at the back of the orthosis in relation to the width and thickness of the strut, stiffness values similar to those displayed by the carbon dorsal leaf spring orthosis can be achieved.

Certain forces, such as mediolateral and fore-aft forces, were excluded from this study. The behaviour of the orthosis has only been regarded in the sagittal plane. If this project continues, additional research will need to be conducted including these forces providing a more comprehensive understanding of the AFOs behaviour across all axes.

A major concern still present in the design is that of stress relaxation. Polymers tend to lose their ability to return to their original state if held in a strained condition for an extended period of time. During walking, the AFO undergoes continuous strain and relaxation. This will most likely have an effect on its stiffness behaviour over time. Life cycle assessments have not been conducted and should be considered before producing an SLS-printed orthosis. It is necessary to investigate how the stiffness behaviour of the orthosis behaves when exposed to cycles of strain and relaxation, both through stress relaxation tests and real-life usage scenarios.

It is also recommended to further look into the chance of fracturing an orthosis. Although some measures have been taken to increase the strength of the orthosis, they have not been validated in a real use-case scenario. The orthoses will need to be tested further to ensure non will break during normal use.

It will also have to be tested if the more flexible and ridged footplates will not break. Reducing the thickness of the footplate will decrease the stiffness along the MTP line and make the footplate more flexible. This is more ideal for people with hyper-extended knees according to the Amsterdam Gait classification types[17]. Although Pa11 is a flexible material and has shown potential (*as depicted in figure 79*), further validation is required.

The same counts for the ridged footplate. One approach could be to introduce an external stiff component, as shown in figure 79. However, a functional prototype using SLS printing will have to be built and used to see if this works.

The current stiffness in the footplate is achieved by making it slightly thicker from the MTP line towards the toes compared to the carbon footplate. This increase in thickness might clamp the toes of the wearer against the roof of the shoe. A solution here might be to make the othopedic custom foot sole 1 to 1,5 mm thinner. It has to be seen however if the production method would allow for this and which result this will have on comfort.

However, the most significant recommendation, in terms of function, is to continue testing with the participant who took part in the user test. He has expressed interest in participating in a follow-up study for a longer duration. The orthoses have already been custom-made to fit his feet and will else be shelved. Having him wear the orthoses for an extended period will provide invaluable insights and help address most concerns.

Comfort
This study mainly focussed on function and replicating the behaviour of the dorsal leaf spring orthosis. Comfort, however, is just as important and it is recommended to run some follow-up studies regarding this aspect. One significant aspect for example is if the AFO rotates at least in some regard around the ankle. Having a rotation point further away from the ankle rotation point will result in rubbing of the skin where the cuff is attached to the calf. Either the geometry will need to be adjusted to align the rotation axis more with the point between the malleoli or a system could be designed around the cuff to bend the top part of the orthosis, keeping it perpendicular to the lower leg. The participant that tested the orthosis did not express any discomfort, but further research needs to be conducted to explore the influence of this design aspect on the overall comfort of the orthosis for more participants.

Another consideration is a derivative from the fore-aft and mediolateral forces that were not taken into account in the design of the current prototype. The SLS orthosis currently gets a lot of stiffness from the curve present in the strut. This curved shape follows the contour of the wearer's leg, ensuring a tight fit close to the skin. Having a well-fitting orthosis close to the skin is considered to be comfortable as the weight of the orthosis is also closer to the leg. However, the human ankle does not rotate solely in the sagittal plane; eversion and inversion also occur during gait. These movements may potentially cause rubbing of the sides of the strut against the leg, compromising comfort.

Perception
The reception of an SLS-printed orthosis has not been included in this study and only one participant was involved in the user testing phase. Considering that medical aids can be a sensitive topic the AFO should conform as best as possible to the wishes of the wearer. It is therefore recommended to further look into the aesthetical preferences and the wearer's perception of an SLS-printed orthosis.

The participant who tested the orthoses intentionally wore black shoes, socks, and requested a black product to effectively conceal the orthoses. Additionally, he always wears long-legged pants to hide his medical aids. This design aspect could be further explored to develop a design that addresses both functional and aesthetic concerns, allowing individuals to feel less ashamed of.

SLS orthoses have the advantage of being colourable and can undergo a vapour polish treatment. These post-processing steps, however, only impregnate to a certain depth. During daily use, wear and tear might damage the surface of the orthoses exposing a rough or differently coloured layer underneath. This might be perceived as aesthetically undesirable. One possible solution could be to apply a top coat that matches the colour of the printed material, but this would limit the option for personalized colouring. A consensus will have to be made here or another solution should be explored.

Model optimization
The current model will prove insufficient for everyday use. Firstly, it is necessary to load solid meshes into Grasshopper instead of the open meshes currently used by Livit Ottobock Care. Certain features in Rhino or Solidworks can be used to convert the files which is currently done manually. Once a new foot model is loaded, it may not display correctly due to specific "choke" points in the model that require manual adjustment. These points are marked in Appendix L and it is recommended that when a new foot model is loaded and the program crashes, these points are examined and adjusted. This usually entails changing a negative value into a positive value or vice versa to make the program work.

This can be corrected by giving the program certain curves as guides to follow. As only a handful of foot models were used in this thesis, time was not invested to streamline this model.

Currently, the trim lines are manually adjusted to define the shape of the orthosis. Implementing a shrink wrap feature could generate the distances of these points based on a single defined value, such as the position of a malleolus or the length of the foot. The model would then generate approximate trim lines originating from that single value that can then be manually tweaked. This will save a lot of time and create consistency in the placement of the trim lines.

The final step, filleting the orthosis, is presently performed in Rhino or Solidworks. These programs are more effective for this task compared to Grasshopper. While it is possible to incorporate this step into the program, no effort was made to do so due to its complexity.

Taking it a step further, incorporating final element analysis into the model is also a possibility. Many such plug-ins exist[58], [59], [60]. Integrating this analysis at the end of the Grasshopper model can give immediate insight into its stiffness behaviour. Moreover, the data obtained can be used again as input in the model to adjust its geometric parameters to generate a new, more optimized model that better approximates the desired stiffness values. Incorporating this loop will prove extremely valuable as certain stiffness values can be specified and the model would automatically run simulations and adjustments to eventually generate a model that precisely meets those criteria. It is recommended, however, to explore this endeavour after all else has been implemented and validated as this will not prove easy.

SLS printing possibilities
A continuation of this project could also focus more on utilizing the fabrication method to a greater extent. In the future, it could be possible to produce an AFO with a custom stiffness tailored to each user. Currently, research is being conducted aimed at determining which stiffness orthosis would best suit a client. This knowledge could be used to prescribe not only a custom-fitted orthosis but also a custom stiff orthosis. SLS printing offers the advantage of delivering consistent results and can produce this custom stiffness without added tooling cost or human error.

Furthermore, exploring aesthetical and ergonomic directions, unique to additive manufacturing could enhance the product in other aspects as well. SLS printing provides a high degree of form freedom that has not yet fully been realised in this project. Some options were brainstormed and are described on the next page. These options serve as a perspective into the future where other aspects such as its aesthetic and improved comfort can come into view after its function has been validated.

SLS prints can be coloured in a wide variety of colours[21]. This could be particularly appealing to a younger audience, as they often have a preference for customized prints on the carbon orthosis[12].

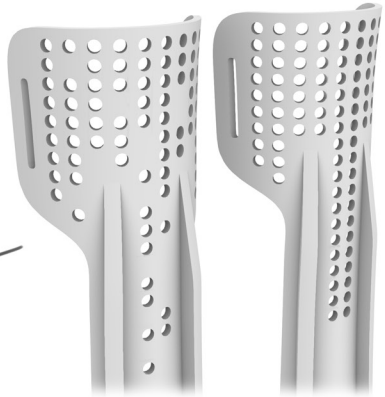

These patterns can also go all the way through the shell of the orthosis in areas where stiffness is of less significance. This feature could lead to a lighter weight more appealing design with certain patterns, again without any added cost.

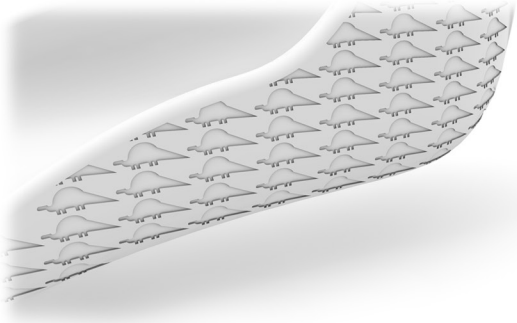

The existing patterns on the carbon orthosis are simply layers added onto the carbon structure. With SLS printing, it becomes possible to incorporate embossings or engravings, offering an alternative to traditional prints. A multitude of patterns could be designed and generated over the orthosis without any added cost or tooling. Even better yet, it is cheaper as it uses less material.

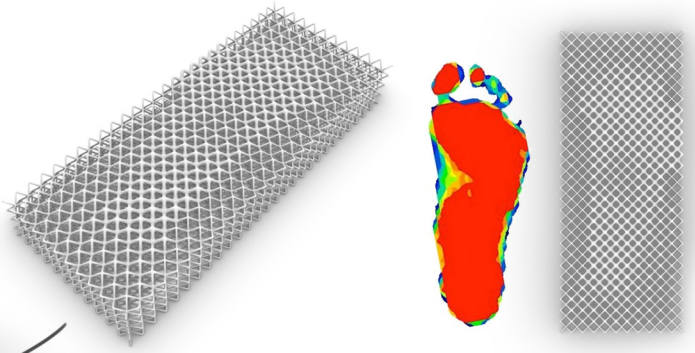

A more advanced feature could be to incorporate cushioning material in the footplate of the orthosis in the form of metamaterials[56], [57]. A pressure map of the foot can be used to generate specific patterns, which could potentially distribute stress more effectively, resulting in increased comfort and again a lighter-weight design.

SOURCES

Literature sources

[1] Foundations for Ankle Foot Orthoses. (n.d.). Physiopedia. https://www.physio-pedia.com/Foundations_for_Ankle_Foot_Orthoses

[2] Rogati, G., Caravaggi, P., & Leardini, A. (2022). Design principles, manufacturing and evaluation techniques of custom dynamic ankle-foot orthoses: a review study. Journal of Foot and Ankle Research, 15(1). https://doi.org/10.1186/s13047-022-00547-2

[3] Faustini, M. C., Neptune, R. R., Crawford, R. H., & Stanhope, S. J. (2008). Manufacture of Passive Dynamic Ankle–Foot Orthoses Using Selective Laser Sintering. IEEE Transactions on Biomedical Engineering, 55(2), 784–790. https://doi.org/10.1109/tbme.2007.912638

[4] Raj, R., Dixit, A. R., Łukaszewski, K., Wichniarek, R., Rybarczyk, J., Kuczko, W., & Górski, F. (2022b). Numerical and Experimental Mechanical Analysis of Additively Manufactured Ankle–Foot Orthoses. Materials, 15(17), 6130. https://doi.org/10.3390/ma15176130

[5] Phillips, R. D. (2019). 3D Printing And Orthotics: A Roundtable Discussion. PodiatryToday, Volume 36, Issue 5.

[6] Industrial 3D-printing: welcome to Parts On Demand. (2022, August 22). Parts on Demand. https://partsondemand.eu/

[7] Quality Management System (QMS) Certification. (2020). In BSI. (BSI/UK/084/MD/0920/en/BLD). The British Standards Institution. https://www.bsigroup.com/nl-NL/medical-devices/medische-hulpmiddelen/onze-diensten/iso-13485-quality-management/

[8] Livit Orthopedie | Orthopedisch specialist in orthesen, prothesen en meer. (2023b, January 26). Livit Orthopedie. https://www.livit.nl/

[9] Foot drop - Symptoms and causes - Mayo Clinic. (2023, January 5). Mayo Clinic. https://www.mayoclinic.org/diseases-conditions/foot-drop/symptoms-causes/syc-20372628

[10] Rao, N., Wening, J. D., Hasso, D., Gnanapragasam, G., Perera, P., Srigiriraju, P., & Aruin, A. S. (2014). The Effects of Two Different Ankle-Foot Orthoses on Gait of Patients with Acute Hemiparetic Cerebrovascular Accident. Rehabilitation Research and Practice, 2014, 1–7. https://doi.org/10.1155/2014/301469

[11] Tomka, O. (2021, June 2). Canberra's Physiotherapy and Medical Bracing Specialists – Momentum. Momentum Sports & Rehabilitation. https://momentumsr.com.au/

[12] Livit carbon layering department (April 14, 2023). Personal communication (internal sources). Livit. https://www.livit.nl/

[13] Whittle, M. (2007). Gait Analysis: An Introduction.

[14] Engel, C. (April 17, 2023). Feedback session, Personal communication (internal sources). Livit. https://www.livit.nl/

[15] Veltmeijer, E. (2019). development of a 3d printed patient specific ankle foot orthosis. Master Thesis TU Delft.

[16] Dept. BioMechanical Engineering, & Harlaar, J. (n.d.). Ankle foot orthosis optimization [Slide show; Pdf].

[17] Fior & Gentz. (2022). CP Guide, A Concept for the Orthotic Treatment of the Lower Extremity in Cerebral Palsy. In https://www.fior-gentz.de/ (Nr. PR0221-GB-2022–03).

[18] Dries, T. (2023) Personal communication (internal sources). Livit. https://www.livit.nl/

[19] Centraal Bureau voor de Statistiek. (n.d.). Uurloon. Centraal Bureau Voor De Statistiek. https://www.cbs.nl/nl-nl/visualisaties/dashboard-arbeidsmarkt/ontwikkeling-cao-lonen/uurloon

[20] Redwood, B., Schöffer, F., & Garret, B. (2018). The 3D Printing Handbook: Technologies, Design and Applications.

[21] Design Guidelines - 3D printing | Parts on Demand. (n.d.). Parts on Demand. https://partsondemand.eu/design-guidelines/

[22] EOS. (2016) PA12-PA2200. Balance 1.0. Unpublished internal company document

[23] EOS. (2001) Product Information EOSINT P/PA2200-Pulver. Unpublished internal company document

[24] Parts on Demand. (2023) PA11 series powered by nature. Unpublished internal company document

[25] Parts on Demand. (2021) PA-640-GSL-Data-Sheet. 2021b. Unpublished internal company document

[26] Parts on Demand. (2023) MDS - PA11GF Black. Unpublished internal company document

[27] ANSYS, Inc. (2022). GRANTA Edupack [Software]. In (www.ansys.com/materials) (Version Vb1)

[28] Holtkamp, F., Ejm, W., J, V. H., Y, V. Z., & Verkerk, M. (2015). Use of and Satisfaction with Ankle Foot Orthoses. Clinical Research on Foot & Ankle, 03(01). https://doi.org/10.4172/2329-910x.1000167

[29] Vinci, P., & Gargiulo, P. (2008). Poor compliance with ankle-foot-orthoses in Charcot-Marie-Tooth disease. European Journal of Physical and Rehabilitation Medicine, 44(1), 27–31.

[30] Knapp, D. (2018). Choosing the optimal PD-AFO for your patient. The Orthotic & Prosthetic Community News Source.

[31] Plagenhoef, S., Evans, F. G., & Abdelnour, T. (1983). Anatomical Data for Analyzing Human Motion. Research Quarterly for Exercise and Sport, 54(2), 169–178. https://doi.org/10.1080/02701367.1983.10605290

[32] DINED. (n.d.). https://dined.io.tudelft.nl/en

[33] Van Ommen, B., & Kleiman, E. (2008b). De Orteam EVO onder de loep [Afstudeerscriptie Bewegingstechnologie]. De Haagse Hogeschool.

[34] Hessert, M. J., Vyas, M., Leach, J., Hu, K., Lipsitz, L. A., & Novak, V. (2005). Foot pressure distribution during walking in young and old adults. BMC Geriatrics, 5(1). https://doi.org/10.1186/1471-2318-5-8

[35] Ortega, J. A., Healey, L. A., Swinnen, W., & Hoogkamer, W. (2021). Energetics and Biomechanics of Running Footwear with Increased Longitudinal Bending Stiffness: A Narrative Review. Sports Medicine, 51(5), 873–894. https://doi.org/10.1007/s40279-020-01406-5

[36] Van den Dool, A. (2023). Feedback sessions, Personal communication (internal sources). Parts on Demand. https://partsondemand.eu/

[37] Bregman, D. B., Rozumalski, A., Koops, D., De Groot, V., Schwartz, M., & Harlaar, J. (2009). A new method for evaluating ankle foot orthosis characteristics: BRUCE. Gait & Posture, 30(2), 144–149. https://doi.org/10.1016/j.gaitpost.2009.05.012

[38] Walbran, M., Turner, K. L., & McDaid, A. (2016). Customized 3D printed ankle-foot orthosis with adaptable carbon fibre composite spring joint. Cogent Engineering, 3(1), 1227022. https://doi.org/10.1080/23311916.2016.1227022

[39] van Es, N. (2023). Personal communication (internal sources). Parts on Demand. https://partsondemand.eu/

[40] Carbon Ankle seven | Dynamic Components | AFO - Ankle Foot Orthosis | Custom Orthotics | Orthotics | Ottobock US Shop. (n.d.). https://shop.ottobock.us/Orthotics/Custom-Orthotics/AFO---Ankle-Foot-Orthosis/Dynamic-Components/Carbon-Ankle-seven/p/17CF1

[41] Dassault systems. (2022). Solidworks simulation [Software]. In Solidworks.

[42] Tempelman., E. NSFD - Engineering bending theory. (2018) Unpublished internal TU Delft Brightspace document

[43] Calculate your 3D print price | Parts On Demand. (2022, 7 januari). Parts On Demand. https://partsondemand.eu/my-parts-on-demand/

[44] ISO 10993-5., ISO 10993-10. (n.d.). Biological Evaluation of Medical Devices - Part 5: Tests for In Vitro Cytotoxicity. International Organization for Standardization. Retrieved from [https://partsondemand.nl/pa11-nylon/]

[45] Wisnom, M. R. (2012). The role of delamination in failure of fibre-reinforced composites. Philosophical Transactions of the Royal Society A, 370(1965), 1850–1870. https://doi.org/10.1098/rsta.2011.0441

[46] Zach. (2022). Curve Fitting in Google Sheets (With Examples). Statology. https://www.statology.org/curve-fitting-in-google-sheets/

[47] Hof, A. L. (2000). On the interpretation of the support moment. Gait & Posture, 12(3), 196–199. https://doi.org/10.1016/s0966-6362(00)00084-9

[48] Waterval, N. F., Brehm, M., Altmann, V. C., Koopman, F. S., Boer, J. J. D., Harlaar, J., & Nollet, F. (2020). Stiffness-Optimized Ankle-Foot Orthoses Improve Walking Energy Cost Compared to Conventional Orthoses in Neuromuscular Disorders: A Prospective Uncontrolled Intervention Study. IEEE Transactions on Neural Systems and Rehabilitation Engineering, 28(10), 2296–2304. https://doi.org/10.1109/tnsre.2020.3018786

[49] Esposito, E. R., Schmidtbauer, K. A., & Wilken, J. M. (2018). Experimental comparisons of passive and powered ankle-foot orthoses in individuals with limb reconstruction. Journal of Neuroengineering and Rehabilitation, 15(1). https://doi.org/10.1186/s12984-018-0455-y

[50] Mavroidis, C., Ranky, R., Sivak, M., Patritti, B. L., DiPisa, J., Caddle, A., Gilhooly, K., Govoni, L., Sivak, S., Lancia, M., Drillio, R., & Bonato, P. (2011). Patient specific ankle-foot orthoses using rapid prototyping. Journal of NeuroEngineering and Rehabilitation, 8(1). https://doi.org/10.1186/1743-0003-8-1

[51] Marques, M., Mendes, E., Viriato, N., & Vaz, M. a. P. (2010). Finite element analysis of ankle foot orthosis to predict fracture conditions during gait. ResearchGate. https://www.researchgate.net/publication/262684543_Finite_element_analysis_of_ankle_foot_orthosis_to_predict_fracture_conditions_during_gait

[52] Taylor, D., Kelly, A., Toso, M., & Berto, F. (2011). The variable-radius notch: Two new methods for reducing stress concentration. Engineering Failure Analysis, 18(3), 1009–1017. https://doi.org/10.1016/j.engfailanal.2010.12.012

[53] McNeel, R., & others. (2010). Rhinoceros 3D, Version 6.0. Robert McNeel & Associates, Seattle, WA.

[54] Arkema Rilsan® PA 11 G BMNO MED Nylon 11. (z.d.). https://www.matweb.com/search/datasheet_print.aspx?matguid=14861cb8cb8e470eba6aaf72089bf716

[55] Stratasys., (2021) Stratasys High Yield Pa11 Material Properties., stratasys.com ISO 9001:2015 Certified

[56] van Leijsen, L. (2020). Application of mechanical metamateri in a parametric 3D printed ankle foot orthosis. Master Thesis TU Delft.

[57] Baatsen, F. F., Van Zuuk, & Van Der Laan, F. (n.d.). Spidershoe; an exploration of a parametrically generate shoe [Slide show]. A project carried out for the course computational design for digital manufacturing. TU Delft

[58] Fenix. (2023, 20 mei). Food4Rhino. https://www.food4rhino.com/en/app/fenix-0?lang=en

[59] Scan&Solve Pro: Structural Simulation for Rhino 6. (2022, 17 mei). Food4Rhino. https://www.food4rhino.com/en/app/scansolve-pro-structural-simulation-rhino-6

[60] Solid Mechanics Simulation for Rhino Users. (2022, 17 mei). Food4Rhino. https://www.food4rhino.com/en/resource/solid-mechanics-simulation-rhino-users

[61] Tracker Video Analysis and Modeling Tool for Physics Education. (z.d.). https://physlets.org/tracker/

Image sources

page 7		*adapted from:*	https://commons.wikimedia.org/wiki/File:Human_anatomy_planes,_labeled.svg https://nl.m.wikipedia.org/wiki/Bestand:Eversion_and_inversion.jpg https://profeet.co.uk/ankle-range-motion-injuries/ https://www.activeforever.com/ankle-foot-orthosis-semi-rigid-afo
page 8	*figure 1*	*retrieved from:*	https://www.livit.nl/product/enkel-voet-orthese/
page 9		*retrieved from:* *retrieved from:*	https://partsondemand.eu/ https://www.livit.nl/
page 12		*retrieved from:*	https://momentumsr.com.au/medical-product-type/ankle/
page 13	*figure 3*	*retrieved from:*	https://www.ottobock.com/nl-nl/product/17AD1000
page 14	*figure 4*	*adapted from:*	Whittle, M. (2007). Gait Analysis: An Introduction. and https://clinicalgate.com/assessment-of-gait/
page 15	*figure 5*	*adapted from:*	Whittle, M. (2007). Gait Analysis: An Introduction. and https://clinicalgate.com/assessment-of-gait/
page 18	*figure 7*	*adapted from:*	*https://upload.wikimedia.org/wikipedia/commons/b/b3/Amsterdam_Gait_Classification_gb.jpg*
page 20	*figure 11*	*retrieved from:*	https://partsondemand.eu/medical-products/
page 24	*figure 14*	*retrieved from:*	Redwood, B., Schöffer, F., & Garret, B. (2018). The 3D Printing Handbook: Technologies, Design and Applications.
page 24	*figure 15*	*retrieved from:*	https://partsondemand.eu/
page 26	*figure 17*	*adapted from:*	https://partsondemand.eu/
page 27	*figure 18*	*retrieved from:*	https://partsondemand.eu/
page 30	*Walk on Flex*	*retrieved from:*	https://www.ottobock.com/nl-nl/product/28U22
	Spiral Matrix	*retrieved from:*	https://www.orthotix.co.uk/shop/ankle-and-foot/carbon-ankle-foot-orthosis/
	Matrix	*retrieved from:*	https://trulife.com/collections/carbon-fiber-dynamic-afos
	EZ stride	*retrieved from:*	https://www.algeos.com/ez-stride-anterior-carbon-fiber-afo
	AFO dynamic	*retrieved from:*	https://www.synergyortho.com/product/dynamic-afo/
	Ypsilon	*retrieved from:*	https://www.allardusa.com/products/foot-drop-afos/foot-drop-mild-stability/ypsilon-flow-2-p34017#lg=1&slide=0
	Walkonreaction	*retrieved from:*	https://shop.ottobock.us/Orthotics/Custom-Orthotics/AFO---Ankle-Foot-Orthosis/Carbon-Fiber-AFO/WalkOn-AFOs/WalkOn-Reaction-Ankle-Foot-Orthosis/p/28U24
	Blue rocker	*retrieved from:*	https://basko.com/nl-nl/Producten/Orthesen-en-Bandages/Onderste-Extremiteit/Details/BlueROCKER-dynamische-enkel-voetorthese
page 32	*figure 23*	*adapted from:*	Whittle, M. (2007). Gait Analysis: An Introduction. and https://clinicalgate.com/assessment-of-gait/
page 32	*figure 24*	*adapted from:*	Whittle, M. (2007). Gait Analysis: An Introduction. and https://clinicalgate.com/assessment-of-gait/
page 33	*figure 25*	*adapted from:*	Whittle, M. (2007). Gait Analysis: An Introduction. and https://clinicalgate.com/assessment-of-gait/
page 35	*figure 26*	*adapted from:*	https://en.wikipedia.org/wiki/Metatarsophalangeal_joints#/media/File:Articulationes_metatarsophalangeae-la.svg

page 35	*figure 27*	*adapted from:*	https://www.researchgate.net/publication/350738471_Energetics_and_Biomechanics_of_Running_Footwear_with_Increased_Longitudinal_Bending_Stiffness_A_Narrative_Review
page 36	*figure 29*	*retrieved from:*	Bregman, D. B., Rozumalski, A., Koops, D., De Groot, V., Schwartz, M., & Harlaar, J. (2009). A new method for evaluating ankle foot orthosis characteristics: BRUCE. Gait & Posture, 30(2), 144–149. https://doi.org/10.1016/j.gaitpost.2009.05.012
page 64	*figure 63*	*adapted from:*	Taylor, D., Kelly, A., Toso, M., & Berto, F. (2011). The variable-radius notch: Two new methods for reducing stress concentration. Engineering Failure Analysis, 18(3), 1009–1017. https://doi.org/10.1016/j.engfailanal.2010.12.012

APPENDIX

Appendix A: Project brief

DESIGN FOR our future

TU Delft

IDE Master Graduation

Project team, Procedural checks and personal Project brief

This document contains the agreements made between student and supervisory team about the student's IDE Master Graduation Project. This document can also include the involvement of an external organisation, however, it does not cover any legal employment relationship that the student and the client (might) agree upon. Next to that, this document facilitates the required procedural checks. In this document:

- The student defines the team, what he/she is going to do/deliver and how that will come about.
- SSC E&SA (Shared Service Center, Education & Student Affairs) reports on the student's registration and study progress.
- IDE's Board of Examiners confirms if the student is allowed to start the Graduation Project.

USE ADOBE ACROBAT READER TO OPEN, EDIT AND SAVE THIS DOCUMENT
Download again and reopen in case you tried other software, such as Preview (Mac) or a webbrowser.

STUDENT DATA & MASTER PROGRAMME

Save this form according the format "IDE Master Graduation Project Brief_familyname_firstname_studentnumber_dd-mm-yyyy".
Complete all blue parts of the form and include the approved Project Brief in your Graduation Report as Appendix 1 !

family name	Baatsen
initials	F.F.
given name	Falko
student number	4594274
street & no.	E
zipcode & city	2
country	N
phone	-
email	E

Your master programme (only select the options that apply to you):

IDE master(s): ★ IPD ○ DfI ○ SPD

2nd non-IDE master:

individual programme: - - (give date of approval)

honours programme: ○ Honours Programme Master

specialisation / annotation: ○ Medisign ○ Tech. in Sustainable Design ○ Entrepeneurship

SUPERVISORY TEAM **

Fill in the required data for the supervisory team members. Please check the instructions on the right !

** chair	Thomassen, E.W.	dept. / section:	SDE/EM
** mentor	Dam, J.J.F. van	dept. / section:	SDE/TS
2nd mentor	Dool, A. C. van den		
organisation:	Parts on Demand B.V.		
city:	Utrecht	country:	Netherlands
comments (optional)	In cooperation with Livit Ottobock Care		

Chair should request the IDE Board of Examiners for approval of a non-IDE mentor, including a motivation letter and c.v..

Second mentor only applies in case the assignment is hosted by an external organisation.

Ensure a heterogeneous team. In case you wish to include two team members from the same section, please explain why.

TU Delft

Procedural Checks - IDE Master Graduation

APPROVAL PROJECT BRIEF

To be filled in by the chair of the supervisory team.

chair Thomassen, E.W. date 01 - 03 - 2023 signature

CHECK STUDY PROGRESS

To be filled in by the SSC E&SA (Shared Service Center, Education & Student Affairs), after approval of the project brief by the Chair.
The study progress will be checked for a 2nd time just before the green light meeting.

Master electives no. of EC accumulated in total: ____ EC

Of which, taking the conditional requirements into account, can be part of the exam programme ____ EC

List of electives obtained before the third semester without approval of the BoE

○ YES all 1st year master courses passed

○ NO missing 1st year master courses are:

name date - - signature

FORMAL APPROVAL GRADUATION PROJECT

To be filled in by the Board of Examiners of IDE TU Delft. Please check the supervisory team and study the parts of the brief marked **.
Next, please assess, (dis)approve and sign this Project Brief, by using the criteria below.

- Does the project fit within the (MSc)-programme of the student (taking into account, if described, the activities done next to the obligatory MSc specific courses)?
- Is the level of the project challenging enough for a MSc IDE graduating student?
- Is the project expected to be doable within 100 working days/20 weeks ?
- Does the composition of the supervisory team comply with the regulations and fit the assignment ?

Content: ○ APPROVED ○ NOT APPROVED

Procedure: ○ APPROVED ○ NOT APPROVED

comments

name date - - signature

Personal Project Brief - IDE Master Graduation

TU Delft

Designing a strong, dynamic SLS-3D printable Ankle-Foot orthosis — project title

Please state the title of your graduation project (above) and the start date and end date (below). Keep the title compact and simple. Do not use abbreviations. The remainder of this document allows you to define and clarify your graduation project.

start date 14 - 02 - 2023 — 10 - 07 - 2023 end date

INTRODUCTION **

Please describe, the context of your project, and address the main stakeholders (interests) within this context in a concise yet complete manner. Who are involved, what do they value and how do they currently operate within the given context? What are the main opportunities and limitations you are currently aware of (cultural- and social norms, resources (time, money,...), technology, ...).

An ankle-foot orthosis (from here on after AFO) is a wearable aid that improves walking patterns by reducing, preventing or helping the movement of the lower limbs to stabilise joints, support weak muscles and in general control the range of motion in the foot and ankle [Figure 1]. It is a supportive device that is strapped on the back of your lower leg and typically extends into the shoe underneath the plantar surface of the foot. The need to wear an AFO usually results from an underlying condition such as peroneal nerve damage, brain/spinal cord problems, muscular dystrophy or from an inherited condition.

Off-the-shelf prefabricated orthoses are commonly used in the short term for an improvable condition. However more commonly a long-term patient-specific AFO is needed as many ergonomic complaints arise when the device needs to be worn for longer periods of time. This project will focus on this second type of AFO. Currently, the last step in the production of these AFOs consists of manually applying the material to a cast and trimming it for a good fit. This is especially true for the dynamic AFOs as these require cutting and applying multiple layers of carbon fibre which takes up a lot of time and makes it expensive.

An alternative to this process may be a more automated production process using 3D printing. This case is therefore carried out for the company PartsonDemand, a selective laser sintering (SLS) 3D printing company for industrial parts. They, in collaboration with Livit/Ottobock, an orthopaedics company, have set up this case to explore the possibilities of manufacturing a (partially) SLS printable AFO providing a comfortable walking experience.

Livit/Ottobock already has CAD files of all their clients and currently uses these to mill a positive cast of the lower leg and foot. This is consequently used for the manual application of either vacuum formed plastic sheets or carbon layering. An alternative to this process may be to directly go from CAD to AFO through SLS printing. It is especially interesting to explore an alternative to the dynamic carbon AFOs as these can be competitive in terms of their cost.

Designing an orthosis using SLS printing as a starting point provides new design opportunities in terms of its form freedom and material properties. SLS-printed AFOs are deemed promising rigid orthoses with potential benefits in terms of their ease of use and comfort [1]. Compared to traditional orthopedic aids, 3d printed AFOs can be lighter in weight and potentially provide a better distribution of pressure on the skin which results in a more comfortable device. However, 3D-printed orthoses are in the early stages of development and further research is needed in terms of their required strength and desired stiffness through exploring various wall thicknesses, material compositions and added external materials as they are still prone to fracturing due to the forces exerted at certain points through walking [Figure 2].

3D-printed othoses are also not yet widely employed as the hardware is considered to be too expensive and many parties are waiting for further validation of methods and materials before investing. PartsonDemand in collaboration with Livit/Ottobock is in a viable position to further explore this field, as they have the orthopaedic knowledge and hardware.

For this project, I want to focus on designing a strong, patient specific SLS-3D printable ankle-foot orthosis for comfortable walking.

space available for images / figures on next page

Personal Project Brief - IDE Master Graduation

TU Delft

introduction (continued): space for images

image / figure 1: An AFO designed by Livit/Ottobock

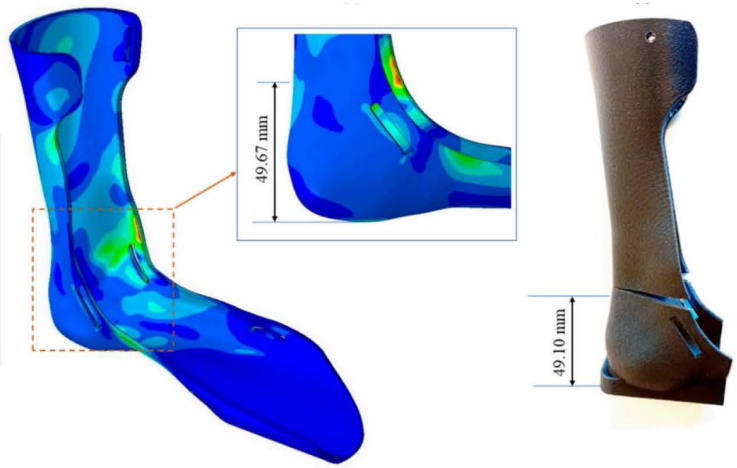

image / figure 2: Typical fracture points SLS printed AFOs [3]

Personal Project Brief - IDE Master Graduation

TU Delft

PROBLEM DEFINITION **

Limit and define the scope and solution space of your project to one that is manageable within one Master Graduation Project of 30 EC (= 20 full time weeks or 100 working days) and clearly indicate what issue(s) should be addressed in this project.

This project focuses on custom-made ankle foot orthoses because they emphasise the advantages of additive manufacturing methods such as SLS printing. This technique excels at one-off part production, such as custom made AFOs, because it does not require any moulds or specific tools. This project will look into the strength of SLS printed parts and their ability to withstand the forces applied to them during normal use.

Livit/Ottobck currently make orthoses through making milling a positive foam cast of the leg using a CAD file and then manually applying the AFO through either thermoplastic vacuum forming or carbon layering. A part of this process is still done by hand. Automation through 3d printing might be a solution for a personalised prescribed orthosis reducing the workload of employees and streamlining the production process potentially saving time. Through this method, a lightweight AFO could be made with more control over its form and its desired rigidity. An SLS-printed orthosis can be designed to meet specific needs to enhance its function, fitting and aesthetic which could improve patient satisfaction, usage compliance, and other health-related concerns [2].

Studies show the potential of 3D-printed AFOs [1], but none have had a promising breakthrough in the market. Using additive manufacturing methods can provide advantages but innovation is not common practice as most orthoses break down after several weeks [3]. Material hardness, porosity or anisotropic properties still limit the lifetime of 3D-printed AFOs.

In this project, I want to focus on designing a strong SLS-printable AFO which can have a patient-specific custom stiffness. SLS-printed AFOs could be a viable option in the orthopedics market through providing a more automated production process, with a slightly reduced production time whilst being competitive in terms of its price.

ASSIGNMENT **

State in 2 or 3 sentences what you are going to research, design, create and / or generate, that will solve (part of) the issue(s) pointed out in "problem definition". Then illustrate this assignment by indicating what kind of solution you expect and / or aim to deliver, for instance: a product, a product-service combination, a strategy illustrated through product or product-service combination ideas, ... In case of a Specialisation and/or Annotation, make sure the assignment reflects this/these.

I am going to design a custom dynamic SLS printable Ankle-Foot orthosis focussing on its strength and customizable stiffness whilst minimizing a compromise in comfort. This will result in a wearable SLS-printed prototype that will be validated through use.

In this project, the goal is to design a (for the most part) SLS-printed custom AFO that improves the gait pattern and resists fracture in day-to-day use. This is done by making and testing a prototype with an emphasis on its resistance against fracture during typical use. The comfort of the orthosis will be considered, along with its variable stiffness that is used for correcting the gait pattern of clients.

The final prototype will be made using a 3D scan of the foot and modelling an AFO based on this data in combination with relevant measurements taken by hand. Small-scale coupon-level prototypes will be made beforehand to test their mechanical properties and performance through material stress testing along with FDM fitting tests to ensure an ergonomic fit.

The design will be validated through quantitative bending stiffness and strength tests for its rigidity. It will be tested qualitatively by being worn by a patient in order to test its comfort and durability in a daily-use scenario. The result will rely on its material properties and physical features to function within its elastic deformation range to facilitate the ideal bending and rotational stiffness without breaking.

Next to this prototype, a template will be provided to replicate the results for a different client. This template will guide PartsonDemand & Livit/Ottobock to adjust the AFO model to suit different feet and reproduce the acquired result.

Initials & Name F.F. Baatsen Student number 4594274

Title of Project Designing a strong, dynamic SLS-3D printable Ankle-Foot orthosis

Personal Project Brief - IDE Master Graduation

TU Delft

PLANNING AND APPROACH **

Include a Gantt Chart (replace the example below - more examples can be found in Manual 2) that shows the different phases of your project, deliverables you have in mind, meetings, and how you plan to spend your time. Please note that all activities should fit within the given net time of 30 EC = 20 full time weeks or 100 working days, and your planning should include a kick-off meeting, mid-term meeting, green light meeting and graduation ceremony. Illustrate your Gantt Chart by, for instance, explaining your approach, and please indicate periods of part-time activities and/or periods of not spending time on your graduation project, if any, for instance because of holidays or parallel activities.

start date 14 - 2 - 2023 10 - 7 - 2023 end date

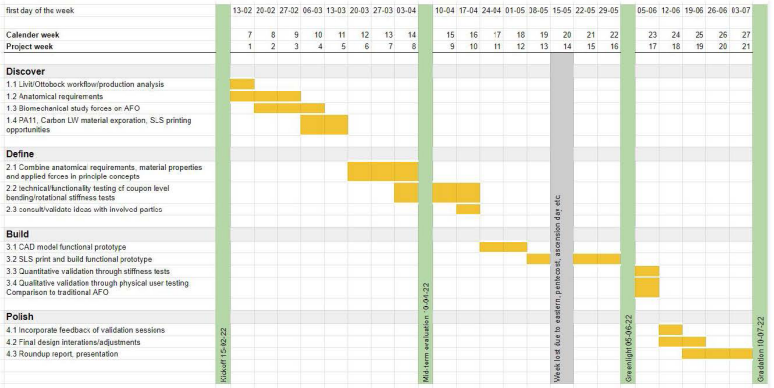

The project is divided into 4 phases and 4 milestones:

During the discovery phase, I will focus on acquiring the relevant knowledge needed for this project. This will be done through literature studies, expert interviews and working together with both Livit/Ottobock and PartsonDemand. At the end of this phase, I hope to deliver a program of requirements regarding the forces, ergonomics and material properties involved to make an SLS-printable AFO.

The second phase is about exploring and testing ideas. The gathered knowledge is combined into measurable biomechanical principles that will be prototyped on a small scale. These prototypes will then be tested in a rudimentary fracture test setup using a push / pull bench. The empirical data of these tests will at the end of this phase, in combination with ergonomic principles, define a concept to be built on a 1-to-1 scale.

From weeks 11 to 16, I will focus on building a patient-specific wearable prototype. This is done through CAD modelling, printing and building the prototype. It will then be validating both qualitative and quantitative through user testing. The result of this phase is a validated full-scale SLS-printed prototype.

My focus will shift towards a final iterated design and recommendations in the last weeks of my project. This phase is used to incorporate all feedback and provide polish to the final report, presentation and other deliverables.

Initials & Name F.F. Baatsen Student number 4594274

Title of Project Designing a strong, dynamic SLS-3D printable Ankle-Foot orthosis

Personal Project Brief - IDE Master Graduation

TU Delft

MOTIVATION AND PERSONAL AMBITIONS

Explain why you set up this project, what competences you want to prove and learn. For example: acquired competences from your MSc programme, the elective semester, extra-curricular activities (etc.) and point out the competences you have yet developed. Optionally, describe which personal learning ambitions you explicitly want to address in this project, on top of the learning objectives of the Graduation Project, such as: in depth knowledge a on specific subject, broadening your competences or experimenting with a specific tool and/or methodology, ... Stick to no more than five ambitions.

I have become increasingly interested in designing and prototyping whilst working with manufacturing techniques during my masters program Integrated Product Design. I like working with the rules that comes with a certain technique and see the opportunities they can offer when you incorporate it into your design process at an early stage. I feel like this not only makes it more likely to be eventually manufactured, as you emphasise producibility, but it also gives early insights into the technical aspects of your final design.

One such technique is additive manufacturing, which has been prevalent throughout my studies. I have made various molds, prototypes or shown functional principles, but these parts were in my case never intended as end products. Designing a finished product using the matured technique of SLS printing is something I would like to explore. I believe in the various application opportunities of this technique and thus hope to see more 3d printed parts as end products in the future. Through this project, I hope to contribute to this industry and help make additive manufacturing more common as a production method.

As a designer, I have come to realise that I enjoy prototyping the most. I excel when I have a concrete concept and am left with technicalities that need to be solved through physical prototyping. I believe that academic knowledge combined with workshop experience help to bridge the gap between a concept and a producible product. Incorporating prototyping in the design process helps me to better validate and iterate my ideas. I aim to continue with this design method in my graduation project as PartsonDemand has stated that they support this work ethic, and that this project could facilitate this. Through this method, I hope to guarantee the manufacturability of my final concept and like to develop myself as an industrial designer who leans somewhat towards the mechanical side. Specifically in this project, I want to gain more competency with (bio) mechanical principles and hope to explore this by making physical prototypes. The field of orthopedics is new to me but I see a strong connection between this field and additive manufacturing that I would like to strengthen.

In this design project, I also see the opportunity to differentiate my CAD modelling experience. A model will need to be made as the end product of this project will be a 3D-printed prototype. I am proficient with Solidworks, but working with more organic shapes such as 3D scanned feet provide new challenges for me. Programs such as Rhino and Grasshopper might be a better fit for this case, which also provide a parametrical approach. Using these programs may provide the opportunity to automatically generate an AFO based on an uploaded 3D model of the lower leg and foot. I want to stress that it will not be a part of this project to automate this process. However, I do want to facilitate the opportunity to implement this later on for PartsonDemand by providing a template with instructions to build upon.

[1] Wojciechowski, E., Chang, A.Y., Balassone, D. et al. Feasibility of designing, manufacturing and delivering 3D printed ankle-foot orthoses: a systematic review. J Foot Ankle Res 12, 11 (2019). https://doi.org/10.1186/s13047-019-0321-6
[2] Choo, Y. J., Boudier-Reveret, M., & Chang, M. C. (2020). 3D printing technology applied to orthosis manufacturing: narrative review. Annals of Palliative Medicine, 9(6), 4262 – 4270. https://doi.org/10.21037/apm-20-1185
[3] Raj, R., Dixit, A. R., Łukaszewski, K., Wichniarek, R., Rybarczyk, J., Kuczko, W., & Górski, F. (2022). Numerical and Experimental Mechanical Analysis of Additively Manufactured Ankle – Foot Orthoses. Materials, 15(17), 6130. https://doi.org/10.3390/ma15176130

FINAL COMMENTS

In case your project brief needs final comments, please add any information you think is relevant.

Initials & Name F.F. Baatsen Student number 4594274

Title of Project Designing a strong, dynamic SLS-3D printable Ankle-Foot orthosis

CONFIDENTIAL INFORMATION

Appendix C: Homesetup stiffness measurements carbon dorsal leaf spring AFO

Strut measurements

	Carbon dorsal leaf spring measurements						
	Heigth on ruler	Weight (kg)	Force (N)	Height (mm)	Moment (Nm))	Angle (degrees)	Measured stiffness (Nm/°)
Dorsiflexion	140	8,1	81	106,5	29,16	16,47997328	1,769420344
	128	6,9	69	94,5	24,84	14,7083039	1,688841907
	125	6,6	66	91,5	23,76	14,26071158	1,666116018
	118	6	60	84,5	21,6	13,2094677	1,635190796
	108	5,3	53	74,5	19,08	11,69200056	1,631884971
	99	4,5	45	65,5	16,2	10,31184913	1,571008244
	94	4,1	41	60,5	14,76	9,539731455	1,547213364
	83,5	3,4	34	50	12,24	7,907162703	1,547963595
	77	2,9	29	43,5	10,44	6,889837456	1,515275225
	72	2,5	25	38,5	9	6,104264141	1,474379187
	66	2,2	22	32,5	7,92	5,158551781	1,535314626
	56,5	1,5	15	23	5,4	3,655595302	1,477187586
	51	1,1	11	17,5	3,96	2,783020754	1,42291429
Plantarflexion	203	0,9	-9	-14	-3,24	-2,227046967	1,454841343
	213	1,5	-15	-24	-5,4	-3,814074834	1,415808613
	220	2	-20	-31	-7,2	-4,921662286	1,462920367
	226	2,4	-24	-37	-8,64	-5,868128565	1,472360379
	236	3	-30	-47	-10,8	-7,438211887	1,451961864
	242	3,4	-34	-53	-12,24	-8,375049783	1,46148385
	253	4	-40	-64	-14,4	-10,08059799	1,428486685
	264	4,7	-47	-75	-16,92	-11,76828893	1,437762116
	272	5,3	-53	-83	-19,08	-12,98299257	1,469614952
	278	5,8	-58	-89	-20,88	-13,88635295	1,503634545
	282	6,1	-61	-93	-21,96	-14,48473356	1,516078974
	299	7,4	-74	-110	-26,64	-16,99082329	1,567905189
	Arm length (m)	0,36				Average plantarflex moment stiffness	1,575593089
	Start value on ruler dorsiflexion(mm)	33,5				Average dorsiflex moment stiffness	1,47023824
	Start value on ruler plantarflexie(mm)	189				Average stiffness	1,525022761

figure 95: Homesetup strut stiffness measurements in plantar flex and dorsiflex directions

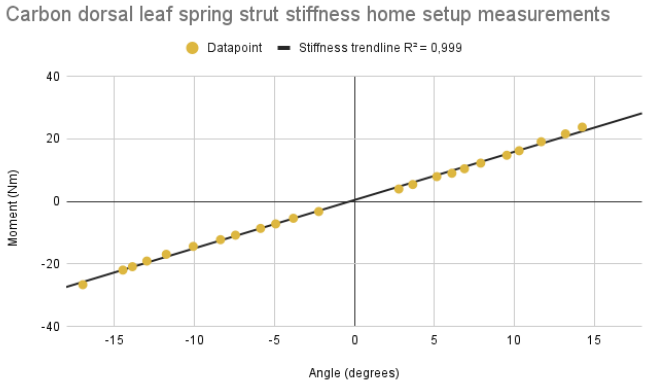

figure 96: diagram of strut stiffness behaviour

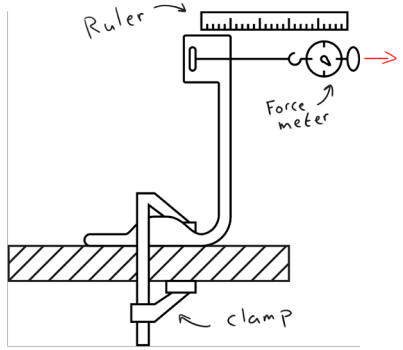

figure 97: schematic representation of test setup

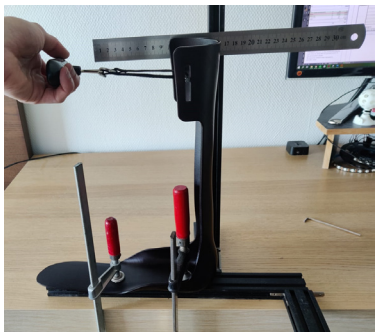

figure 98: Representation of test setup

MTP line measurements

MTP Dorsal leaf spring EVO Livit

Heigth on ruler	Weight (kg)	Force (N)	Height (mm)	Moment (Nm)	Angle (degrees)	Measured stiffness (Nm/°)
37,5	5,9	59	37,5	5,015	23,80594352	0,2106616777
31	5,3	53	31	4,505	20,03721017	0,2248316987
30	5,9	59	30	5,015	19,44003483	0,2579727889
27	6	60	27	5,1	17,62229723	0,2894060822
25	5,5	55	25	4,675	16,38954033	0,2852428991
21,5	4,6	46	21,5	3,91	14,19473761	0,2754541934
20	4,3	43	20	3,655	13,24051992	0,2760465619
19,5	3,9	39	19,5	3,315	12,92075034	0,2565640473
17,5	3,4	34	17,5	2,89	11,633634	0,2484176484
17	2,7	27	17	2,295	11,30993247	0,2029189834
18	2	20	18	1,7	11,95658424	0,1421810749
9,5	1,7	17	9,5	1,445	6,377180624	0,2265891599
6	1,2	12	6	1,02	4,037710621	0,2526184008
5	1	10	5	0,85	3,366460663	0,2524906972
4,5	0,8	8	4,5	0,68	3,030476846	0,2243871293
3	0,6	6	3	0,51	2,02136494	0,2523047619
2,5	0,4	4	2,5	0,34	1,684684318	0,2018182258
Arm length (m)	0,085					
Start value on ruler dorsiflexion(mm)	0				**Average stiffness**	0,2399944724

figure 99: MTP dorsal leaf spring AFO stiffness home setup measurements

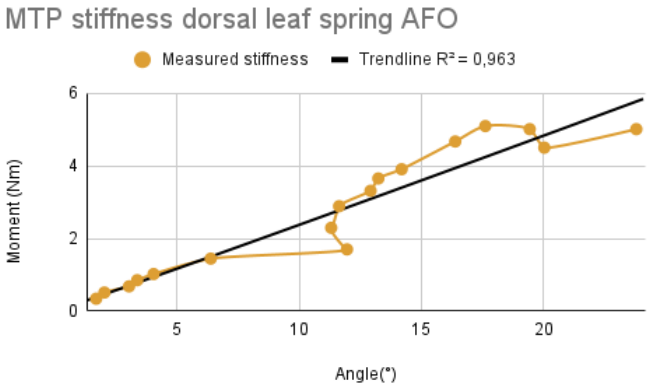

figure 100: diagram of MTP stiffness behaviour

figure 101: Representation of MTP setup

Appendix D: Idea orientation

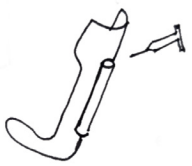

Injection with epoxy resin or other high stiffness liquid material can be used to provide stiffness in designed compartments.

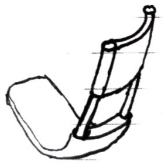

arbon rods where the flexability is needed, SLS prints for support above and below the rotational bend

Strutwidth parameter to influence stiffness (I wonder if this is strong enough)

Thick external strut supporting all stress

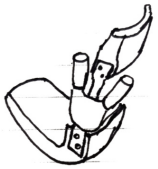

Use existing Livit Ottobock Care hinge component, only SLS foot ankle cast prints

Is this stiffness in the right position? or too far above
the ankle to be affective in any sort?

Cut the strut in half and place it on both sides of the leg for the same stiffness but a thinner-walled design

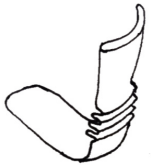

Use the flexability of PA11 or PA12 for the spring function of the AFO

Printed afo with carbon layering on top for increased stiffness. Or Fiber glass -> how does it adhere? does this work, would it bond?

Create a countermoment of some sort, through a spring system, weight or balance to counteract the stiffness

Springs as force to deliver the rolloff of a dynamic AFO

Stepper motor or dynamo could deliver resistance moment?

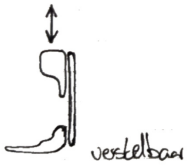

Length changeable strut. Would have influence on the stiffness but could have concequences on comfort ,-> shorter arm is more pressure on skin

Springdampner in joint design. Replace spring for desired stiffness

Capsule of some sort around the ankle placement with metal rod or other stiff stick placed in it.

Pol on foot idea, results on pressure on sheen. Shape is possible in SLS, how thick would it be?

If the material is too stiff; translate stiffness requirements into adjustable density (through generated holes). More holes = more flexible

Extra strap around top of foot for extra strength and stress distribution --> what is the influence of this on the stiffness?

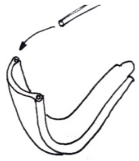

Carbon kitepole insert idea Erik. Inserting carbon would increase stiffness as the material properties are superior to SLS printable materials

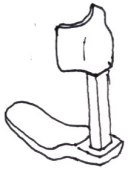

Interchangeable metal rod for required stiffness. (Either material changes stiffness or thickness)

Thick U form around the ankle --> would this increase moment of inertia or not at all?

Backstrips through thicker fin design? --> bigger moment of inertia without adding too much material

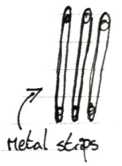

Backstrips through thicker fin design? --> could be made from a different material screwd onto it. Metal strips/carbon layered/ carbon LW strips?

Aluminium strut profile screw-on idea

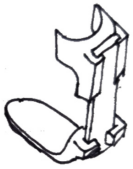

Carbon plate idea. Verenstaal could work or other plates with a high youngs modulus and flexability

Bladveer idee

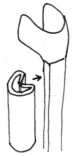

Reinforcement of the strut from the sides

Nosagveer in notches for flexible spring storage

Torsion spring attachment for ankle moment influence

Use tensile strength of a stiff rubber like material. A thin wire could be present inside the shoe as to minimize AFO thickness. Downside; only works in one way

Deep slots in AFO for carbon rods. Slide in from the top, maybe a cap on it to block them from getting out

Using an externally produced carbon layered strut in combination with SLS printed fitting components

Ropes to tension the stut
-> provide enough stiffness

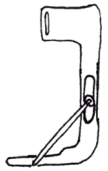

metal rods with a roller for stiffness in both directions

Fan like spring structures for strut support

Appendix E: AFO thickness relevance analysis

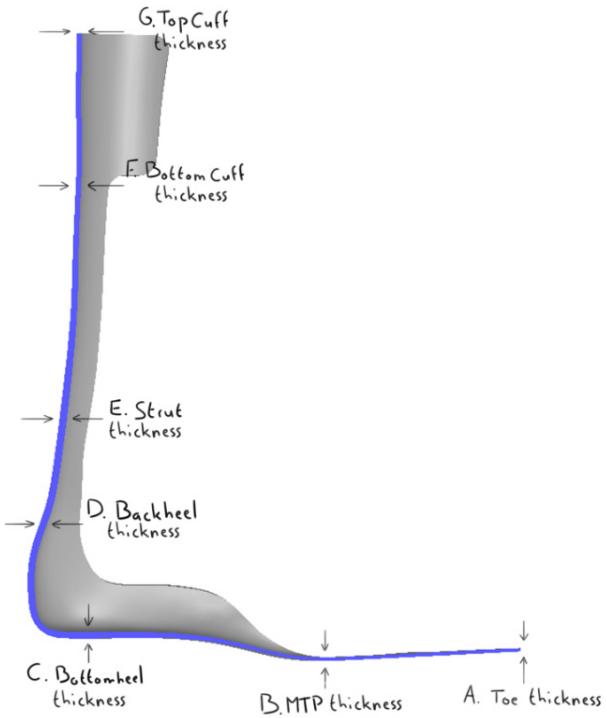

Different thickness values at points C, D and E were generated and consequently simulated through FEA to determine their effect on the displace present when a force of 60N is applied at the height of the cuff.

A:2mm B:2mm C:4mm D:5mm E:5mm F:3mm G:3mm

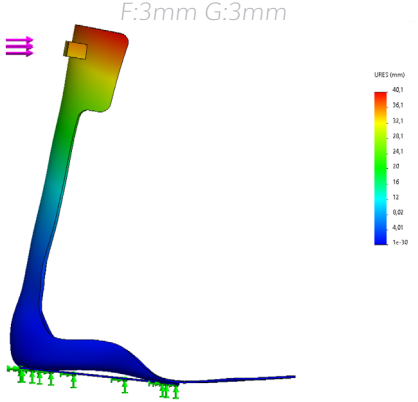

A:2mm B:2mm C:4mm D:5mm E:6mm F:3mm G:3mm

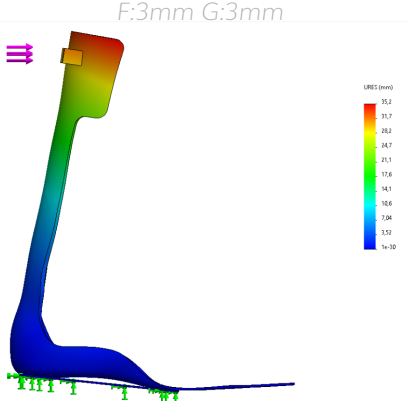

A:2mm B:2mm C:5mm D:5mm E:6mm F:3mm G:3mm

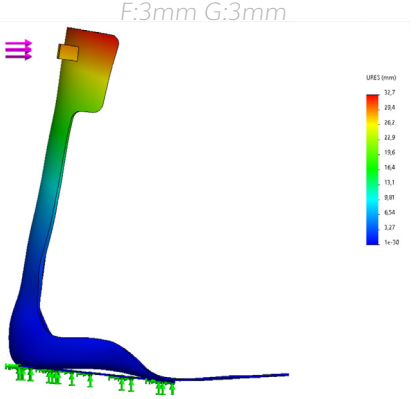

A:2mm B:2mm C:4mm D:4mm E:5mm F:3mm G:3mm

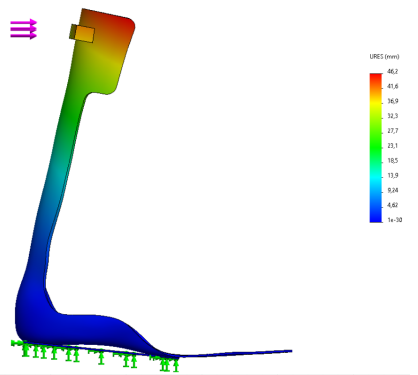

A:2mm B:2mm C:5mm D:4mm E:4mm F:3mm G:3mm

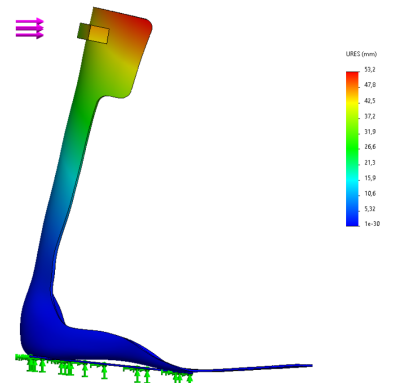

A:2mm B:2mm C:3mm D:5mm E:6mm F:3mm G:3mm

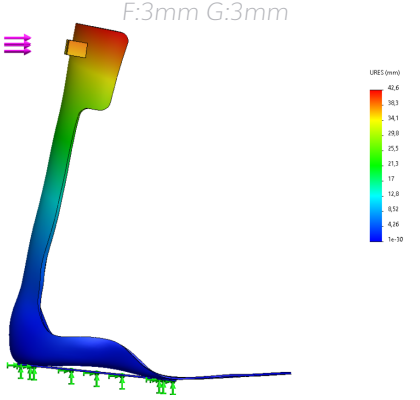

A:2mm B:2mm C:5mm D:5mm E:5mm F:3mm G:3mm

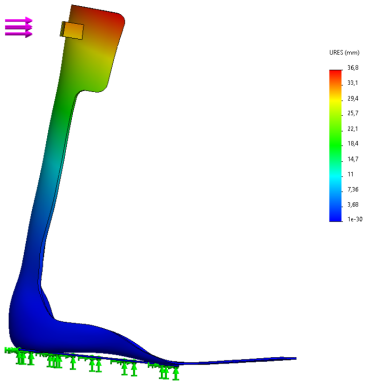

A:2mm B:2mm C:4mm D:3mm E:4mm F:3mm G:3mm

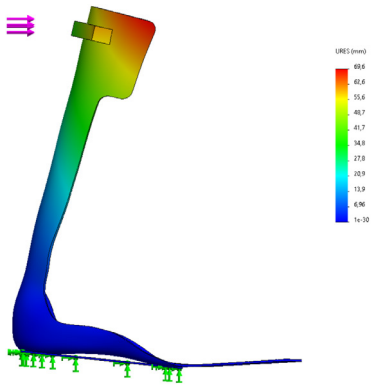

Appendix F: data comparison for 3 piece prototype

3 piece prototype PA11 strut simulated stiffness						
	Weight (kg)	Force (N)	Height (mm)	simulated Moment (Nm))	Angle (degrees)	Measured stiffness (Nm/°)
Dorsiflexion	8	80	85,7	28,8	13,39034607	2,150803262
	6	60	65,8	21,6	10,35805888	2,085332807
	4	40	44,7	14,4	7,077999616	2,034473125
	2	20	22,7	7,2	3,608040408	1,995543061
	0	0	0	0	0	0
Plantarflexion	2	-20	22,9	-7,2	3,639744228	-1,978160978
	4	-40	45,5	-14,4	7,203356111	-1,999068181
	6	-60	67,4	-21,6	10,60427953	-2,036913487
	8	-80	88,3	-28,8	13,78131398	-2,089786216
	Arm length (m)	0,36			Average dorsiflex moment stiffness	2,066538064
					Average plantarflex moment stiffness	-2,025982215

figure 102: simulated stiffness data for 3 piece prototype with PA11 strut

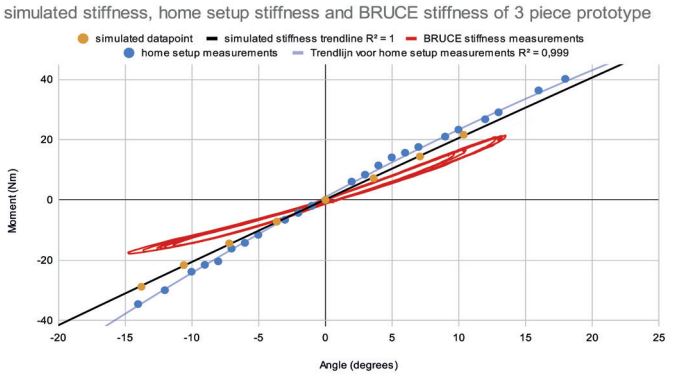

figure 103: comparison graph between BRUCE, home and simulated measurements

3 piece prototype PA11 strut homesetup measurements							
	Heigth on ruler	Weight (kg)	Force (N)	Height (mm)	Moment (Nm))	Angle (degrees)	Measured stiffness (Nm/°)
Dorsiflexion	157	10	100	112,5	35	17,81888891	1,964207767
	146	9	90	101,5	31,5	16,17215902	1,947791879
	125	7,1	71	80,5	24,85	12,95276451	1,918509363
	119	6,5	65	74,5	22,75	12,01647656	1,893233834
	109	5,6	56	64,5	19,6	10,44164186	1,877099431
	99	5	50	54,5	17,5	8,850694047	1,977246068
	88	4,1	41	43,5	14,35	7,08471688	2,025486726
	84	3,6	36	39,5	12,6	6,438992961	1,956827733
	78	3,2	32	33,5	11,2	5,467369272	2,048517202
	71	2,5	25	26,5	8,75	4,329847792	2,020856256
	66	2	20	21,5	7	3,515180849	1,991362692
	61	1,7	17	16,5	5,95	2,699088403	2,204447988
	54	1,1	11	9,5	3,85	1,554789411	2,476219592
Plantarflexion	165	1	-10	-8,5	-3,5	-1,391195467	2,515821884
	170	1,6	-16	-13,5	-5,6	-2,208885075	2,535215645
	175	2,2	-22	-18,5	-7,7	-3,02567551	2,544886249
	186	3,5	-35	-29,5	-12,25	-4,817828486	2,54263929
	192,5	4,2	-42	-36	-14,7	-5,872628281	2,503138169
	198	4,7	-47	-41,5	-16,45	-6,762070638	2,432686803
	204,5	5,3	-53	-48	-18,55	-7,80899246	2,375466502
	209	5,8	-58	-52,5	-20,3	-8,53076561	2,37962229
	213	6,1	-61	-56,5	-21,35	-9,170067115	2,328227235
	217,5	6,7	-67	-61	-23,45	-9,886531241	2,371913812
	233	8,3	-83	-76,5	-29,05	-12,32932276	2,35617159
	245	9,5	-95	-88,5	-33,25	-14,19021227	2,343164384
	Arm length (m)	0,35				Average plantarflex moment stiffness	2,023215887
	Start value on ruler dorsiflexion(mm)	44,5				Average dorsiflex moment stiffness	2,435746154
	Start value on ruler plantarflexie(mm)	156,5				Average stiffness	2,221230415

figure 104: homesetup stiffness data for 3 piece prototype with PA11 strut

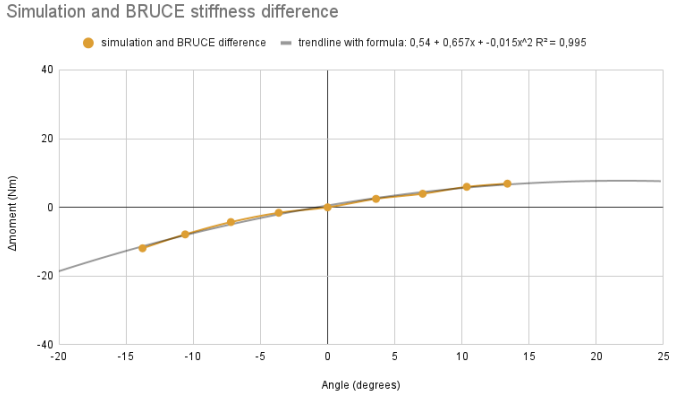

figure 105: difference between BRUCE measurements and simulated stiffness

Appendix G: Ridge design exploration

<- Long fins straight back

negative moment: 1,86Nm/deg

positive moment: 1,53Nm/deg

score: 0,823

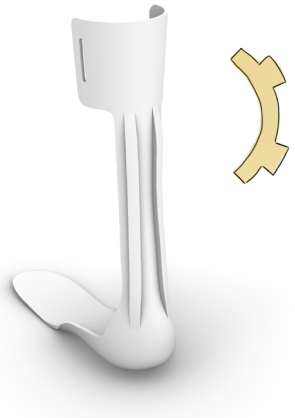

<- Broad, slightly normally offset fins

negative moment: 2,32Nm/deg

positive moment: 1,73

score: 0,75

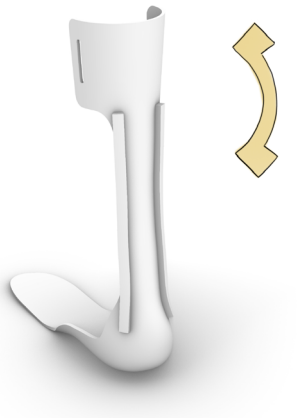

<- Fins on the edge of the strut

negative moment: 1,94Nm/deg

positive moment: 1,63

score: 0,840

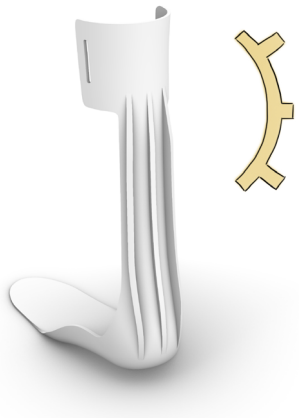

<- Three fin design

negative moment: 1,61Nm/deg

positive moment: 1,39Nm/deg

score: 0,863

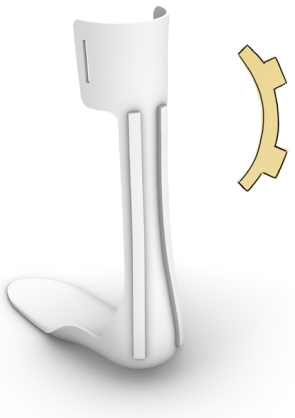

<- Follow curve of heel at the bottom instead of straight fins

negative moment: 1,73Nm/deg

positive moment: 1,58Nm/deg

score: 0,913

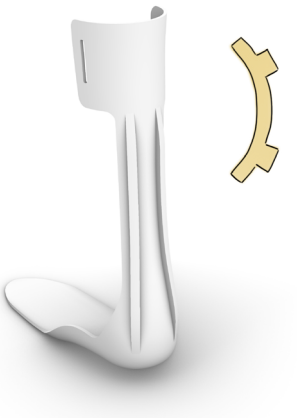

<- dissolving fins to fit better in a shoe

negative moment: 1,92Nm/deg

positive moment: 1,79Nm/deg

score: 0,932

<- Anti-curve for more symetrical shape

negative moment: 1,90Nm/deg

positive moment: 1,67Nm/deg

score: 0,879

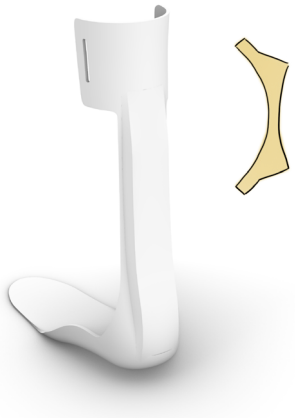

<- More organic, more flat anti- curve

negative moment: 1,88Nm/deg

positive moment: 1,75Nm/deg

score: 0,931

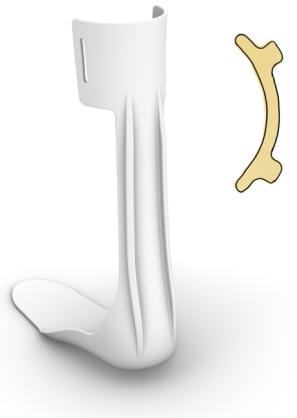

<- Filleted, dissolving fins

negative moment: 1,83Nm/deg

positive moment: 1,72Nm/deg

score: 0,940

Appendix H: MTP Pa11 sample measurements

Several PA11 samples with variable thicknesses that mimicked the shape of the foot sole were calculated and measured to determine their stiffness.

Figure 106: Samples used in the test

MTP 3,5 ~ 3,5 mm thickness sample

Heigth on ruler	Weight (kg)	Force (N)	Height (mm)	Moment (Nm)	Angle (degrees)	Measured stiffness (Nm/°)
42,4	4,1	41	39,4	4,6207	19,26966271	0,2397914312
40,8	3,8	38	37,8	4,2826	18,54164475	0,2309719584
36	3,5	35	33	3,9445	16,32070503	0,2416868629
31,2	3	30	28,2	3,381	14,04820501	0,2406713169
27,2	2,5	25	24,2	2,8175	12,11905848	0,2324850568
25,2	2,3	23	22,2	2,5921	11,14363138	0,2326081967
22,4	2,1	21	19,4	2,3667	9,767084118	0,242313875
18,4	1,7	17	15,4	1,9159	7,781046223	0,2462265286
14	1,3	13	11	1,4651	5,574654373	0,2628144997
10,8	0,9	9	7,8	1,0143	3,959144213	0,2561917287
8	0,6	6	5	0,6762	2,540294233	0,2661896371
Arm length (m)	0,1127					
Start value on ruler (mm)	3				Average stiffness	0,2447228265

MTP 3 ~ 2,5 mm thickness sample

Heigth on ruler	Weight (kg)	Force (N)	Height (mm)	Moment (Nm)	Angle (degrees)	Measured stiffness (Nm/°)
39,2	1,6	16	34,2	1,8032	16,88097227	0,1068184919
28	1,1	11	23	1,2397	11,53462065	0,1074764431
22,8	0,8	8	17,8	0,9016	8,975237258	0,100454169
16,8	0,5	5	11,8	0,5635	5,977247018	0,09427416975
Arm length (m)	0,1127					
Start value on ruler (mm)	5				Average stiffness	0,1022558184

MTP 3,5 ~ 3 mm thickness sample

Heigth on ruler	Weight (kg)	Force (N)	Height (mm)	Moment (Nm)	Angle (degrees)	Measured stiffness (Nm/°)
40	3	30	37	3,381	18,17527898	0,1860219039
36,8	2,7	27	33,8	3,0429	16,69457997	0,1822687366
34,4	2,5	25	31,4	2,8175	15,5686767	0,1809723494
31,6	2,3	23	28,6	2,5921	14,23941914	0,1820369198
28	2	20	25	2,254	12,50727401	0,180215129
24	1,7	17	21	1,9159	10,55518143	0,1815127492
20,4	1,4	14	17,4	1,5778	8,776722046	0,1797709887
15,6	1	10	12,6	1,127	6,379248168	0,1766665868
10,8	0,5	5	7,8	0,5635	3,959144213	0,1423287382
Arm length (m)	0,1127					
Start value on ruler (mm)	3				Average stiffness	0,1768660113

MTP 3 ~ 3 mm thickness sample

Heigth on ruler	Weight (kg)	Force (N)	Height (mm)	Moment (Nm)	Angle (degrees)	Measured stiffness (Nm/°)
36	2	20	33	2,254	16,32070503	0,1381067788
31,2	1,7	17	28,2	1,9159	14,04820501	0,1363804129
24	1,3	13	21	1,4651	10,55518143	0,138803867
18,4	0,9	9	15,4	1,0143	7,781046223	0,130355221
13,6	0,6	6	10,6	0,6762	5,373148267	0,1258480069
Arm length (m)	0,1127					
Start value on ruler (mm)	3				Average stiffness	0,1338988573

Figure 107: Measured data of MTP samples

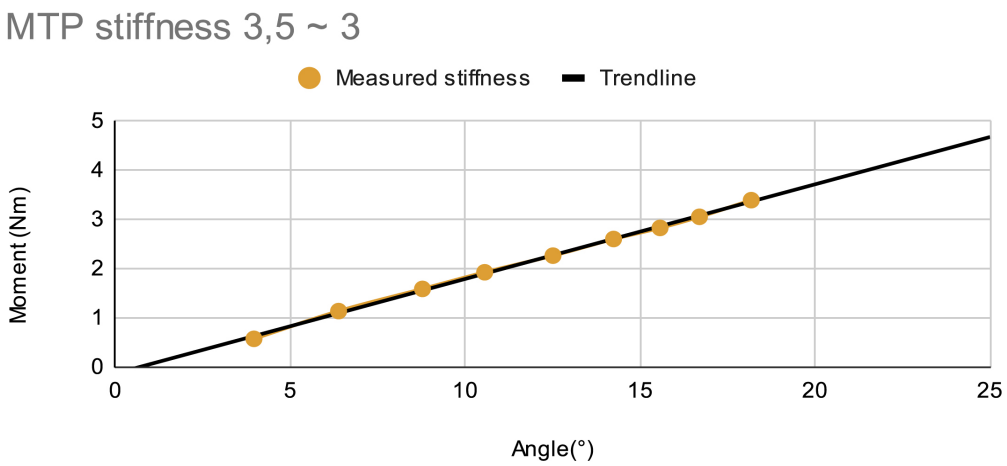

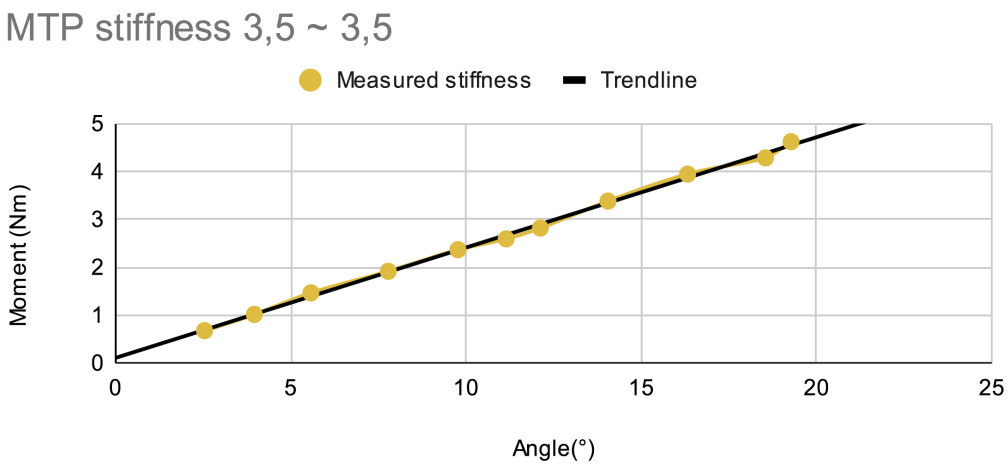

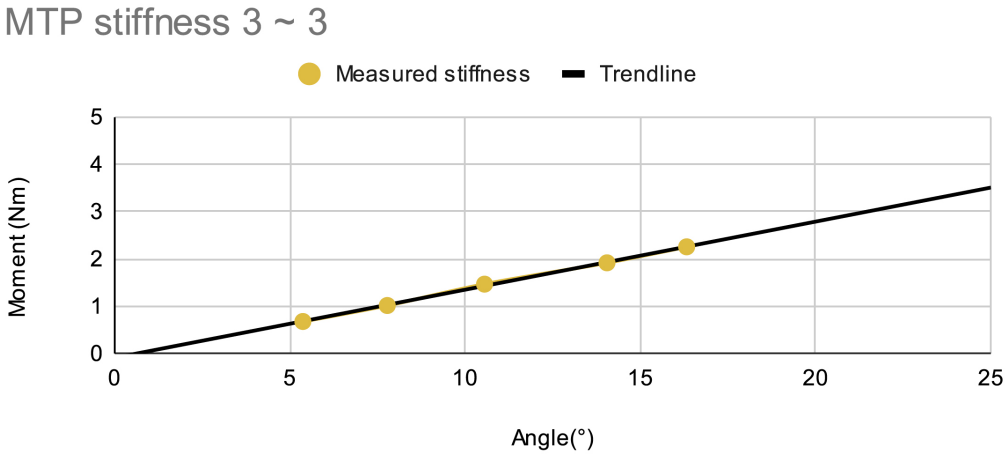

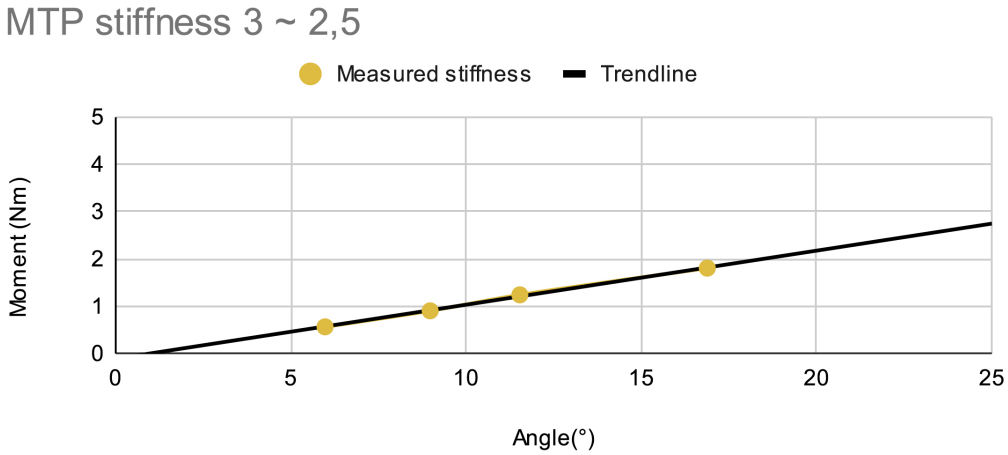

Figure 108: Graphs of measured stiffness in MTP samples

Appendix I: Ridge prototype BRUCE measurements

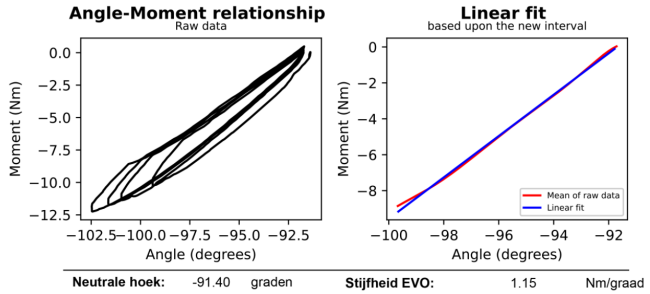

Figure 109: Dorsiflexion measurements 1

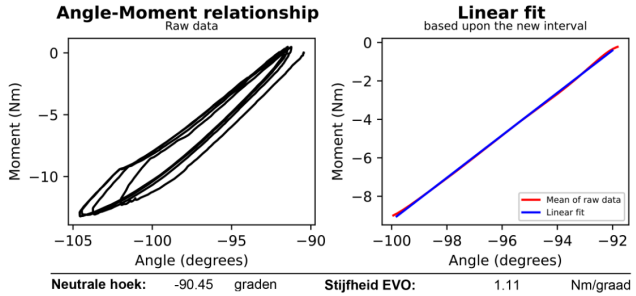

Figure 110: Dorsiflexion measurements 2

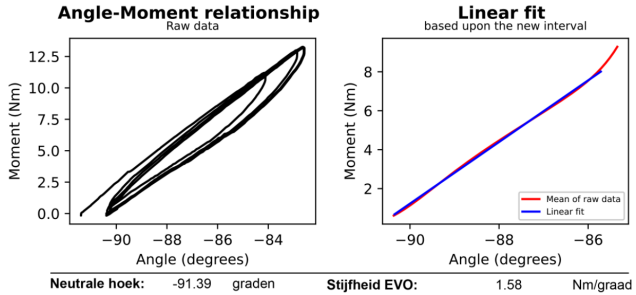

Figure 111: Plantar flexion measurements 1

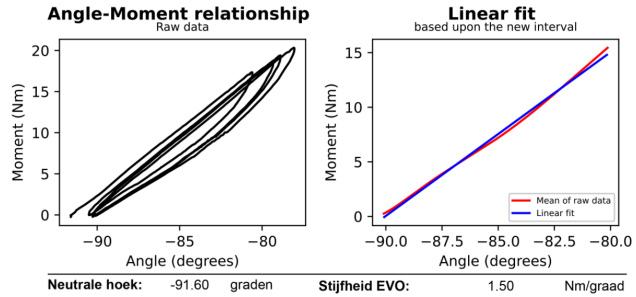

Figure 112: Plantar flexion measurements 2

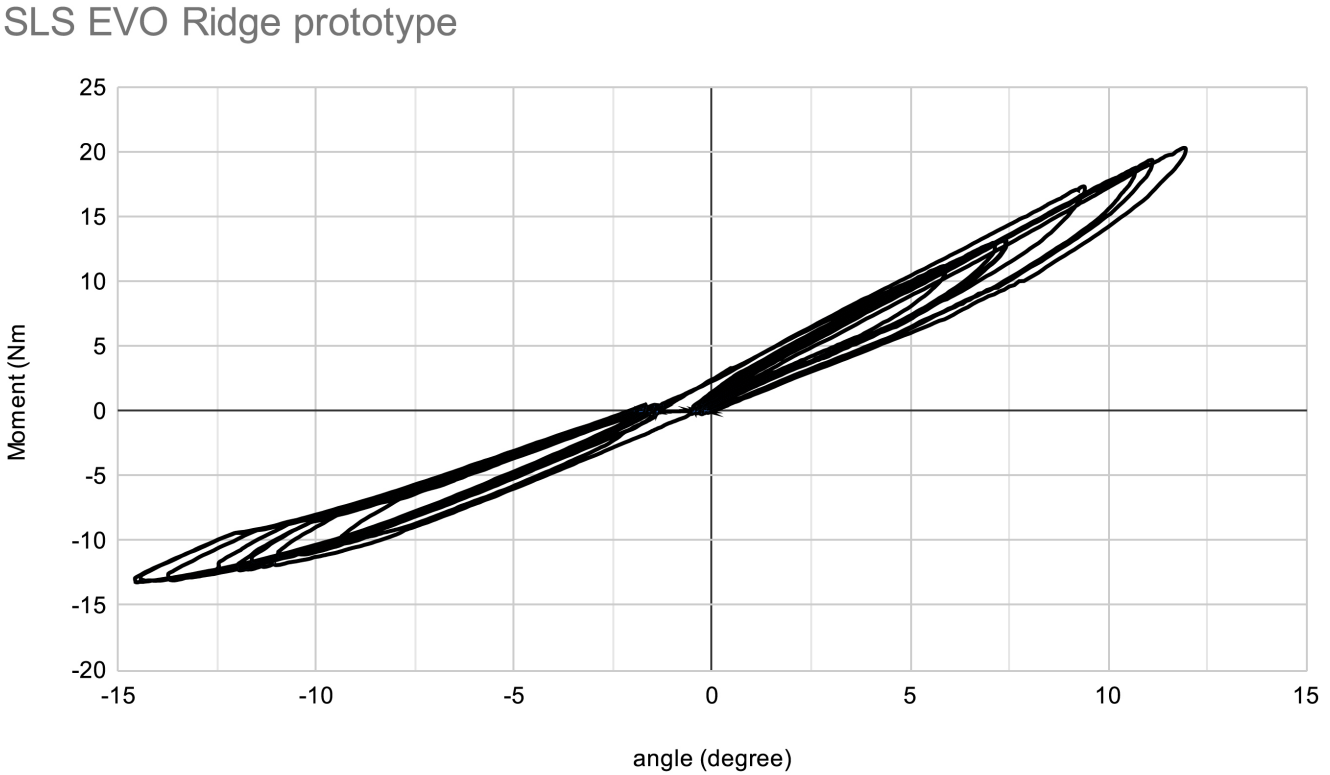

Figure 113: Combined data

Appendix J: MTP stiffness Ridge prototype

MTP stiffness Ridge prototype

Heigth on ruler	Weight (kg)	Force (N)	Height (mm)	Moment (Nm))	Angle (degrees)	Measured stiffness (Nm/°)		
35	0	0	0	0	0	0	0	0
45	0,5	5	10	0,75	3,814074834	0,1966400851	0,36	3,814074834
47	0,6	6	12	0,9	4,57392126	0,1967677074	0,72	3,814074834
53	0,8	8	18	1,2	6,842773413	0,1753674903	0,6	4,763641691
56	1,1	11	21	1,65	7,969610394	0,2070364696	0,6	5,237476067
60	1,4	14	25	2,1	9,462322208	0,2219328357	0,84	5,710593137
64	1,5	15	29	2,25	10,94218541	0,2056261995	0,72	5,710593137
64	1,6	16	29	2,4	10,94218541	0,2193346128	0,84	6,654425046
69	2,1	21	34	3,15	12,77124256	0,2466478875	0,96	8,53076561
74	2,4	24	39	3,6	14,5742162	0,2470115683	1,2	8,997143421
79	2,7	27	44	4,05	16,34817155	0,2477341266	1,08	9,462322208
83	3	30	48	4,5	17,74467163	0,2535972542	1,32	9,926245507
43	0,6	6	8	0,9	3,052882515	0,2948033525	1,44	10,38885782
43	0,3	3	8	0,45	3,052882515	0,1474016762	1,44	10,85010463
47	0,7	7	12	1,05	4,57392126	0,2295623253	1,68	10,85010463
54	1	10	19	1,5	7,219020825	0,2077844124	1,68	11,08019922
57	1,2	12	22	1,8	8,343891584	0,2157266764	1,68	11,76828893
58	1,4	14	23	2,1	8,717456965	0,2408959412	1,92	12,22512268
61	1,6	16	26	2,4	9,833563964	0,2440620724	1,8	13,58599121
65	1,8	18	30	2,7	11,30993247	0,2387282158	1,92	13,58599121
66	1,8	18	31	2,7	11,67673783	0,2312289647	2,16	14,03624347
69	2,1	21	34	3,15	12,77124256	0,2466478875	2,16	14,48473356
73	2,4	24	38	3,6	14,21585347	0,2532384008	2,52	15,81919395
74	2,6	26	39	3,9	14,5742162	0,2675958657	2,52	15,81919395
73,5	2,8	28	38,5	4,2	14,39517866	0,2917643538	2,4	17,1362745
77	3,2	32	42	4,8	15,64224646	0,3068612947	2,88	17,57125878
45	0,5	5	11	0,75	4,194182788	0,178819102	3,36	17,78797254
48	0,7	7	14	1,05	5,332158882	0,1969183633	3,12	18,00416161
54	0,9	9	20	1,35	7,594643369	0,1777568655	2,88	18,00416161
57	1,2	12	23	1,8	8,717456965	0,2064822353	3,84	19,29004622
57,5	1,4	14	23,5	2,1	8,903961957	0,2358500643	2,88	20,13630343
71	2	20	37	3	13,8563515	0,2165072097	3,24	20,13630343
78	2,4	24	44	3,6	16,34817155	0,2202081125	3,6	21,80140949
85	2,7	27	51	4,05	18,77803322	0,2156775394	3,6	22,61986495
84	3	30	50	4,5	18,43494882	0,2441015727	3,24	23,02549201
Arm length (m)	0,15				Average stiffness:	0,220751964		
Start value on ruler dorsiflexion3(mm)	35							
Start value on ruler dorsiflexion2(mm)	35							
Start value on ruler dorsiflexion1(mm)	34							

figure 114: Raw data of measured MTP tests

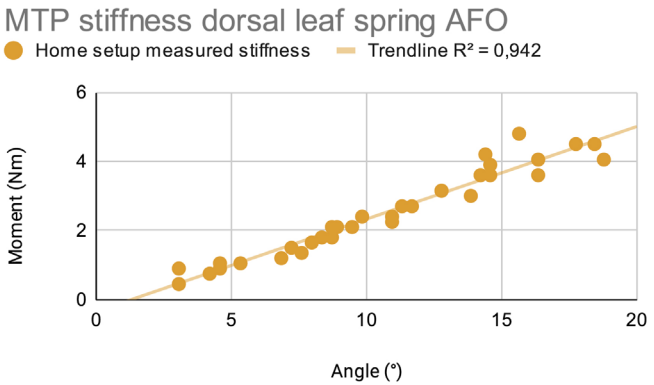

figure 115: moment set out against angle of measured MTP stiffness

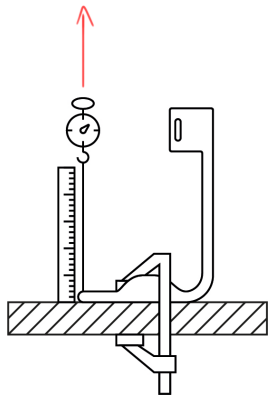

figure 116: MTP measurment setup overview

Appendix K: Model interface to customize parameters

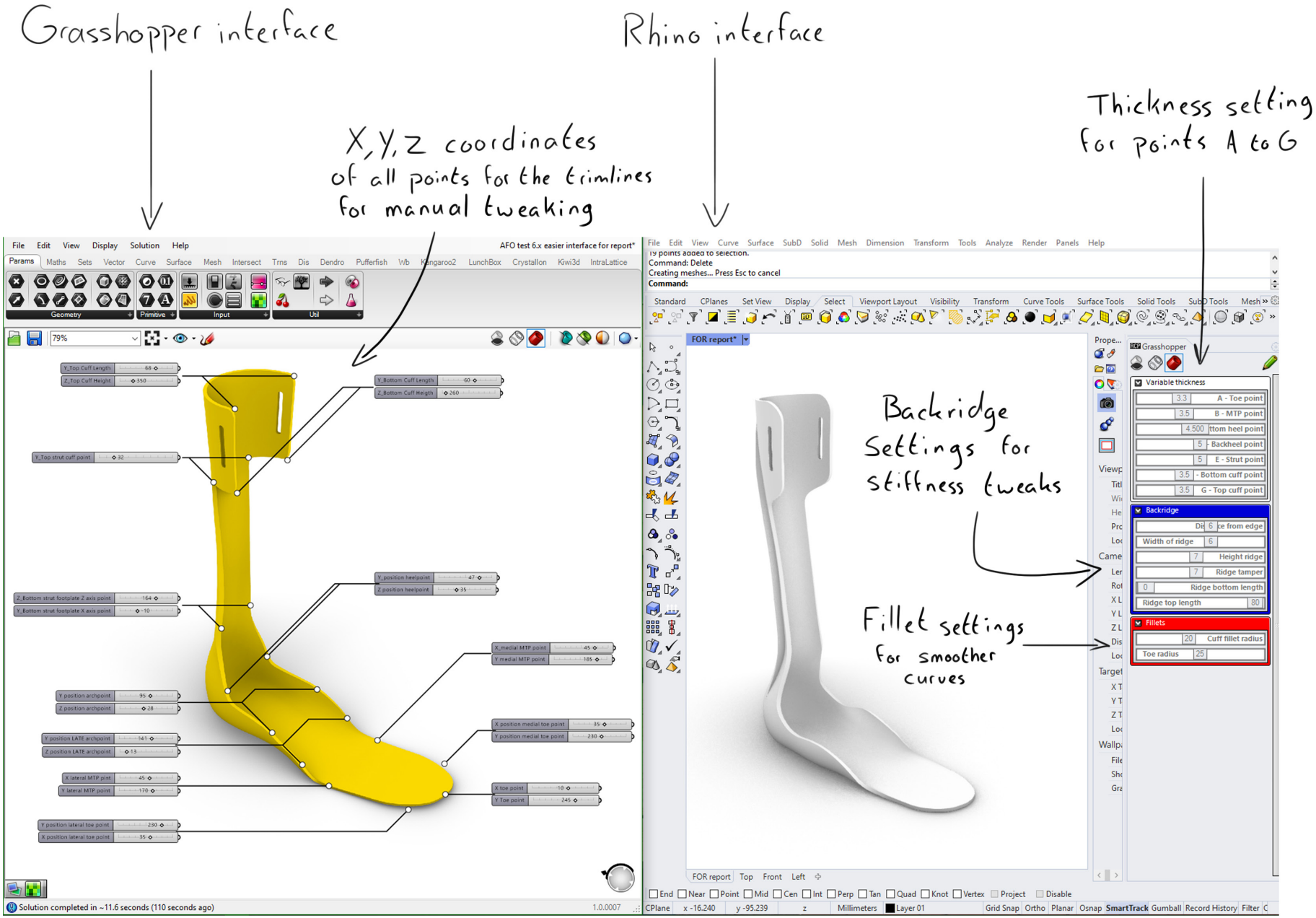

Figure 117: Grasshopper and Rhino interface with changeable parameters influencing the model. All values are in mm.

Appendix L: Grasshopper model

The arrows in the model refer to 'choke' points. It is recommended to examine these points in the model first when a new footmodel is loaded into the program for troubleshooting.

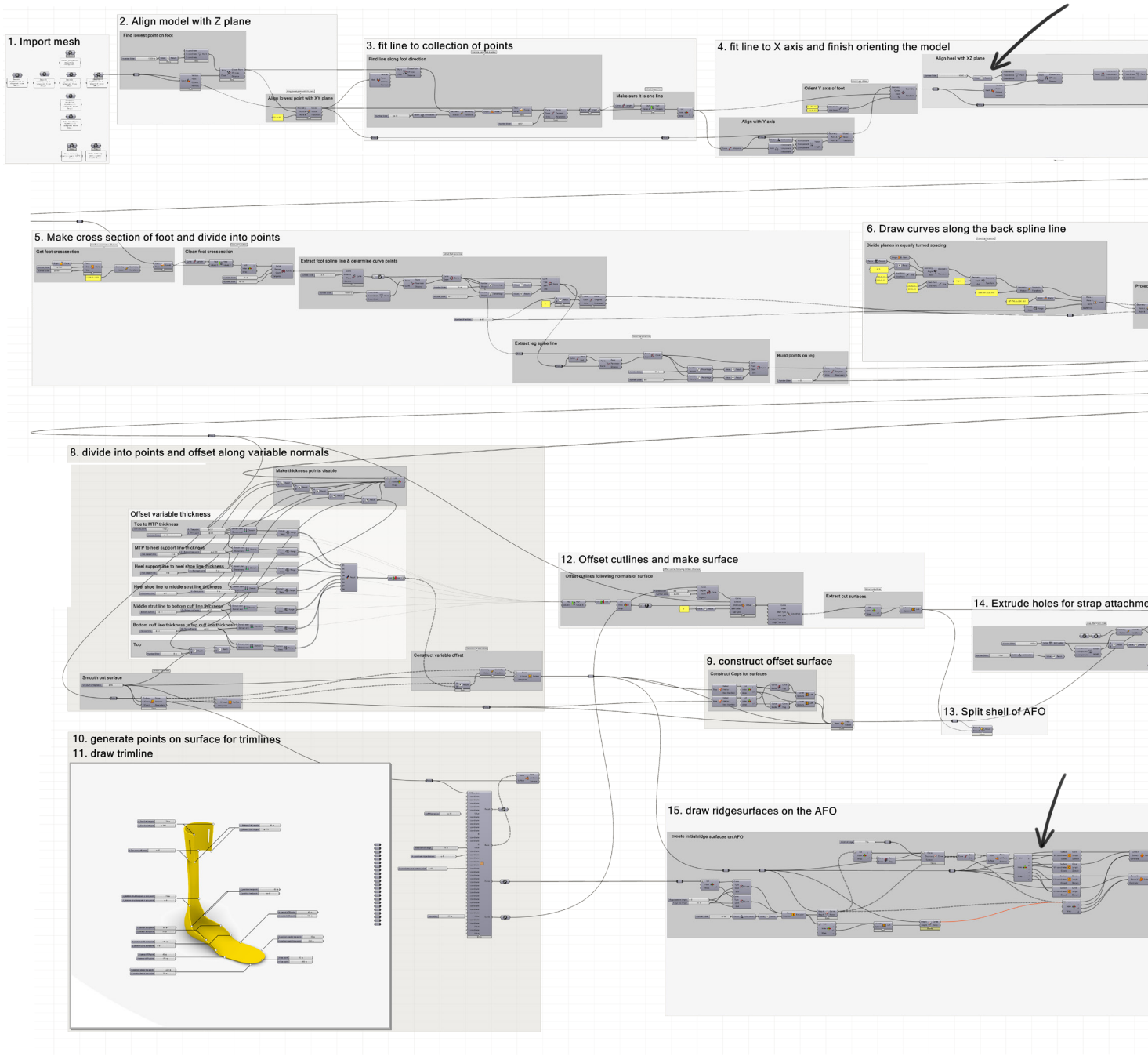

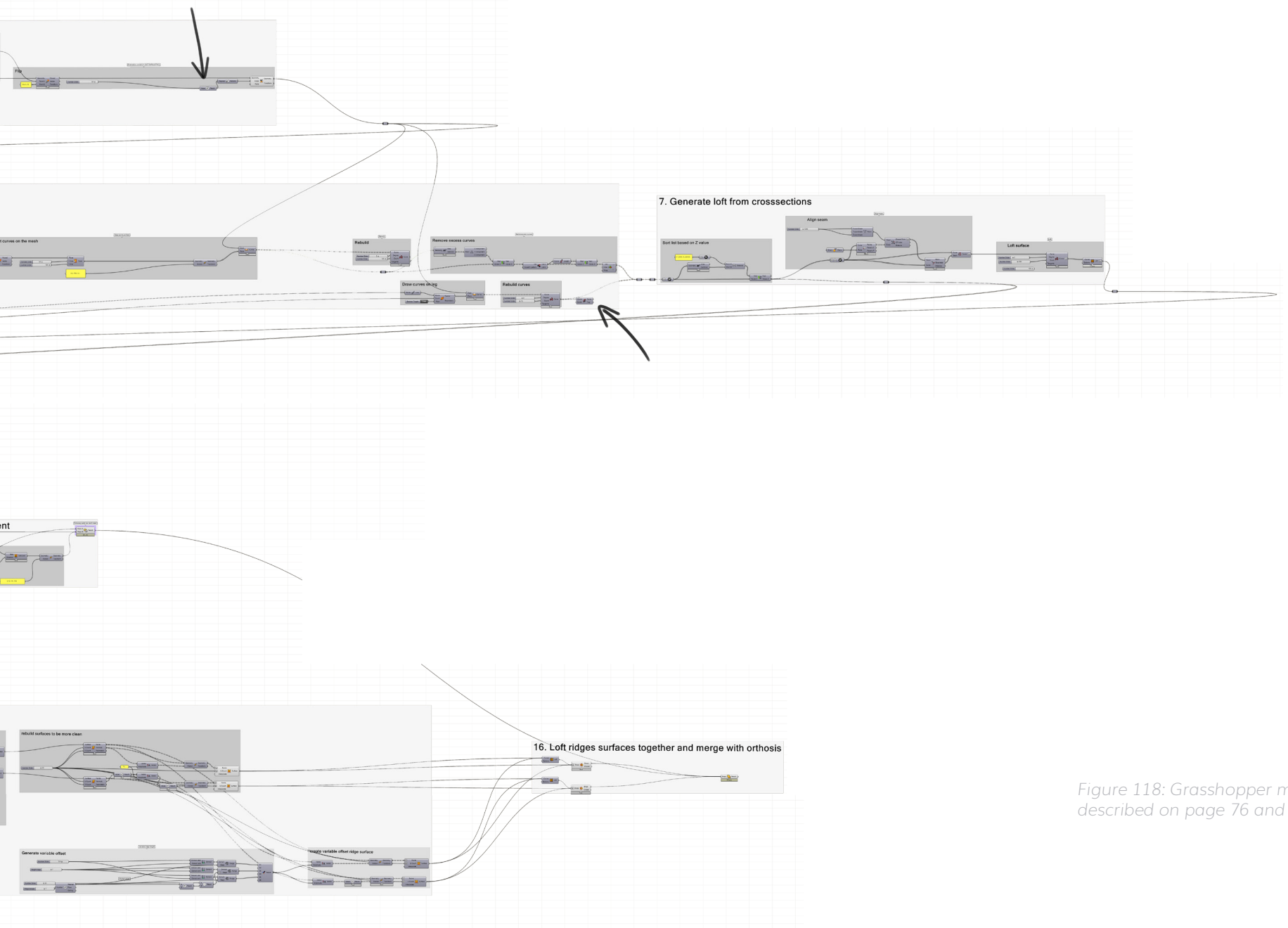

Figure 118: Grasshopper model buildup, each step is described on page 76 and 77 for further explanation

Appendix M: User test setup and concent form

Studie naar de invloed van een SLS geprinte orthese op het gangbeeld van een carbon dorsale veer enkel-voet orthese gebruiker

Deze studie wordt uitgevoerd als onderdeel van de opleiding Industrieel Ontwerpen aan de TU Delft in samenwerking met Parts on Demand en Livit Ottobock Care. Als u vragen heeft naar aanleiding van deze studie, kunt u ten alle tijden contact opnemen met: Falko Baatsen,

CONFIDENTIAL INFORMATION

Het doel van dit onderzoek is om inzage te krijgen in de ergonomie en invloed op het gangbeeld van een alternatief geproduceerde enkel-voet-orthese. Dit onderzoek is onderdeel van een Masterscriptie rondom de verkenning van een SLS 3D geprint alternatief voor de carbon gelaagde dorsale voetorthesen, momenteel geproduceerd door Livit Ottobock Care. Parts on Demand is als belanghebbende betrokken als excusief uitvoerend producent van de SLS-3D geprinte onderdelen. Dit onderzoek is deel van het overkoepelende onderzoek om de bruikbaarheid van een SLS geprinte orthese te achterhalen zodat, indien mogelijk, de bruikbaarheid van het product verbeterd kan worden.

Dit onderzoek zal ongeveer 120 minuten in beslag nemen. De data zal geanonimiseerd en gebruikt worden in de verslaglegging van dit thesis project. Dit zal gepubliceerd worden in de TU Delft repository en inzag zal verschaft worden voor Parts on Demand en Livit Ottobock Care.

In dit onderzoek zal van u gevraagd worden een looptraject af te leggen met de huidige carbon dorsale veer voorzieningen en om hetzelfde traject af te leggen met SLS geprinte loopvoorzieningen. Dit bestaat uit het lopen van +- 5 minuten op een rolband. Hierin zal de enkel en onderbeen positie vastgelegd en gedocumenteerd worden door middel van camera opnames geschoten vanuit het sagitalle vlak. Dit zal 3 keer gedaan worden; een keer zonder loophulpmiddel, een keer met de carbon dorsale veel ortheses en een keer met de SLS geprinte ortheses. Achteraf aan dit onderzoek zal u aan aantal vragen gesteld worden over het gebruik van het product en hoe u het ervaren heeft.

Gedurende de studie zal informatie verzameld worden (in de vorm van schriftelijke aantekeningen, foto's en video's tijdnes de gangbeeld analyse en geluidsopnamen tijdens het interview) met betrekking tot het productgebruik. De informatie zal alleen voor het onderzoeksteam beschikbaar zijn. De gegevens zullen anoniem worden geregistreerd. De data vergaard aan de hand van dit onderzoek zal vervolgens online opgeslagen worden. Wij zullen ons best doen uw antwoorden vertrouwelijk en geanonimiseerd te houden. Dit zal gedaan worden door middel van het onherkenbaar maken van foto's in het verslag. De digitale data direct vergaard tijdens het onderzoek zal opgeslagen worden op een lokale telefoon, camera en laptop waar het niet langer op zal staan dan 5 dagen. De data zal dan opgeslagen worden op een server van Nextcloud met ISO/IEC 27001-2013 beveiliging tegenover datalekken.

Uw deelname aan dit onderzoek is volledig vrijwillig, en u kunt zich elk moment terugtrekken zonder reden op te geven. U bent vrij om vragen niet te beantwoorden.

Als u besluit mee te doen aan deze studie, willen we u vragen om een toestemmingsformulier te tekenen. Deze kunt u tekenen bij aanvang van de bijeenkomst.

De test zal uitgevoerd worden in de revalidatie locatie te Eindhoven, Blixembosch. Mede onder begeleiding van Chantal Engel.
contactgegevens uitvoerende onderzoeker:
Falko Baatsen

CONFIDENTIAL INFORMATION

Toestemmingsformulier

Gelieve de juiste vakjes aan te vinken

	JA	NEE
1. Ik heb de informatie over het onderzoek gedateerd 24-05-23 gelezen en begrepen, of deze is aan mij voorgelezen. Ik heb de mogelijkheid gehad om vragen te stellen over het onderzoek en mijn vragen zijn naar tevredenheid beantwoord.		
2. Ik doe vrijwillig mee aan dit onderzoek, en ik begrijp dat ik kan weigeren vragen te beantwoorden en mij op elk moment kan terugtrekken uit de studie, zonder een reden op te hoeven geven.	☐	☐
3. Ik begrijp dat mijn deelname aan het onderzoek de volgende punten betekent: - Ik toestemming geef dat fotos tijdens het onderzoek gemaakt worden, die mogelijkerwijs geanonimiseerd gebruikt kunnen worden in de verslaglegging van het overkoepelende onderzoek - Ik toestemming geef dat videos tijdens het onderzoek gemaakt worden, die gebruikt zullen worden voor de evaluatie van het product - Ik toestemming geef dat mijn digitale bestanden en metingen gebruikt worden in de productie van de SLS ortheses.	☐	☐
4. Ik begrijp dat de studie zal plaatsvinden op 26-06-23 om 10:00 te Eindhoven, Blixembosch	☐	☐
5. Ik begrijp dat mijn deelname risico's met zich meebrengt op het gebied van valincidenten of uitglijden. Ik begrijp dat deze risico's worden geminimaliseerd door ondersteuning door middel van aanwezig traliewerk om aan vast te pakken of menselijke ondersteuning. De SLS orthese zal op breuk getest zijn tot een buighoek van 20 graden dorsaalflexie en 20 graden plantair flexie.	☐	☐
6. Ik begrijp dat de volgende stappen worden ondernomen om het risico van een data breuk te minimaliseren, en dat mijn identiteit op de volgende manieren wordt beschermd in het geval van een data breuk: - De data vergaard tijdens het onderzoek zal maximaal 5 dagen ongeanonimiseerd op een lokale harde schijf staan, waarna het vernietigd wordt - De data zal vervolgens geanonimiseerd worden en opgeslagen op een server van Nextcloud met ISO/IEC 27001-2013 beveiliging tegenover datalekken	☐	☐
7. Ik begrijp dat de persoonlijke informatie die over mij verzameld wordt en mij kan identificeren, zoals mijn naam, digitale gegevens en geboortedatum niet gedeeld worden buiten buiten dit onderzoek	☐	☐
8. Ik begrijp dat de persoonlijk identificeerbare data die over mij verzameld wordt, vernietigd wordt op 30-06-23.	☐	☐
9.Ik begrijp dat na het onderzoek de geanonimiseerde informatie gebruikt zal worden voor de verslaglegging van dit thesis project. Dit zal gepubliceerd worden in de TU Delft repository en inzag zal verschaft worden voor Parts on Demand en Livit Ottobock Care.	☐	☐
10. Ik geef toestemming om mijn antwoorden, ideeën of andere bijdragen anoniem te quoten in resulterende producten.	☐	☐

Ondertekeningen

_____	_____	_____
Naam deelnemer	Handtekening	Datum
_____	_____	_____
Naam onderzoeker	Handtekening	Datum

Ik, Falko, **de onderzoeker**, verklaar dat ik naar het beste van mijn vermogen, heb verzekerd dat de deelnemer begrijpt waar hij/zij vrijwillig mee instemt.

Appendix N: Gait analysis of user test

The gait of the user was analysed by placing a camera at 2 meters away from a treadmill, capturing the sagittal plane view, while the participant walked at a pace of 3 meters per hour for approximately 1 minute each time.

Trackers in the form of white stickers with bright dots were placed at the ankle joint, the 5th metatarsophalangeal joint and the knee joint.

The data was then analysed in Tracker[61], a video analysis and modelling tool, where the points were auto-tracked and the angle was measured between them with the centre point being the ankle joint (*figure 123*) that was set out against time.

TThis process was repeated three times for each orthosis, as seen in figure 119 to 121. To offset the angle, a line perpendicular to the line from the ankle joint to the knee joint was drawn through the ankle joint, and the remaining angle was subtracted from the values. Trendlines were then drawn over the data to better visualise their means.

The combined trendlines and a 'healthy' gait adopted from Whittle[13] can be found in figure 122.

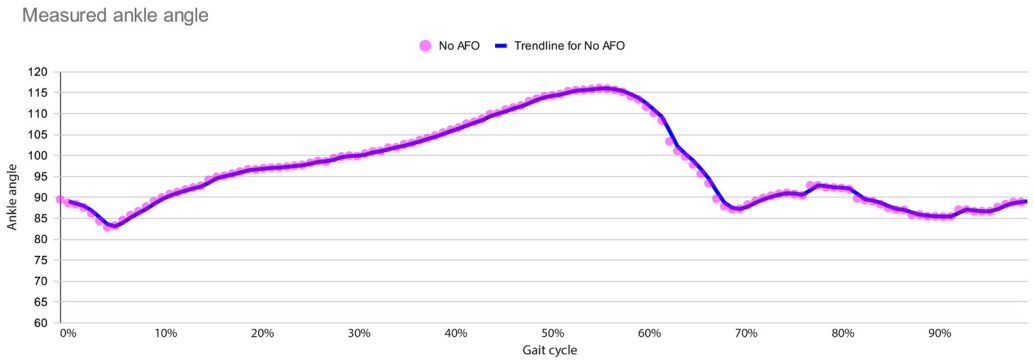

figure 119: Ankle angle measurements without wearing orthoses for a full gait cycle

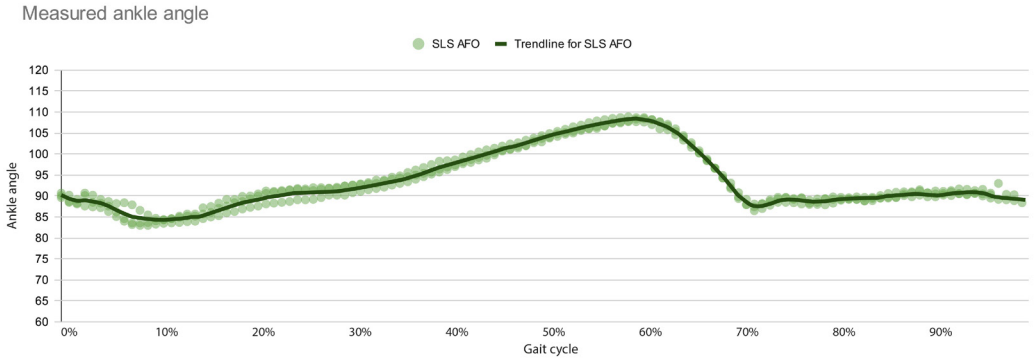

figure 120: Ankle angle measurements whilst wearing SLS orthoses for a full gait cycle

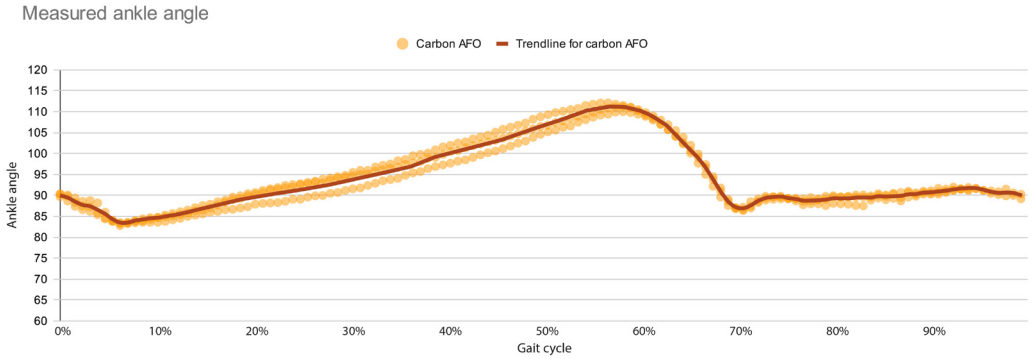

figure 121: 3 Ankle angle measurements whilst wearing carbon dorsal leaf spring orthoses for a full gait cycle

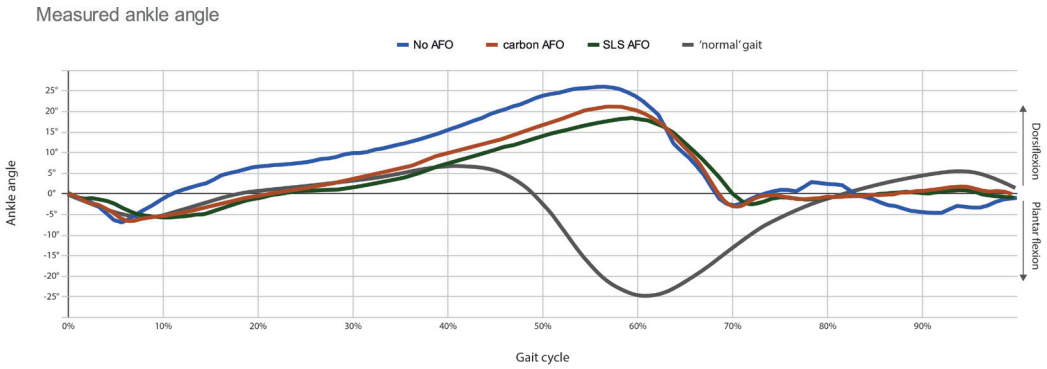

figure 122: ankle angle during a full gait cycle of the participant when no AFOs are worn, when carbon AFOs are worn, when SLS printed AFOs are worn and a 'normal' gait cycle as depicted by Whittle[13]

figure 123: Analysis of the ankle angle offset against time in Tracker[61]